The role of central amygdala neuron subpopulations in appetitive behaviours

Dissertation der Fakultät für Biologie

der Ludwig-Maximilians-Universität München

Federica Fermani

München, den 29.11.2021

Erstgutachter: Prof. Dr. Rüdiger Klein

Zweitgutachter: Prof. Dr. Laura Busse

Tag der Abgabe: 29.11.2021

Tag der mündlichen Prüfung: 26.07.2022

The work presented in this dissertation was performed in the laboratory of Prof. Dr. Rüdiger Klein, Department of Molecules – Signaling – Development, Max- Planck Institute of Neurobiology, Martinsried, Germany.

EIDESSTATTLICHE ERKLÄRUNG

Ich versichere hiermit an Eides Statt, dass die vorgelegte Dissertation von mir selbständig und ohne unerlaubte Hilfe angefertigt ist.

München, den 29.11.2022

Federica Fermani

ERKLÄRUNG

Hiermit erkläre ich, dass die Dissertation nicht ganz oder in wesentlichen Teilen einer anderen Prüfungskommission vorgelegt worden ist und ich mich anderweitig einer Doktorprüfung ohne Erfolg nicht unterzogen habe.

München, den 29.11.2022

Federica Fermani

Abstract

Nutrient ingestion is regulated by homeostatic needs, that increase the motivation to eat when energy stores are low, and by hedonic pathways that increase the desire to consume rewarding food even when there is abundant energy. Animals looking for food must constantly rely on environmental signals in order to discriminate between dangers and rewards. The amygdala comprises a collection of nuclei including the basolateral complex (BLA) and the central amygdala (CeA). The CeA, with its lateral (CeL) and medial (CeM) divisions orchestrates a wide range of behaviours, including defensive and appetitive responses. The CeA, indeed, is a node within different structures known to process taste and interoceptive information and integrates emotionally salient environmental stimuli to generate appropriate behaviours[1]. All the studies presented in this thesis investigate the role of CeA in appetitive behaviours.

In the first study, I combined behavioural, optogenetic and *in vivo* recordings of neuronal activity, to explore the roles of different CeA subpopulations in associative learning of contextual food cues. Using a behavioural task of appetitive conditioning, in which the mice explore an arena across different cues looking for food, I found that two CeA subpopulations, Somatostatin (Sst) and Protein kinase C delta (PKCδ), acquire a specific response to context-positive environmental cues. Interestingly, while the proportion of food responsive cells was higher in Sst neurons, only optogenetic inhibition of PKCδ impaired both the learning and the retrieval of contextual food memory, suggesting their involvement in linking the sensory characteristics of the environment with the salience of the food reward. However, Sst cells could be responsible for correlating the physical properties of the food, such as texture and taste, with the context.

In the second study, I examined the role of 5-Hydroxytryptamine receptor 2A (Htr2a) and Sst neurons in CeL versus CeM in consummatory and rewarding behaviours. Although CeA has been recently studied in appetitive paradigms, the relative contribution of the two major CeA subdivisions is still relatively unclear. The role of CeA^{Htr2a} neurons in feeding, previously described in our lab[2], raised the question of whether their function is specific to feeding, or they are involved in other consummatory behaviours such as drinking. Moreover, the activity of Sst neurons (that partially overlap with Htr2a), has been shown as positively reinforcing and their inhibition in the CeL reduced water intake[3]. For these reasons, I investigated the

involvement of Htr2a and Sst neurons in CeA, CeM and CeL in drinking, feeding, and rewarding behaviours.

To do so, we generated a novel transgenic mouse line that expresses a Tamoxifen-inducible version of the Flp recombinase under regulatory elements of the Wfs1 gene (Wfs1-*FlpoER*) where the FlpoER is expressed specifically in the majority of $CeL^{Htr2a/Sst}$ neurons. Crossing Htr2a-*Cre*/Sst-*Cre* and Wfs1-*FlpoER* mice generates double transgenic intersectional mice in which $CeL^{Htr2a/Sst}$ cells are positive for both Cre and Flp, while $CeM^{Htr2a/Sst}$ cells are positive for Cre only. Stimulation of CeM^{Htr2a} and CeM^{Sst} neurons promoted drinking and positive reinforcement behaviour. Stimulation of CeM^{Htr2a}, but not CeM^{Sst}, neurons increased food intake. Photoactivation of the corresponding CeL subpopulations failed to elicit appetitive responses. Ongoing analysis of intra-CeA and long-range projections will provide further insights into the specific roles of CeL and CeM subpopulations in appetitive responses.

In summary, this work extends our knowledge about the role of CeA in different appetite behaviours, analysing the function of the different CeA neuronal subpopulations and of the two main CeA subdivisions, CeL and CeM.

1. Introduction

1.1 Neuroanatomical features of the amygdala

1.1.1 The amygdala: structure and molecular diversity

1.1.1.1 Amygdaloid complex nuclei

The amygdala is an almond-shape structure found deep in the temporal lobe implicated in a variety of functions, ranging from attention, to memory, from emotion to fear[1]. Although modest in size, the amygdala complex contains a heterogeneous collection of multiple anatomically defined nuclei with distinct cytological, connectional and functional characteristics[4]. These nuclei are further divided into subdivisions with extensive inter and intranuclear connections.

Classically, the amygdaloid complex can be separated into three groups based on structural similarity and originality during development. The first is a specialized ventromedial expansion of the striatum, comprising the central (CeA) and medial (MeA) nuclei and anterior area (AAA), that together with the dorsal substantia innominata (SI) and the bed nucleus of the stria terminalis (BNST), form the central extended amygdala[5]. A second region, the superficial or cortical-like group, is related to the caudal olfactory cortex and comprises the nucleus of the lateral olfactory tract (NLOT), the cortical nucleus (COA) and the postpiriform and piriform amygdala (PAA) areas[5]. Finally, the deep or basolateral group (BLA), a ventromedial extension of the claustrum, which includes the lateral (LA) and basal (BA), basomedial (BM) and posterior nuclei[5] (Figure 1.1). There is also another set of nuclei that cannot be easily encompassed in the previous groups that includes the intercalated cell masses and the amygdalohippocampal area[5]. Previous studies underlined some important differences between the basolateral and central nuclei of the amygdala in morphology of cells and electrophysiological properties. In the BLA, two main populations are present: pyramidal spiny neurons and GABAergic neurons. The first group differs from the cortical spiny neurons in some cytological characteristics as well as in the organisation - it is not rigid in one plane with parallel apical dendrites, but completely random. For these reasons, it is more appropriate to call these cells pyramidal-like neurons. The second group resembles stellate cells of the cortex and is clearly involved in the formation of local circuits[5].

The centromedial nuclei have both histochemically and developmentally distinctive characteristics from the cortical nuclei. In particular, the CeA has three subregions: the capsular subdivision (CeC), the lateral (CeL), and the medial subdivision (CeM). The main cell type in the CeA is medium spiny neurons, which are distinctly different from the cortical-like neurons found in the BLA and morphologically defined as striatal-like, consistent with the different embryological origin of the two nuclei. Moreover, central nuclei projections are mainly GABAergic, while basolateral projections are glutamatergic. This supports the general conclusion of the difference between the two nuclei[5]. CeA neurons can be classified into three different electrophysiological types: late-firing, low threshold bursting, and regular spiking[6]. The majority of the neurons in the capsular part are late firing, while in the medial part, they are mostly low threshold or regular spiking. A combination of all three types is present in the lateral part of the CeA[7].

Structurally the CeM contains more densely packed neurons of variable diameter, while the CeL consists of more diffuse and uniform medium-size cells[8].

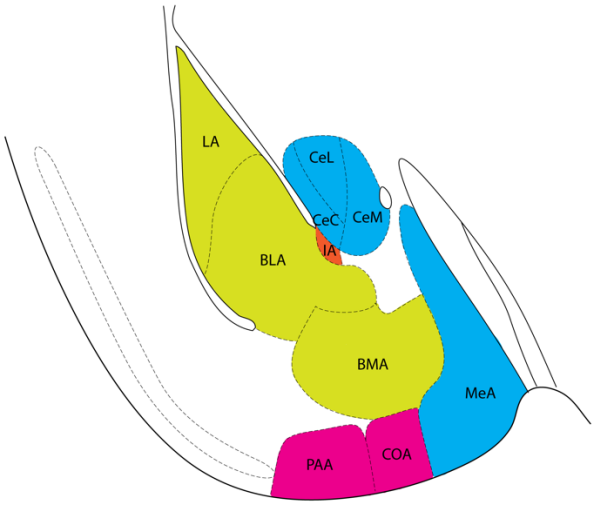

Figure 1.1: Nuclear divisions of the amygdala complex

Coronal representation of the amygdala complex highlighting its three main nuclei: the basolateral (lime), centromedial (blue) and superficial (magenta). The intercalated cells appear in orange. The basolateral part is composed of LA (lateral amygdala), BLA (basolateral amygdala), BMA (basomedial amygdala); the centromedial part is constituted of CeC (centrocapsular amygdala), CeL (centrolateral amygdala), CeM (centromedial amygdala), MeA (medial amygdala). The cortical area comprises PAA (piriform amygdala area), and COA (cortical amygdala area).

1.1.1.2 Molecular diversity of the CeA

The amygdala complex exhibits a wealth of neuropeptides that, acting as neurotransmitters or neuromodulators, are very important in understanding the physiology of the structure[9].

CeA neurons express neuronal peptides such as neurotensin[10] and somatostatin (Sst), which spread quite diffusely within the CeA, substance-P, found almost exclusively in the medial part, and Leu-enkephalin (ENK), in the lateral part[11]. Immunohistochemical investigations have reported the presence of neuropeptide Y (NPY), vasoactive intestinal peptide (VIP), cholecystokinin (CCK), and calcitonin gene-related peptide (CGRP)[12] positive cells in the CeA[9,13]. ENK neurons are present within the CeA and especially in the CeL[14], pro-opiomelanocortin (POMC) positive neurons were not observed in the amygdala[15] while fibres mostly localized respectively in the lateral, capsular and medial part[16]. Neurotensin (Nts) immunoreactive neurons comprise the largest population of cells in the CeA, preferentially distributed in the CeL, where a considerable number of corticotropin-releasing-hormone (CRH) positive neurons are present[17]. Tachykinin 2 (Tac2) is present in both the central and basal nuclei[18].

The CeA also expresses a large variety of receptors, such as the widely expressed dopamine D2 receptor (D2R), which is related to food rewards, and a lower percentage of neurons which express the melanocortin 4 receptor (MC4R), involved in the regulation of homeostatic balance and controlling the motivation for food[19]. Recently a detailed description of the main markers in the different subdivisions of the CeA was made[3]: Calcr1 (Calcitonin receptor 1) and PKCδ (protein kinase δ) are expressed in the CeC; CRH, Htr2a (5-Hydroxytryptamine receptor 2A) Nts, PKCδ, Sst and Tac2 in the CeL; and Htr2a, Nts, Sst and Tac2 in the CeM. In the CeC, Calcrl labels 89% of PKCδ neurons and does not overlap with Sst. In the CeM there is only minimal overlap between CRH, Nts, Sst, and Tac2; Htr2a neurons were found to coexpress CRH, PKCδ, Nts, Sst and Tac2 in the CeL while only Nts, Sst and Tac2 in the CeM [3].

1.1.2 Neurocircuits of the amygdala

1.1.2.1 Afferent connections

Each amygdaloid nucleus receives input from multiple and distinct brain regions[14], and projects to cortical and subcortical regions.

The major source of sensory input is from the cerebral cortex[20] which sends glutamatergic and ipsilateral[21] projections, entering the amygdala via the external capsule[22]. The amygdala receives olfactory, somatosensory, gustatory, visceral, auditory, and visual inputs in this way. Olfactory projections mostly reach the BLA[5], while somatosensory inputs from primary somatosensory areas target both the BLA and the CeA[23,24].

Other information reaches the amygdala from projections from the pontine parabrachial nucleus (PBN), thalamic nuclei (TH), and medial portion of medial geniculate (MGM), all of which are involved in the transmission of nociceptive stimuli[25]. Gustatory and visceral primary areas in the anterior and posterior insular cortex (IC) project to the BLA and the CeA[23], the thalamic nucleus (thalamic gustatory nucleus) to the BLA and the CeL[26,27], while the PBN targets the CeL[28]. The amygdala receives auditory information via projections from the cortex (CTX)[29] and thalamic medial geniculate[25], and visual cortical projections from thalamic and high-order visual areas[20,30].

The amygdala receives a variety of polymodal sensory information from the prefrontal cortex to both the BLA and the CeA[31], and from the perirhinal cortex and the hippocampus (HPC) that projects strongly and reciprocally to the BLA and more sparsely to the other nuclei[20]. Additionally, the LA and the CeA receive inputs from the hypothalamus (HYP), and the CeA is the major target for midbrain, pons, medulla projections[5] (Figure 1.2).

1.1.2.2 Intra connectivity

The amygdala receives sensory information with an affective value and translates it into the correct behavioural responses projecting to different brain regions[32,33]. The flow of information has a highly localized representation, and since the inputs converge in different nuclei, it is important to understand how they integrate through intra-amygdaloid connections[4].

Synaptic connectivity is generally unidirectional within the amygdala complex, with glutamatergic neurons in the BLA forming excitatory synapses on neurons of both the CeL and CeM of the CeA[34]. The LA, the main relay station for visual and auditory inputs[20], projects to the BL and the BM[8] and indirectly, through the basal nuclei[35,36,37], to the CeC and the CeM, the principal source of brainstem projections[11].

However, there are exceptions that make the information flow reciprocal and not just unidirectional from the lateral to medial area, as previously postulated[38]. For example, almost all the amygdala nuclei project to the lateral area, and reciprocal projections are of substantial density[39]. Also, the organization of the central nucleus is different: it receives projections from the lateral and basal parts but sends limited projections back. Further, the inputs into the CeA are largely restricted to the medial and capsular part.

There are also extensive connections within the CeA[40]. The capsular and lateral subdivisions significantly project to the medial and lateral parts, while the medial division largely sends projections out of the amygdala but also moderately projects to the capsular subdivision[40]. The lateral subdivision, which forms the largest projections to the other CeA regions, does not receive many reciprocal connections but receives extra-amygdaloid inputs from cortical and subcortical regions, suggesting a role of integration of inputs to the complex[5].

To summarise, when information enters the complex, it is processed in parallel in different amygdala nuclei and enters the output region, the CeA, where the different stimuli are gathered and the appropriate behavioural responses are elicited[4].

1.1.2.3 Efferent connections

The amygdala complex projects to the cortical, hypothalamic and brainstem regions. There are reciprocal connections between lateral and basolateral nuclei to cortical sensory areas. The BLA innervates the hippocampus, the perirhinal and prefrontal cortex, the nucleus accumbens[41,42], and the thalamus[5]. Activation of the central nucleus induces autonomic responses, in turn activating the brainstem neurons that control the autonomic system, or stimulating hypothalamic nuclei that modulate these centres[43]. The medial nucleus of the CeA projects to the hypothalamus, BNST, midbrain, pons, and medulla[11], as well as the periaqueductal gray (PAG)[44], parabrachial nucleus[45], and nucleus of the solitary tract (NTS)[46]. In addition, all the subdivisions of the CeA target the BNST, as well as various hypothalamic regions, thus influencing ingestive, reproductive, and defensive behaviour[47](Figure 1.2).

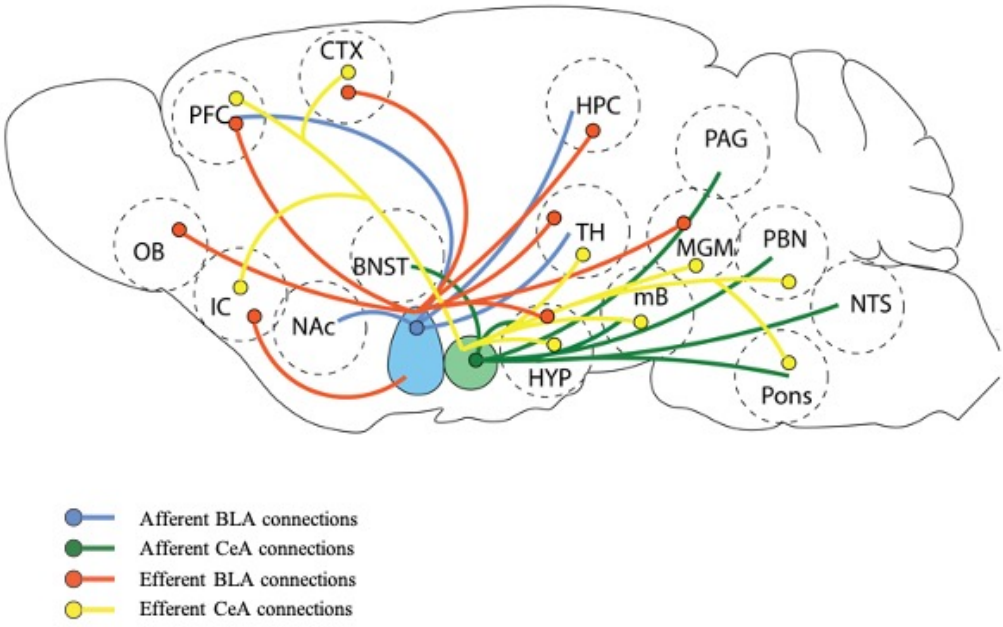

Figure 1.2: Schematic representation of amygdala afferents and efferents

Diagram showing BLA (blue) and CeA (green) connections. BLA afferents (blue), BLA efferents (red), CeA afferents (green), and CeA efferents (yellow). OB, olfactory bulbs; IC, insular cortex; NAc, nucleus accumbens; BNST, bed nucleus of the stria terminalis; PFC, prefrontal cortex; CTX, cortex; HPC, hippocampus; TH, thalamus; HYP, hypothalamus; mB, midbrain; MGM, medial geniculate; PAG, periaqueductal grey; PBN, parabrachial nucleus; NTS, nucleus of the solitary tract.

1.2 Functions of the amygdala

The amygdala is a brain region important in emotional processing and its function is well-conserved across time and species[1]. The first evidence underlining a role of this brain region in connecting stimuli with their emotional meaning came from lesion studies in non-human primates, demonstrating an impairment in acquiring behavioural responses to shock-predictive cues[1,48]. Subsequent experiments of amygdala lesions in rodents revealed a functional conservation across species with the involvement of the amygdala in the recognition of fearful stimuli in an emotional learning paradigm called fear conditioning[1]. Starting from these experiments, the amygdala complex was studied in much further detail using aversive and rewarding behavioural tasks, disentangling specific functions of the BLA and the CeA[1,49].

In this thesis, I will focus specifically on the circuit of the CeA. The CeA orchestrates a broad variety of different behaviours, from defensive to appetitive responses[50,51] and its network comprises recurrent inhibitory circuits with functionally and genetically defined cell types that select and control different behavioural outputs[3,52,53]. Moreover, the importance of investigating the anatomical roles of the CeL and CeM subregions of the CeA is becoming prominent[3]. The CeA is involved in both learning and in innate behaviours: while more accepted information about the CeA and its subpopulations is related to defensive behaviour, much less is known about appetitive and rewarding behaviour. Furthermore, some of the published work on CeA subpopulations is controversial. This may have to do with the fact that previous work did not consider the CeL and CeM fractions separately. A single molecularly defined population can be, in fact, further divided by spatial location. My thesis work analysed the role of the CeA both in learned and innate appetite behaviours, examining the role of three main neuronal subpopulations, Htr2a, PKCδ, and Sst, considering their location in the CeL or CeM subregions. In the following part of the introduction related to the amygdala function, I will describe the involvement of the CeA in learning and innate behaviours, with particular attention to the role of these three subpopulations.

1.2.1 The central amygdala and learned behaviour

1.2.1.1 The central amygdala and appetitive Pavlovian conditioning

The classical view of the amygdala emphasises its role on negative, unpleasant emotions, such as fear, and on linking environmental stimuli with aversive sensory inputs. However, recent evidence supports a role for the amygdala in also processing positive emotions, such as learning the beneficial biological value of stimuli[54-57].

To carry out its reward-related functions, the amygdala interacts with various cortical and subcortical structures, including the nucleus accumbens, midbrain dopaminergic system, the basal forebrain cholinergic system, and the prefrontal cortex[58]. Many studies in rodents and non-human primates identified a role for the amygdala in the association of reward value with initially neutral stimuli[58]. In such tasks, animals need to learn which stimulus or place to choose in order to obtain a reward (usually food or water), or to choose one positive stimulus (S^+) rather than a distracter stimulus (S^-). Severe impairments in several measures of stimulus-reward learning can be observed through aspiration lesions where most of the amygdala is mechanically removed[59-61].

Pavlovian approach responses to a specific conditioned stimulus (CS) engage the central amygdala: a stereotyped response to a previously neutral stimulus is elicited by the pairing of the reward with that stimulus. LA lesions prevent amphetamine place preference conditioning, a procedure through which the animals learn to associate a spatial location with the reinforcing effects of the drug[62], while CeA lesions prevent conditioned responses to reward-predictive cues[56]. Amygdala lesions impair the ability to respond to cues in the face of changing reward value, being involved in learning the current value of the overall situation of an organism at a given moment[1,63].

One study reported that lesions of the CeA, but not the BLA [64], impair stimulus-reward association. In this study, rats were presented with two identical visual stimuli - one on either side of a cup; but the presentation of the stimulus is followed by food delivery only on one side. Rats usually learn to approach the stimulus that appears on this side, reflecting a Pavlovian association between the stimulus and the food delivery, but this kind of behaviour is impaired by lesions of the CeA[65]. Optogenetic stimulation of the CeA paired with a particular sucrose

reward in rats amplifies and narrows incentive motivation to that particular target. In addition, pairing CeA activation with a specific reward precisely amplifies the will to pursue one reward, even at the expense of earning another alternative reward of comparable value. Reward-paired stimulation of the BLA does not lead to the similar result as stimulation in the CeA[66].

1.2.1.2 Central amygdala and conditioned taste aversion

Feeding is a goal-directed behaviour essential for the survival of all animals, but this behaviour accompanies the possibility of ingesting noxious substances that may be a threat to life. For example, animals often learn to avoid a poisonous bait, but only if they survive the poisoning. When the ingestion of a substance is followed by a gastrointestinal malaise, animals have an innate predisposition to form "associations" between foodstuff and visceral distress and, as a vital adaptive reaction protecting them against repeated intake of dangerous food, they reject its ingestion again.

A brain region playing a key role in anorexic behaviour is the PBN, a region with a heterogeneous population of neurons in the brainstem that mediates the suppression of appetite after ingestion of toxic food or after a bacterial infection. Experimentally, these conditions are generated by injection of lithium chloride (LiCl), lipopolysaccharide (LPS), or anorectin hormones such as amylin and cholecystokinin in rodents[67]. In particular, a population of neurons expressing the calcitonin gene related peptide (CGRP) in the outer external lateral subdivision of the PBN and projecting to the lateral capsular part of the CeA, forms a very important connection involved in appetite suppression.

Optogenetic and chemogenetic-based activation of this specific projection suppresses food intake. On the contrary, its inhibition increases food intake in situations when animals wouldn't normally eat[67]. The specific connection between CGRP neurons in the PBN and the CeA may mediate the discomfort that results from adverse conditions during which it is usually unfavourable to eat.

1.2.1.3 The amygdala and Pavlovian fear conditioning: from a serial to a parallel circuit model

The amygdala has long been known to be the neuroanatomical centre of fear memory. Early studies in 1937 revealed that resection of large portions of the temporal lobe in monkeys caused 'psychic blindness'[68], with animals showing loss of previously acquired fear responses[48]. The central role of the amygdala in emotional learning and memory was then intensely studied using Pavlovian fear conditioning. This is a form of associative learning in which an initially neutral stimulus (conditioned stimulus [CS]), such as a tone, is paired over time with a different noxious stimulus (unconditioned stimulus [US]), such as a foot shock[34]. As a result, the CS elicits defensive or fear responses, such as freezing, when presented alone[69].

In the early 1990's, it was initially proposed that the convergence of synaptic inputs about the CS and the US leads to the potentiation of synapses conveying CS information to the LA. In the original 'serial model'[70], auditory and somatosensory information reaches the LA from the thalamic[29,71] and cortical[22,72] regions and is then relayed to the CeA[73] which, projecting to areas of the brainstem and hypothalamus, controls the expression of defensive behaviour[69,74].

Prior to conditioning, the CS inputs are relatively weak, being unable to elicit fear responses. In contrast, the US inputs are stronger and capable of eliciting robust responses in LA neurons. Since CS and US inputs converge onto LA neurons, during fear conditioning the CS inputs are active during strong postsynaptic depolarization caused by the US. As a result, the CS becomes stronger and more effective at driving LA neurons that can subsequently activate downstream structures[75]. However, recent evidence suggests that the 'serial' model can be overtaken by a 'parallel' one. The BLA and the CeA have a coordinating function, working both in parallel and independently to control different aspects of emotional learning[76].

The BLA mediates associations between predictive stimuli and the biological properties of events and the CeA mediates the associations of predictive stimuli with their effective or emotional properties. In contrast, in reward-related learning, the BLA mediates the emotional significance of reward while the CeA establishes the general affective responses that underlies the nonspecific reinforcing effects of these events. It does not seem required and there is no direct indication that the BLA and the CeA must function serially, rather it seems more probable that they function in parallel and simultaneously.

1.2.1.4 Fear conditioning: a new circuit model. The role of the CeL and the CeM

Recent evidence supports a role in the learning process for the CeA, previously considered as simply a passive relay station, since it has many of the same characteristics that originally implicated the LA as the main site for fear learning. In fact, the CeA receives projections from the auditory cortex[20] and the thalamus[27], raising the possibility that it could receive direct CS input. It also gets somatosensory (US) information from the insular cortex[20] and from the parabrachial nucleus, which transmits pain information[77,78]. High frequency stimulation of thalamic inputs induces an N-methyl-D-aspartate-receptor (NMDA) receptor-dependent long-term potentiation (LTP) in the CeA[79-81] and inactivation of the CeA during fear conditioning or local blockade of NMDA receptors results in impaired acquisition of responses[82,83]. This is strong evidence that activity-dependent plasticity in the CeA is necessary for acquisition of fear conditioning[79,84].

While the original model proposed direct projections from the LA to the CeA, it was pointed out that there is no direct link between the LA and the CeM[85], highlighting a very important role for CeL GABAergic neurons in relaying CS information to the CeM.

The CeM is the main output station for the expression of conditioned fear as the CeM projects to the ventrolateral periaqueductal grey (vlPAG), mediating the freezing response[43,86], to the dorsal vagal complex (DVC), modulating cardiovascular response[87], and the lateral hypothalamus (LH), regulating blood pressure[43]. CeM-PAG projecting cells receive direct CeL oxytocin-receptor expressing neurons projections, while CeL oxytocin receptor negative neurons innervate CeM-DVC output cells[87] (Figure 1.3). Since the CeM output neurons are under tonic inhibitory control of the CeL, a model in which the CeL to CeM inhibition or disinhibition could modulate the CeM output after fear conditioning has been proposed. Bilateral optogenetic-based activation of the CeM induced strong and reversible freezing responses, in a similar way to inactivation of the CeL, proving that the CeM is necessary and sufficient for driving freezing behaviour and the CeM is under tonic inhibition of the CeL[88]. Bilateral inactivation of the CeA and the CeL during the learning phase results in a memory deficit during the retrieval. The same expression deficit was observed with inactivation during the retrieval of the CeA and the CeM, not the CeL. This data indicates a functional dissociation of the CeL and the CeM during acquisition/expression of fear conditioning and an activity dependent neuronal plasticity in the CeL.

1.2.1.5 The role of CeL PKCδ and Sst neurons in fear conditioning

The CeL is an essential component of the neuronal circuit of fear conditioning and contains two functionally distinct neuronal subpopulations forming local inhibitory circuits which inhibit the CeM output neurons. One population acquires CS excitatory responses (CeL_{ON} neurons), while another, largely overlapping with PKCδ positive neurons, displays strong inhibitory response after conditioning (CeL_{OFF} neurons). CeL_{OFF} neurons project to CeM cells projecting to the PAG, inhibiting the output and regulating conditioned freezing (Figure 1.3). CeL_{ON} cells receive glutamatergic inputs, involved in synaptic plasticity, from various brain structures including the BLA, insular cortex and brainstem, in particular from the parabrachial nucleus[79].

Afferents from the PBN make very strong synapses onto the CeL[89] neurons and could function as a signal enabling the induction of synaptic plasticity at other inputs. PKCδ neurons (CeL_{OFF}) activity is inversely correlated with the activity of CeL_{ON} units, suggesting reciprocal inhibition. Exposure to the CS not only inhibits CeL_{OFF} unit spiking but also increases CeM unit activity, with a short latency, implying an inhibitory connection. Moreover, genetic silencing of PKCδ neurons generates a statistically significant enhancement of conditioned freezing[90] without affecting CeL_{ON} cells. The presence of reciprocal inhibitory connections between CeL_{ON} and CeL_{OFF} neurons suggests that when the CS is presented, the excitation of the CeL_{ON} cells causes inhibition of CeL_{OFF} neurons, resulting in the disinhibition of CeM fear output neurons. Once the role of the CeL_{OFF} cells was elucidated, the CeL_{ON} cells were identified as Sst positive. Sst neurons constitute a major CeA population and are intermingled with Sst negative neurons, the majority of which are PKCδ positive. Fear conditioning potentiates excitatory synaptic transmission onto Sst CeL neurons, while weakening that into Sst CeL negative neurons, largely through a presynaptic mechanism in synapses driven by inputs from the LA[91]. Reversible silencing of Sst neurons in the CeA during the learning phase of fear conditioning causes a reduction of freezing, while optogenetic activation elicits freezing behaviour[91]. CeL neurons exhibit mutual inhibition and fear conditioning-induced synaptic modifications cause Sst (CeL_{ON}) neurons to be preferentially activated. Once activated, Sst neurons are sufficient to release fear responses, inhibiting the CeL output (CeL_{OFF}) without inhibiting PAG-projecting CeM neurons. The experience-dependent potentiation of excitatory synaptic transmission onto Sst CeL neurons is crucial, since fear memory is stored and enables the expression of conditioned fear, while its suppression severely impairs fear memory[91].

Recent studies indicated that the CeL, in addition to gating the activity of the CeM to induce fear expression, also sends long-range projections to the PAG and the paraventricular nucleus of the thalamus (PVT), two areas involved in defensive behaviours. These neurons, predominantly Sst positive, can directly inhibit PAG neurons, and display an excitatory synaptic plasticity during fear conditioning, participating in fear learning and regulating fear expression independently of the CeM[92].

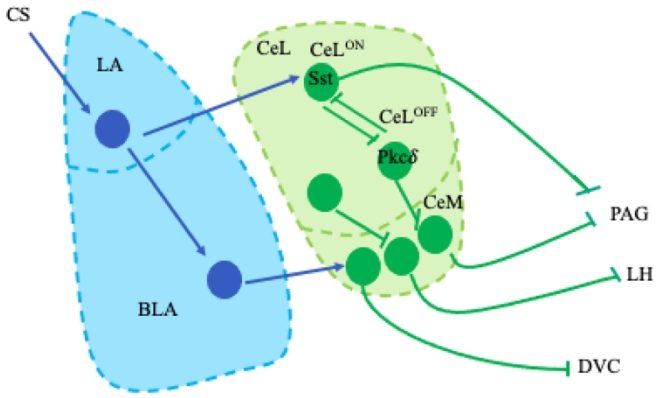

Figure 1.3: Model of the amygdala fear conditioning circuit

Information about the CS from the LA is sent to the CeA via two distinct routes: BLA glutamatergic projections to the CeM, and LA glutamatergic neurons to Sst CeL_{ON} cells. Sst CeL_{ON} GABAergic neurons inhibit PKCδ CeL_{OFF} cells, releasing the inhibition on CeM neurons. The concomitant increase in neuronal activity of CeL and CeM neurons generates freezing behaviour, through inhibition of the PAG, and an increase in blood pressure and heart rate, through the LH and DVC.

1.2.1.6 Passive and active defensive behaviour

CeA^{Sst} neurons are essential for the acquisition and recall of conditioned freezing behaviour, an index of defensive responses. To further investigate the contribution of this subpopulation in the generation of defensive behaviour, mice were tested in a conditioned lick suppression task in which a CS, predicting a noxious US, suppresses water licking in water-deprived mice[53]. Sst neurons become responsive to threat-predicting sensory cues (CS) in a learning-dependent manner, and their activation suppresses ongoing actions (licking) converting an active defensive behaviour to a passive response. Conversely, inhibition of the same neurons promotes active defensive behaviour. CeA^{Sst} neurons control the behavioural output of an animal: high activity induces passive actions, such as freezing and lick suppression, while low activity induces active responses, such as running or active avoidance. Thus, CeA^{Sst} neurons acquire learning-dependent sensory responsiveness and their activity needs to be adjusted flexibly for the expression of adaptive defensive behaviours[53] . It would be of great interest to manipulate the CeL^{Sst} and CeM^{Sst} independently to investigate which subregion is responsible for defensive behaviour.

1.2.2 Central amygdala and innate behaviour

1.2.2.1 Homeostatic and hedonic feeding

Feeding is a complex behaviour essential for an organism's survival and central regulation of food intake is a key mechanism contributing to energy homeostasis. In addition to survival and basic metabolic processes, feeding can also be driven just by the reward, or the sensory perception of pleasure[93].

The hypothalamus is the best studied brain region in the neuronal control of appetite and metabolism. Within the arcuate nucleus, two genetically distinct neuronal populations positively and negatively influence feeding behaviour: agouti-related peptide (AgRP) neurons that promote feeding, weight gain[94] and intense food-seeking behaviour[95], and anorexigenic pro-opiomelacortin (POMC) neurons that, when activated, avoid eating and generate weight loss[96,97]. AgRP neurons are inhibited by leptin, a hormone predominantly made by adipose cells, and activated by ghrelin, released mainly by the stomach, while the opposite happens for POMC cells[98].

The most studied brain regions promoting motivated food consumption and processing the hedonic value of the food are the ventral tegmental area (VTA), the nucleus accumbens (NAc) and the LH, with the VTA and the NAc forming the mesolimbic dopamine system. Dopamine signalling, in addition to its role in reward, is a critical component of voluntary feeding and motivated behaviour. Intracranial self-stimulation of regions of the dopamine system has often been found to promote feeding[93]. The LH was historically treated as a feeding centre, since its ablation produces starvation[99], whereas electrical stimulation elicits feeding[100]. Recently it has been shown that the inhibitory projections from the BNST to the glutamatergic LH neurons promotes high-caloric food consumption and self-stimulation behaviour[101]. Conversely, inhibition of the connection between NAc and LH GABAergic neurons suppresses hedonic feeding[102]. Moreover, activation of the GABAergic innervation of the LH to the VTA supports positive reinforcement and place preference, increasing dopamine release in the NAc[103].

Although the homeostatic and hedonic circuits are often treated independently, there are functional and anatomical overlaps that imply considerable interaction between the two and require further investigation.

1.2.2.2 The central amygdala and feeding behaviour

The role of the CeA in regulating feeding has been uncertain for a long time[104,105]. Infusion of the CeA by different neuromodulators, including the ones regulating the melanocortin system or opiod signaling, has been found to modulate food intake[106-108]. Nevertheless, CeA lesion studies reported very conflicting results[109,110] pointing out the importance of manipulating different CeA cell types independently.

Once the connection between CGRP neurons in the PBN and the CeA was described as being involved in appetite suppression[67], further investigations of the CeA-targeted neurons suggested the involvement of a subpopulation of GABAergic cells expressing PKCδ in the CeL[104]. PKCδ cells are activated by different anorexigenic signals like lithium chloride, cholecystokinin and lipopolysaccharide, as well as by bitter tastants and satiety. Optogenetic-based activation of the PKCδ positive neurons drastically reduced feeding in mice that had been deprived of food for 24 hours, while optogenetic inhibition caused a significant increase in feeding in satiated mice[104].

To investigate which output brain regions could be involved in exerting this inhibitory influence on feeding, anterograde tracing experiments were conducted that revealed that PKCδ neurons project locally to PKCδ negative neurons in the CeA (to both the CeL and the CeM), and with long range projections to the bed nucleus of the stria terminalis (BNST) and the lateral parabrachial nucleus (LPB)[104]. Optogenetic activation of the two projections did not show any effect on feeding behaviour. However, food intake during inhibition of PKCδ negative cells in food deprived mice was partially but significantly inhibited[104]. Since the CeA is involved in regulation of fear and anxiety, aversive states are considered to be a cause of reduced appetitive behaviours like feeding. Activation of PKCδ neurons was performed during fear and anxiety paradigms resulting in an anxiolytic effect[104]. These data suggest that PKCδ neurons have a central role in mediating the inhibitory influence on feeding through a local CeA inhibitory circuit and represent the first inhibitory relay in the central processing of inhibitory influences on food intake[104].

Recently, a GABAergic population of CeA neurons expressing Htr2a but not PKCδ was identified[2]. Optogenetic and chemogenetic-based manipulations of Htr2a neurons showed the

opposite feeding behaviour as compared to that seen in PKCδ neurons. Activation of Htr2a cells promotes feeding in satiated mice, and their inhibition reduces food consumption during food deprivation. Moreover, chemogenetic activation in fasted mice decreases the anorexic properties of LiCl and LPS and also rescues the effect of bitter food. Ablation of CeA^{Htr2a} neurons did not change the daily food intake or the weight of the mice given *ab libitum* food[2], suggesting, together with the previous data, that their role is not in maintaining energy homeostasis, but in modulating the rewarding properties of food and their activity is intrinsically positively reinforcing. Given that Htr2a and PKCδ neurons both reside in the CeA, the local circuit interaction was investigated. Htr2a neurons were found to receive input from PKCδ and Htr2a cells in similar proportions. Moreover, PKCδ neurons receive monosynaptic inputs from Htr2a, revealing a reciprocal connection within the CeA[2].

Since the PBN was already found to have a role in appetitive suppression, the long-range projections of Htr2a neurons to this brain region was studied, revealing that inhibition of PBN neurons mediated by Htr2a is positively reinforcing and modulates food consumption. Furthermore, Htr2a neurons partially function through local inhibition of PKCδ neurons and partially through inhibition of neurons in the PBN, leading to sustained eating behaviour via both local and long-range circuit mechanisms[2].

The functional antagonism of rewarding Htr2a neurons and anorexigenic PKCδ neurons implicates the CeA in the control of antagonistic consummatory behaviours via reciprocal inhibitory connections between defined CeA cell types. An additional CeA subpopulation, prepronociceptive-expressing cells (Pnoc) having little co-expression of both PKCδ and Htr2a neurons, was shown to be involved in food consumption.[111]. Using genetic, electrophysiological and behavioural approaches, a new CeA circuit necessary for regulation of hedonic but not homeostatic feeding was described[111]. Inhibition of the Pnoc subpopulation decreases palatable food consumption and ablation reduces high-fat-driven increases in bodyweight and adiposity. Interestingly, activation of Pnoc cells or their terminals does not promote feeding, suggesting their role in promoting the reinforcing properties of calorically dense, palatable food[111].

1.2.2.3 The central amygdala and prey hunting behaviour

The already known role of the CeA in food intake[2], the evidence of neuronal activation in the CeA during prey hunting[112] and the fact that CeA neurons densely project to brainstem premotor circuits involved in craniofacial control[113,114], made the CeA a possible brain region to investigate predatory hunting. Optogenetic and chemogenetic-based activation of CeA neurons promotes predatory-like attacks upon artificial and real prey. Manipulation of CeA projections to the midbrain PAG matter is fundamental to initiate prey pursuit, such as predator stalking and running toward prey. Projections to the brainstem reticular formation are instead necessary for positioning lethal bites on prey[115]. Currently, the role of CeA subpopulations in hunting is unknown.

1.2.2.4 The central amygdala and innate fear

Fear is a powerful emotion that greatly influences animal behaviour and can be induced by innate and learned mechanisms. These two kinds of fear can be experienced simultaneously and are regulated by distinct neural pathways[116] that need to have potential interactions to integrate the final information and generate the appropriate behaviour for survival.

Innate fear is conserved and acquired over the course of evolution, while learned fear is mutable and depends on individual's fearful experiences. Animals can experience these two types of fear simultaneously and, if the risk levels of both fears are comparable, usually innate fear has priority over the learned fear. The central amygdala works as an integrator for both olfactory mediated innate and learned fear. Recently it has been shown that Htr2a expressing cells control both as a hierarchy generator, prioritising innate over the learned fear[117]. In order to test innate and learned fear simultaneously, a new behavioural paradigm was applied: mice were food deprived and food pellets were placed at both ends of the two arms of a Y-maze and presented with an innate fear inducing odorant in one arm, and a learned fear inducing odorant, previously paired with electric foot shocks, in the other[117]. Normally mice eat the food in the arm with the learned fear inducing odorant, prioritizing innate over learned fear. Inhibition of Htr2a cells in the CeA significantly upregulates the innate freezing response, while activation significantly downregulates it.

It has already been demonstrated that learned freezing behaviours are controlled by the ventral periaqueductal gray (vPAG)[118,119] while innate avoidance and risk assessment behaviours are

regulated by the dorsal periaqueductal gray (dPAG)[120,121], making them two possible important regions controlling innate and learned freezing. Inhibition of Htr2a cells in the CeA increased both innate freezing and the expression of immediate early genes in the dPAG while decreasing it in the vPAG. Previous experiments showed that Htr2a cells regulate the hierarchical relationship between innate and learned freezing responses, in which the former predominates. Innate-fear inducing odorants suppress learned fear responses through the activity of Htr2a cells[117].

1.2.3 The central amygdala in emotional and sensory regulation

1.2.3.1 Central amygdala PKCδ neurons and anxiety

Anxiety is defined as an inappropriate fear reaction to specific stimuli or to less specific and more generalized states of apprehension and vigilance[122]. Fear and anxiety are two different defensive behavioural programs: mice presented with an immediate and predictable threat respond with freezing or flight-or-fight responses, while unspecific cues for threat predictions promote avoidance and risk assessment behaviour[123]. The central amygdala has been proposed to have a role in anxiety, in particular, optogenetic stimulation of BLA terminals in the CeA has an acute, reversible, anxiolytic effect while inhibition of the same projections increases anxiety-related behaviour. The same effects were not observed by directly manipulating the soma of the same cells in the BLA. Thus, a selective glutamatergic BLA projection to the CeA can promote anxiolysis[124].

Anxiety states are often associated with fear generalisation - the generation of acute fear responses to stimuli that do not predict an aversive outcome. Fear responses have been studied using an auditory fear conditioning paradigm in which animals learn to associate an initially neutral stimulus (CS, such as a tone) with an aversive unconditioned stimulus (US, such as a foot shock). In anxiety disorders the discrimination between a CS paired with a US (CS^+) and a non-paired CS (CS^-) is diminished. PKCδ neurons seem to be a key element in neuronal circuitry controlling anxiety. To prove this, mice underwent discriminative fear conditioning and were tested 24 hours later with contemporary activation of PKCδ neurons, resulting in an increased fear generalisation result, calculated as the ratio between CS^- and CS^+ freezing[123]. The same mice tested in the elevated plus maze (EPM) during PKCδ activation spent less time in the open arms, corresponding to an anxiogenic effect, whereas inhibition was anxiolytic[124].

Therefore, in the CeA there are two subpopulations of neurons that modulate anxiety in an opposite way[123,124].

1.2.3.2 Central amygdala PKCδ and Sst neurons and pain

Pain perception is essential for survival and the brain can influence behavioural responses in opposite ways to different painful stimuli. The CeA receives nociceptive inputs via the spino-ponto-amygdaloid pain pathway[77,125] and from the PBN [126], as well as affective and cognitive information from the BLA. In recent years, the CeA has been described as a nociceptive centre ideally positioned to link experience, context and emotional states with behavioural responses to painful stimuli[50,127,128]. A recent study focused on the role of two CeA non overlapping populations, PKCδ and Sst neurons, demonstrating that the CeA can function as a pain rheostat, attenuating or exacerbating pain-related behaviours in mice.

Using a sciatic nerve cuff model of neuropathic pain, it was shown that the dual and opposing function of the CeA is encoded by opposing injury-induced changes in the excitability of PKCδ and Sst neurons: PKCδ cells increase firing, while Sst cells decrease excitability following injury. Moreover, activation of PKCδ neurons increases pain (pronociception) and activation of Sst neurons decreases it (antinoception) showing an opposing function in the modulation of pain-related behaviours[129]. Recent *in vivo* calcium imaging and optogenetic experiments revealed a distinct population of GABAergic CeA neurons activated by general anaesthesia. Optogenetic activation or inhibition of these neurons regulates pain-related behaviours bidirectionally, decreasing or increasing the pain sensation in mice, respectively. The general anaesthesia neurons partially overlap with PKCδ and proenkaphalin1 (Penk1) positive neurons. However, a specific subset of neurons involved in general anaesthesia was not found, opening the possibility of the involvement of a heterogeneous ensemble of CeA neurons. These results demonstrate the important role of the CeA in both pain and analgesia, revealing a previously unknown mechanism underlying the bidirectional control of pain in the brain[130].

1.2.4 Physiological regulation of fluid intake and thirst

1.2.4.1 Fluid homeostasis

Fluid satiation is a critical homeostatic signal to stop drinking, preventing potentially lethal consequences of overhydration. Fluid homeostasis is crucial in maintaining the correct cell size required for proper functionality and stable blood volume and pressure, which is required to transport nutrients and oxygen around the body[131]. An increase in blood osmolarity of just one percent can trigger the sensation of thirst, a sensation that is sufficient to motivate the animal to find and consume water. Animals, in fact, can sense their changing of internal needs and generate the correct behavioural response to restore homeostasis[131]. To maintain homeostasis and ensure survival, physiological imbalances produce motivational drives, specific goal-directed behaviours that vary in duration, intensity and valence[132-136]. This is in agreement with the 'drive reduction' hypothesis that states that animals learn particular behaviours in order to reduce the level of an aversive drive state[137].

For wild animals, water is not always immediately available and looking for it could require taking a risk, or sacrificing other vital behaviours like mating or feeding. For this reason, water seeking is a motivated behaviour, and the animals need to weigh survival demands and environmental risks in order to meet these goals. Thirst motivates water seeking and consumption both by a positive and negative valanced mechanism. While thirst is an aversive state and animals are motivated to work to suppress this aversive feeling[138], fluid satiation is extremely pleasant, particularly after dehydration[139]. Another key component for fluid homeostasis is salt (NaCl), the major osmotic component of the extracellular fluid (ECF)[140,141]. An animal is fully satiated when both water and NaCl have been replenished.

Signalling regarding fluid status derives from three different preabsorptive inputs: predictive cues, oropharyngeal inputs, and oesophageal and gastric inputs. Placing a water bottle in a cage of a thirsty mouse rapidly inhibits calcium activity in thirst-related neurons in the supraoptic nucleus before drinking has commenced suggesting that these neurons receive signalling about water-predicting cues[142]. Inputs from the oral cavity and the stomach also signal fluid satiation, so it appears to be a combination of signals in an appropriate temporal sequence for fluid satiation, most likely carried by the vagal nerve[143]. Longer term, fluid absorbed into the systemic circulation and reduction of plasma osmolarity restores fluid homeostasis, which is

detected by postabsorptive signals such as baroreceptors, osmoreceptors, and sodium sensors, which further diminishes fluid and salt intake when water is in excess[140,144,145].

The amount of fluid ingested reaches the central nervous system where the activity of different neuronal populations, initially identified by lesions, pharmacological and immunohistochemical studies of Fos expression[140,141]. Recently, similar experiments have been carried out by designer receptors exclusively activated by designer drugs (DREADD) and optogenetic-based manipulation to prevent or decrease fluid intake. The fluid satiation neural circuit partially overlaps with that of thirst, and there is an interplay of signals within brain regions as well as within different neuronal populations in the same brain region.

1.2.4.2 Thirst regulation

The nucleus of the solitary tract (NTS) and area postrema (AP) receive peripheral inputs about the body's fluid status[146] and mediate fluid satiation. Lesions of these regions increase water and salt intake[147], while activation suppresses both of them[148]. Neurons from the NTS project to the PBN, a key brain region in the regulation of fluid intake. Injection of antagonists, for example methysergide a serotonin receptor antagonist, or proglumide, a cholecystokinin antagonist, increases salt and water intake[149].

Recently, a subpopulation of neurons in the PBN expressing oxytocin-receptor (Oxtr) was characterised as a key regulator of the fluid satiation neurocircuit, having very rapid neuronal responses due to the preabsorptive information it receives via the NTS[148], acting to decrease water intake in order to prevent hypervolemia. Activation of Oxtr-neurons decreases noncaloric fluid intake, but not food intake, after fasting or salt intake after salt depletion. Conversely, inactivation increased saline intake after dehydration and hypertonic saline injection[148]. This effect is similar to intra-PBN injections of methysergide and proglumide, suggesting possible co-expression of these receptors.

Both the NTS and PBN project to the CeA and BNST, an integrative centre of visceral and somatic sensory regions[150,151]. Electrolytic lesions of the CeA and BNST in rats decrease salt but not water intake and these two regions express Fos after sodium depletion[152-154]. NaCl

intake is mediated by endogenous opiods in the CeA, since injection of opioid receptor antagonist decreases NaCl intake[155], which is instead increased by PBN deactivation[156].

The paraventricular hypothalamic nucleus (PVH) and the supraoptic nucleus (SON) contain magnocellular neurons expressing vasopressin and oxytocin[157]. Once osmolarity increases, oxytocin and vasopressin act to restore fluid homeostasis increasing antidiuresis and sodium excretion. Oxytocin-expressing neurons in the PVH (Oxt^{PVH}) decrease water intake when activated with a milder effect compared to $Oxtr^{PBN}$ activation, since only a subset of these neurons is activated[148].
A major forebrain region coordinating fluid intake is the lamina terminalis that, thanks to three nuclei: the subfornical organ (SFO), the organum vascolosum of the lamina terminalis (OVLT), and the median preoptic nucleus (MnPO)[140,158]; primarily signals thirst and increases fluid and salt intake when activated.

Activation of MnPO neurons motivates mice in water-satiated conditions to perform an operant task, where lever pressing leads to a unit of water reward. Experiments of real time place preference revealed the mice avoid the chamber paired with photoactivation of the same neurons, in line with the classical theories of learning and motivation, suggesting that deviations from homeostatic points are aversive and animals perform motivated behaviour to reduce these aversive states. SON vasopressin neurons projecting to the posterior pituitary (VP_{PP} neurons) decrease activity after mice are presented with water-predicting cues and after mice drink the water. Conversely, their activity increases upon food availability following food restriction[142].

Drinking water in response to thirst, for example following fluid loss, is a pleasant experience, while drinking water after thirst has been satiated is unpleasant. Functional MRI experiments in humans showed that the pleasantness of drinking is associated with activation in the anterior cingulate cortex and the orbitofrontal region, while the unpleasantness of overdrinking with activation in the midcingulate cortex, insula, amygdala and periaqueductal grey[139]. The initiation of drinking is triggered by water depletion, while drinking is terminated quickly when animals have ingested a sufficient amount of water[159]. For such accurate fluid regulation, the brain needs to check internal water balance and fluid ingestion on a real-time basis[160,161]. The lamina terminalis is the principal brain structure for sensing and regulating this internal water balance[158,162]. The SFO and the OVLT are two major osmosensory sites, due to the lack of the

normal blood-brain barrier and direct contact with the peripheral system. Optogenetic and chemogenetic-based activation of excitatory nitric oxide synthase positive neurons in SFO (SFO^{nNOS}) drives immediate drinking behaviour[163], while stimulation of inhibitory cells suppresses water intake[164].

MnPO GABAergic neurons that express glucagon-like peptide 1 receptor (GLP1R) are activated upon drinking and inhibit SFO thirst neurons. The responses are induced by the ingestion of fluids but not food and are time-locked to the onset and offset of drinking. Loss of function of the same neurons lead to an overdrinking phenotype. These neurons facilitate satiety of thirst by monitoring real-time fluid ingestion. While the main brain regions involved in fluid homeostasis have been identified it would be important to understand how this neural circuitry interacts with feeding and other ingestive behaviours and what impact it has on the motivational and reward systems.

The role of the CeA in drinking is not clear. A previous publication demonstrated that inhibition of CeL^{Sst} neurons in water deprived mice reduces water intake[3], but no gain of function experiments were performed, and no further investigation of other CeA subpopulations was undertaken. In this thesis work, I will investigate the role of different CeA neurons in the CeL and CeM in drinking.

1.7 Advanced behavioural manipulation and *in vivo* imaging

1.7.1 Optogenetic manipulation

The ability to activate and silence genetically specified neurons in a temporally precise fashion provides scientists with the opportunity to investigate the causal role of specific neuronal populations in mouse behaviour[165]. Transiently perturbing neuronal activity in specific circuits and observing the consequences on behaviour is an increasingly powerful approach[166,167]. Optogenetic-based manipulation integrates genetic targeting and optical stimulation to achieve temporally precise manipulation of genetically and spatially defined cell types[168] and raises the possibility of testing whether specific cells and projections are necessary or sufficient for initiating or altering animal behaviour[169].

Optogenetic-based manipulation uses light-sensitive transmembrane proteins, opsins, that respond to light either by pumping ions into or out of the cell or by opening an ion channel. The expression of these molecules makes it possible to silence or activate neurons in response to light. Halorhodopsins and archaerhodopsins are used for optical silencing[170], while channelrhodopsins are used for optical activation[171]. Microbial-type rhodopsins represent membrane ion transport proteins; channelrhodopsin-1 (ChR1) and ChR2 are light-gated proton channels from the green alga *Chlamydomonas reinhardtii*. This channel opens rapidly after absorption of a photon to generate a large permeability for monovalent and divalent cations causing cell depolarization simply by illumination[172]. Recently, the channelrhodopsin protein was modified to change from an unspecific cation channel into a chloride-conducting channel, and the selective chloride-conducting-channelrhodopsin iC ++ was developed and found to be very efficient for optical inhibition of neurons. The archaeal light-driven chloride pump (NpHR) from *Natronomonas pharaonic* allows temporally precise optical inhibition of neuronal activity, through either knockout of single action potentials or sustained blockade of spiking[173]. The gene archaerhodopsin-3 (Arch)[174] from *Halorubrum sodomense* enables near-100% silencing of neurons when virally expressed in the mouse brain and illuminated with yellow light. It recovers from light-dependent inactivation, unlike other chloride pumps that enter long-lasting inactive states following light stimulation[165]. While optogenetic activation of long-range projecting axons is temporally precise[175], silencing of these connections has always been ineffective[176]. Halorhodopsin only partially suppresses neurotransmitter release, archeorhodopsin triggers an elevated spontaneous neurotransmission[177], and both require continuous light to sustain their activity[173]. In order to solve this issue, a mosquito-derived homolog of the mammalian encephalosin/panopsinprotein (OPN3) was optimised to be expressed in neurons. The targeting-enhanced OPN3 (eOPN3) protein was shown to suppress synaptic release in the mouse hippocampus, cortex and mesencephalus, having robust behavioural effects[177].

Opsins are fused to fluorescent proteins to facilitate their visualization and delivered via a virus that infects broad sets of cells or more specific subpopulations that express the Cre recombinase. In this case, the gene of interest is flanked by lox sites in the virus so that the Cre causes the deletion of a stop sequence or reverses the gene sequence from a backward-to-forward direction[178]. Adeno-associated viruses express opsins under cell specific promoters, such as synapsin-1 for neurons, or simply pancellularly, for example the CAG[179] promoter, to infect some cell types preferentially over others. Devices that deliver light, such as implanted

optical fibres, need to reach the deep target and experiments are commonly performed at least four weeks after viral delivery.

1.7.2 *In vivo* calcium imaging

The brain orchestrates a wide array of functions, from perceiving the outside world to coordinating behaviour and preserving past experiences. To do this, neurons interact with each other to form circuits with the capability to mediate sensory information into the appropriate behaviour outcome.

One approach to monitoring circuit-specific activity dynamics is *in vivo* calcium imaging. During periods of increased neuronal activity, dynamic fluctuation of calcium levels can be monitored with genetically encoded calcium indicators, such as GCaMP[180,181]. Neuronal activity causes rapid changes in intracellular free calcium. Calcium imaging experiments rely on this principle to track the activity of neuronal populations. Genetically encoded protein sensors can be targeted to specific cell types to study neuronal activity over time[180]. Multiple rounds of structure guided design have made the single fluorophore sensor GCaMP the most widely used protein calcium sensor. GCaMP consists of circularly permuted green fluorescent protein (cpGFP), the calcium-binding protein calmodulin (CaM) and CaM-interacting M13 peptide. CaM-M13 complex is in proximity to the chromophore; calcium-dependent conformational changes in CAM-M13 cause increased brightness with calcium binding[180]. Calcium concentration, inside the cell, transiently rises during neuronal activity and this can be measured by an increased fluorescent signal that indicates changes in neuronal activity.

Imaging of neuronal activity using *in vivo* two-photon microscopy provides unprecedented cellular and subcellular spatial resolution but with the great limitation that the imaging must be performed in head-fixed mice, greatly impairing the assessment of naturalistic behaviour[182]. Two new methods for using freely moving mice have been developed to try to bypass this problem: mini-epifluorescent microscopes used in conjunction with gradient index (GRIN) lens microendoscopes[183] and fibre photometry[184,185]. Both systems take advantage of devices that are small enough to fit on an animal's head and light enough to be carried. Moreover, they are capable of recording neuronal activity many millimetres deep within the brain. Mini-epifluorescent microscopes allow repeated measures of somatic calcium activity dynamics of

hundreds of genetically and spatially defined neurons in a single animal[183]. Fibre photometry uses optical fibres to detect bulk changes in calcium mediated fluorescence in the soma or terminals of genetically defined neurons[184]. Although this method lacks cellular resolution, it can provide interesting insights into the synchronous activity dynamics within a microcircuit. However, with the help of calcium imaging techniques, it is possible to gain an insight into the endogenous activity of specific neurons during behaviour.

1.7.3 Intersectional genetics

Optogenetic manipulations and calcium imaging in specific neuronal populations depend on the selective expression of genetically encoded tools in the subpopulation of interest. Moreover, the improvement of transcriptomic and connectomic techniques has highlighted that one neuronal subpopulation is often defined by multiple features, not only one. To overcome this difficulty, a new technique, called INTRSECT was developed, where scientists generated adeno-associated viruses (AAV) with two orthogonal recombinase (Cre and Flp) recognition sequences in synthetic introns in order to allow their expression when just two defined parameters are expressed in the cells[186]. For example, EYFP or ChR2-EYFP expression can be restricted to cell populations depending on Cre and Flp recombinases: one or two introns are inserted into a gene with one or two reading frames and the starting configuration of the exons, together with the recombinase recognition sites (lox and FRT), determine which combination of Cre and Flp is necessary for the expression of the virus. Finally, the introns containing the recombinase sites can be removed during mRNA splicing allowing the protein to be expressed and functional. In addition to EYFP and ChR2-EYFP, many other fluorescent proteins, calcium indicators, and excitatory and inhibitory opsins have been developed. Cre ON-Flp ON (Con/Fon) vectors guarantee expression only in the presence of both recombinases, while the Flp and NOT Cre (Coff/Fon) vectors are expressed in the presence of the Flp but not the Cre, and the Cre and NOT Flp (Con/Foff) in the presence of the Cre but not the Flp[186] (Figure 1.4). Thanks to this intersectional approach, multiple-feature-dependent optogenetic inhibition and excitation and *in vivo* imaging will be possible.

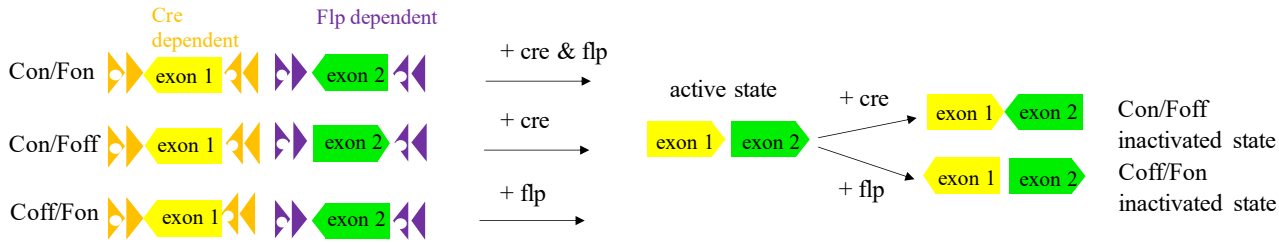

Figure 1.4: INTRSECT

Single intron intersectional construct for a single open reading frame (ORF) in three designs: Cre and Flp, Cre and NOT Flp, Flp and NOT Cre. Activity of the Cre and Flp recombinases to move the single configurations to the active and inactivated states.

2. Materials and methods

2.1 Animals

Htr2a-cre (STOCK Tg[*Htr2a-cre*] KM208Gsat/Mmucd) and *PKCδ-cre* (Tg(Prkcd-glc-1/CFP,- Cre)EH124Gsat) BAC transgenic lines were imported from the Mutant Mouse Regional Resource Center. *SOM-IRES-cre* (SSTtm2.1(cre)Zjh/J) mice were acquired from The Jackson Laboratory. TdTomato (B6.Cg- Gt(ROSA) 26Sortm9(CAG- tdTomato)Hze/J) [187], FPDI (B6;129S6Gt(ROSA)26Sortm9 (CAG-mCherry, -CHRM4*)Dym)[188], and FL-hM3Dq (B6.Cg-Gt(ROSA)26Sortm3.2(CAG-EGFP,CHRM3*/mCherry/Htr2a)Pjen)[189] were as described previously. Wfs1-flpER BAC transgenic mice were generated in our lab. All mice were backcrossed into a C57BL/6NRj background (Janvier Labs - http://www.janvier-labs.com). 3-6 months old male mice were used for the place preference assay combined with optogenetic manipulation of $CeA^{PKC\delta}$ and CeA^{Sst} cells, as well as for the open field task. Eight to 18 months old male and female mice were used for the place preference assay combined with Ca^{2+} imaging of $CeA^{PKC\delta}$ and CeA^{Sst} cells. 4-14 months old males and females were used for the feeding, drinking, and rewarding experiments. Mice were kept on a 12-h light/dark cycle. All behavioural experiments were conducted during the light phase of the cycle.

2.2 Viral constructs

The following AAV viruses were purchased from the University of North Carolina Vector Core (https://www.med.unc.edu/genetherapy/vectorcore: AAV_5-Ef1a-DIO-eNpHR3.0-mCherry, AAV_5-Ef1a-DIO-mCherry, AAV_5-Ef1a-DIO-hChR2(H134R)-EYFP-WPRE-pA, AAV_5-Ef1a-DIO-EYFP-WPRE-pA, AAV_5-hSyn-Con/Fon-hChR2(H134R)-EYFP-WPRE, AAV_5-hSyn-Con/Fon-EYFP-WPRE, AAV_5-hSyn-Con/Foff-hChR2(H134R)-EYFP-WPRE, AAV_5-hSyn-Con/Foff EYFP-WPRE. The AAV_5-Syn.Flex.GCaMP6s virus was obtained from Addgene. AAV_8-nEF-Con/Foff iC++ - EYFP and AAV_8-nEF-Con/Foff – EYFP viruses were provided by the lab of Prof. Dr. Karl Deisseroth, Stanford University, Stanford, California, United States.

2.3 Stereotaxic surgeries

2.3.1 Viral injections

Mice were anaesthetized using isoflurane (Cp-pharma) and placed on a heating pad on a stereotaxic frame (Model 1900 – Kopf Instruments). Carprofen (Rimadyl – Zoetis) (5 mg/kg body weight) was given via subcutaneous injection. Mice were bilaterally (unilaterally only for calcium imaging experiments) injected with 0.3 µl of virus in the CeA by using the following coordinates calculated with respect to bregma: for the CeA and CeL: −1.20 mm anteroposterior, ± 2.87 mm lateral, −4.65 to -4.72 mm ventral; for the CeM −1.155 mm anteroposterior, ± 2.87 mm lateral, −4.65 to -4.72 mm ventral. Virus was allowed to be expressed for a minimum duration of 3 weeks before histology or behavioural paradigms. For animals not undergoing implant surgery, the incision was sutured.

2.3.2 Optic fibre implants

Mice used in optogenetic experiments were, immediately after viral injection, implanted with optic fibres (200-µm core, 0.22 NA, 1.25-mm ferrule - Thorlabs) above the CeA (−4.35 mm ventral from bregma). The skull was first protected with a layer of histo glue (Histoacryl, Braun), the fibres were then fixed to the skull using UV light-curable glue (Loctite AA3491 - Henkel) and the exposed skull was covered with dental acrylic (Paladur - Heraeus).

2.3.3 GRIN lens implantation and baseplate fixation

Three weeks after GCaMP6s viral injection in the CeA, mice were implanted with a gradient index (GRIN) lens. At the same coordinates of the injection, a small craniotomy was made and a 20G needle was slowly lowered into the brain to clear the path for the lens to a depth of -4.5 mm from bregma. After retraction of the needle, a GRIN lens (ProView lens; diameter, 0.5 mm; length, ~8.4 mm, Inscopix) was slowly implanted above the CeA and then fixed to the skull using UV light-curable glue (Loctite AA3491 - Henkel). The skull was first protected with histo glue (Histoacryl, Braun), and the implant fixed with dental acrylic (Paladur - Heraeus). 4 to 8 weeks after GRIN lens implantation mice were “baseplated”: under anaesthesia. Briefly, in the stereotaxic setup, a baseplate (BPL-2; Inscopix) was positioned above the GRIN lens, adjusting the distance and the focal plane until the neurons were visible.

The baseplate was fixed using C&B Metabond (Parkell). A baseplate cap (BCP-2, Inscopix) was left in place to protect the lens.

2.4 Behaviour

2.4.1 Conditioned place preference

For the conditioned place preference behaviour, we used a custom-built arena made of a rectangle-shaped chamber (45x15 cm) and a triangle shaped chamber (45x30 cm), that differed in the texture of the floor and pattern on the walls, separated by a corridor.
During the first day the mice could explore the arena for 20 min; we considered the least preferred chamber to be the one in which they spent less time and we paired this chamber (context+) with food during the following training days. The mice were food restricted and maintained at 85% of their initial body weight for all days of the behaviour experiments. During the next four days, mice were sequestered in the neutral context (context-) for 15 min and then transferred to the context+ for 15 min where the food pellet was positioned. On the last day of the experiment, mice were allowed to navigate freely in between the two chambers in the absence of food. The preference for the context+ was measured for a period of 10 min as a readout for contextual appetitive conditioning. The animals expressing either eNpH3.0 or mCherry in the CeA and implanted with optic fibres received constant bilateral stimulation of 561-nm intracranial light, during the whole 30 min of the conditioning or during the retrieval test. For this, mice were tethered to optic-fibre patch cables (Doric Lenses or Thorlabs) connected to a 561 nm CNI laser (Cobolt) via a rotary joint (Doric Lenses) and mating sleeve (Thorlabs).

2.4.2 Open field

Mice were allowed to explore a custom-built plexiglas arena (40 cm×40 cm×25 cm) for 10 min. During the whole experiment, mice received constant 561-nm intracranial light bilaterally through optic-fibre patch cords connected to a 561 nm CNI laser.

2.4.3 Drinking behaviour

Mice were bilaterally tethered to optic fibre patch cables (Doric Lenses or Thorlabs) via a mating sleeve (Thorlabs). The patch cables were connected via a rotary joint (Doric Lenses) to a 473nm or 561nm (CNI lasers) laser. Photoactivation was conducted with 10-15mW 10ms, 473nm light pulses at 20 Hz, using a pulser (Prizmatix) controlled by the Ethovision software XT 14 (Noldus). Photoinhibition experiments were conducted with 561nm 15mW constant light. For the water deprivation experiments, mice were water deprived and trained to drink in a 32 cmx35 cm plastic arena for 30 minutes. This training was mainly done to habituate the mice to the new setup and train them to drink from specific pipettes. For the photoactivation experiments, mice were then tested the following two days in the setup with access to water with a sequence of 10 min laser OFF/10 min laser ON and 30 min laser ON/30 min laser OFF or simply for 30 min laser ON. The two experiments were performed in a randomized order. For the experiments in normal conditions, the same protocols were used, but the mice had *ad libitum* water in their cage. For the photoinhibition experiments, mice had access to water for 30 min with constant photoinhibition. The amount of water was manually measured.

2.4.4 Feeding behaviour

The experiments were conducted in a 32 cmx35 cm plastic arena containing two plastic cups in opposite corners, one with precision pre-weighed food pellets (20 mg each). Experiments were conducted over 40 min sessions and the remaining food was weighed. Mice were bilaterally tethered to optic fibre patch cables (Doric Lenses) and connected via a rotary joint (Doric Lenses) to a 473nm (CNI lasers). Photoactivation experiments were conducted with 10-15mW 10ms, 473nm light pulses at 20Hz. The day before the experiment, mice were habituated to the new food by placing some of these pellets into the cage together with the normal food.

2.4.5 Palatable reward consumption

Mice were food deprived for 16 hours and allowed to consume a palatable reward solution (Fresubin, 2kcal/ml) for 30-45 min. The mice went back to *ad libitum* food and the following day were tested for 30 min for Fresubin consumption with constant photoinhibition (561nm, 10mW) for the animals expressing eNpHR3.0 and corresponding controls, and with 20 Hz 473nm photostimulation for the animals expressing IC++ and controls.

2.4.6 Real-time place preference

ChR2-expressing mice and corresponding controls were allowed to freely navigate in a custom-made plexiglas two-chambered arena (50x25x25cm) for 20 min. ChR2-expressing mice and controls received 20 Hz 473nm photostimulation in one compartment. The experiment was repeated for two consecutive days alternating the photostimulated chamber. The laser was controlled with Ethovision XT 14 (Noldus).

2.4.7 Conditioned flavour preference

Water deprived mice, for two consecutive days, were given the choice between two non-nutritive flavoured liquids (0.3 % grape or cherry and 0.15% saccharin) for 30 min. The preferred taste was identified as the taste of the two that the mice drank more of. The conditioning was conducted over four consecutive days with two sessions per day. The least preferred taste was paired with optogenetic activation. In conditioning session one, the least preferred taste was paired with 20 Hz 473nm photostimulation for 15 minutes. In conditioning session 2, the mice were presented with the other taste in the absence of photostimulation. The order of the sessions was inverted each day, occurring 4-6 hours apart. Conditioned flavour preference was tested the day after the final conditioning session, when the mice were presented with both tastes.

2.5 *In vivo* calcium imaging of freely moving mice

All imaging experiments were conducted on freely behaving mice. GCaMP6s fluorescence signals were acquired using a miniature integrated fluorescence microscope system (nVoke – Inscopix) secured in the baseplate holder before each imaging session. Mice were habituated to the miniscope procedure for 3 days before behavioural experiments for 30 min per day. Settings were kept constant within subjects and across imaging sessions. Imaging acquisition and behaviour were synchronized using the data acquisition box of the nVoke Imaging System (Inscopix), triggered by the Ethovision XT 14 software (Noldus) through a TTL box (Noldus) connected to the USB-IO box from the Ethovision system (Noldus). Compressed images were obtained at 1200 pixels by 800 pixels and 10 frames per second using the Inscopix acquisition software (Inscopix). We recorded the activities of CeA neurons during habituation, day 1 and day 3 of conditioning and recall.

2.6 Calcium imaging data analysis

2.6.1 Extraction of ΔF/F and temporal registration with behavioural data

For imaging data processing and analysis, all videos recorded from one imaging session were combined into a single image stack using the Inscopix data processing software (version 1.3.0 – Inscopix) and saved as a tiff. The miniscope 1-photon imaging signal extraction pipeline (MIN1PIPE)[190], which returns fully processed ROI components with spatial footprints and temporal calcium traces as outputs, was used to process the tiff files. The data go through different steps of neural enhancing, hierarchical movement correction, and neural signal extraction that combine a first seeds-cleansing step followed by a simplified spatiotemporal CNMF. Behavioural data were finally temporally aligned to the calcium traces using linear interpolation and unix time stamps as references for both datasets.

2.6.2 Longitudinal registration of ROIs

ROIs from several recording sessions were longitudinally registered using CellReg Matlab GUI[191]. In brief, the roifn output variable from the Min1pipe that contained the processed vectorised ROI footprints for each session was transformed in matlab using:
roi_use = permute(reshape(roifn, pixh, pixw, n), [3, 1, 2]), where n is the number of ROIs.
Transformed ROIs footprints were then registered using CellReg and the following parameters: alignment type: translations and rotations (max rotation in degrees: 30). A maximal distance of 12 microns was used to compute the probabilistic model. The initial and final cell registrations were performed using spatial correlation models. The resulting cell_to_index_map file was used to identify identical ROIs from one day to another, calculating the total number of recorded cells per animal and the number of overlapping neurons during the whole recording session.

2.6.3 Regressors and correlation analyses

Regressors were built as previously described[192]. For this, the behaviour of each mouse in the positive context, food zone or 'on top of the food'(square-wave data sets), was convolved with a kernel with an exponential decay based on the measured half-decay time for GCaMP6s (~0.150 s)[180]. The resulting predicted calcium traces were then used to compute Pearson correlation coefficients with the corresponding calcium traces. To classify neurons as 'memory

cells' or 'food responsive cells', we examined which coefficients arise above chance by correlating our fluorescent traces to 1000 random regressors that were constructed after randomly shuffling the real behavioural dataset by bouts of 10s. A threshold of at least 2.58 deviation from the standard error of the random coefficients mean (corresponding to the 99% confidence interval) was required to assign a cell to a particular functional group.

2.6.4 Classification of neurons preferentially active in the positive context

To quantify which neurons were preferentially active in the positive context compared to the neutral one during conditioning, ΔF/F transients were z-scored at each time point using the following formula: (F(t) – Fm)/SD, where F(t) is the ΔF/F value at a time t, Fm, and SD are the mean and standard deviation of the baseline calculated from time point when the animals were in the neutral context. An average of the single z-scored time points was then calculated for when the animal was located in the positive context. Neurons were considered to be preferentially active in the positive context when the averaged z-scored value exceeded the 1.96 threshold (corresponding to the 95% confidence interval).

2.6.5 Decoding of positive context locations

To decode the location of the mice in the positive context during recall, a logistic regression classifier was used. For decoder training and testing, neuronal Ca^{2+} signals expressed as ΔF/F was used. For each animal, classifiers were trained on 70% of the data during recall and tested on the remaining 30%. We computed the prediction score as the average of correct predictions over a 10-fold cross-validation procedure. Correct predictions were defined as the ratio of TP/(TP+FP+FN) where TP is the number of true positives, FP the number of false positives and FN the number of false negatives.

To evaluate the statistical significance of decoding performance, we trained logistic regression decoders on temporally shuffled behavioural data. For this, behavioural data were split into 7 sec bouts and randomly shuffled. This was repeated five times. The shuffled prediction score was defined as the average of correct predictions of these five repetitions.

2.6.6 Alignment of calcium responses to positive context entries

ΔF/F transients were z-scored with the baseline calculated from time points when the animals were in the neutral context (see formula above in: 2.6.4 Classification of neurons preferentially active in the positive context). We omitted short bouts whose duration was below 2.5 sec to exclude epochs when the animals were only briefly going in and out of the corridor space without properly entering the positive context. Z-scored calcium responses of single neuron to positive context entry were then averaged in a time window from 3 s before transition to 4.5 s after. Cells were finally sorted in descending order based on their activity response upon entry in the context+.

2.6.7 Heatmaps of spatial Ca2+ activity

To plot a heatmap of the average spatial activity of one selected cell we used the raw ΔF/F data. The total activity in a specific x-y location was normalized to the total time the animal spent in that location. x-y data were discretised in 50 x 50 pixels.

2.7 Histology

At the conclusion of experiments, mice were anesthetized with ketamine/xylazine (Medistar and Serumwerk) (100 mg/kg and 16 mg/kg, respectively) and transcardially perfused with phosphate-buffered saline (PBS), followed by 4% paraformaldehyde (PFA) (1004005, Merck) (w/v) in PBS.
Extracted brains were post-fixed overnight at 4°C in 4% PFA (w/v) in PBS, embedded in 6% agarose and sliced using a Vibratome (VT1000S - Leica) into 50-µm free-floating coronal sections.

2.8 Immunohistochemistry

Brain sections were blocked at room temperature for two hours in 5% donkey serum (Biozol JIM-017-000-121) diluted in 1X PBS 0.5% TritonX-100 and then incubated with primary antibody at 4°C overnight in the same solution. Primary antibodies: goat anti-mCherry (1:1000) (Origene AB0040-200), chicken anti-GFP (1:500) (Aves, GFP-1020), rabbit anti-Wfs1 (1:200)

(made by the lab of Prof. Dr. Jens F. Rehfeld, Dept. of Clinical Biochemistry, Copenhagen, Denmark).
After primary antibody, the sections were washed in 1X PBS (3x 10 minutes) and incubated in secondary antibody in 1X PBS 0.5% TritonX-100 at 4°C overnight. Secondary antibodies: Alexa Fluor donkey anti-rabbit/goat/chicken 488/Cy3/647, (1:300) (Jackson). After 3x10 min washes in 1X PBS, sections were incubated in DAPI and coverslipped (Dako).

2.9 Microscopy

Epifluorescence images were obtained with an upright epifluorescence microscope (Zeiss) with 5×/0.15 or 10×/0.3 objectives (Zeiss). Confocal images were obtained using a Leica SP8 microscope with a 20X/0.75 IMM objective. The brightness and contrast of the images were minimally processed with ImageJ software (NIH) to reduce the noise. For all quantifications of brain sections, ImageJ was used to manually count the cells.

2.10 Statistical analysis

No statistical methods were used to pre-determine sample sizes. The numbers of samples in each group were based on those in previously published studies. Statistical analyses were performed with Prism 7 (GraphPad) and all statistics are indicated in the figure legends.
T-tests or two-way ANOVA with Bonferroni post-hoc test were used for individual comparisons of normally distributed data. Normality was assessed using Shapiro-Wilk test. When normality was not assumed, Mann-Whitney U test and Wilcoxon signed-rank test (for paired observations) were performed for individual comparisons. A one-way repeated measures ANOVA or Friedman's test (as a non-parametric equivalent) were used for within-subjects comparisons followed respectively by Bonferroni post hoc analysis or Dunn's multiple comparison test. After the conclusion of experiments, virus-expression, optic-fibre and GRIN-lens placement were verified. Mice with very low or null virus expression were excluded from analysis.

3. Results

3.1 Encoding of environmental cues in central amygdala neurons during foraging

An organism's survival depends on its ability to evaluate whether environmental cues predict a threat or an opportunity and to learn to associate surrounding signals with the possibility of finding food. The CeA, although traditionally thought to be the main effector station of the amygdala complex, has been recently proposed to have an important role in the formation of memories that link sensory information to aversive or rewarding representations[70]. Furthermore, the CeA provides the output pathway through which these memories are translated into behavioural actions. To understand how the surrounding environment modulates plasticity in the CeA and produces the right behaviour, I performed a conditioned place preference behavioural paradigm, in which mice learn to associate external cues with the availability of the food, while optogenetically manipulating different CeA neuronal populations or recording their activity *in vivo.* In this way, I could investigate the possible roles of CeA neuronal subpopulations in associative learning of contextual food cues and in the formation of appetitive memories represented in a semi-naturalistic setting.

3.1.1 Inhibition of $CeA^{PKC\delta}$ but not CeA^{Sst} cells impairs contextual appetitive conditioning

To investigate the role of different neuronal subpopulations in the CeA and their role in the acquisition of contextual appetitive memories, I set up a conditioning place preference behavioural paradigm. On the first day, *ad libitum* fed mice were free to explore a two-chamber arena for 20 min. The chambers presented different shapes, floor texture and wall patterns. I identified the least preferred chamber as the one where the mouse spent the minority of the time on this first day, and paired it with food for four consecutive 'training' days. After this habituation, mice were food restricted and every day sequestered in each chamber for 15 min with access to food only in the least preferred chamber, termed the 'positive context' (context+). During the recall, mice were allowed to freely navigate in the setup and I measured the time they spent in the positive context in the absence of the food as a readout for contextual appetitive learning (Figure 3.1 A).

The results obtained with WT animals showed that, after conditioning, the mice had a preference of 70% for the positive context (Figure 3.1 B). Afterwards, I tested PKCδ-*Cre* and Sst-*Cre* mice, injected with AAV_5-Ef1a-DIO-eNpHR3.0-mCherry or, as a control AAV_5-Ef1a-DIO-mCherry in the CeA (Figure 3.1 C). Mice were subjected to the same behavioural test, with constant inhibition of PKCδ or Sst neurons during the training in both chambers. The results showed that control animals preferred the context+ during the test, however, photoinhibition of Sst neurons did not alter the behaviour. Conversely, silencing PKCδ neurons impaired learning, with mice lacking their preference for the context previously paired with the food (Figure 3.1 D-F). Moreover, only $CeA^{PKC\delta}$ inhibited mice spent significantly less time in the food zone (the corner of the context+ where the food was placed during training) (Figure 3.1 G-I), with no difference on frequency entering the context as compared to the control group (Figure 3.1 J).
There was no difference in the velocity during recall for both groups (Figure 3.1 K), ruling out any locomotor effects by inhibiting PKCδ and Sst neurons.

To avoid a possible effect of the neuronal inhibition on the food consumption, as a consequence influence on the behaviour outcome, I analysed the food consumption of the PKCδ and Sst animals and found no difference between the control and the inhibition group (Figure 3.1 L).

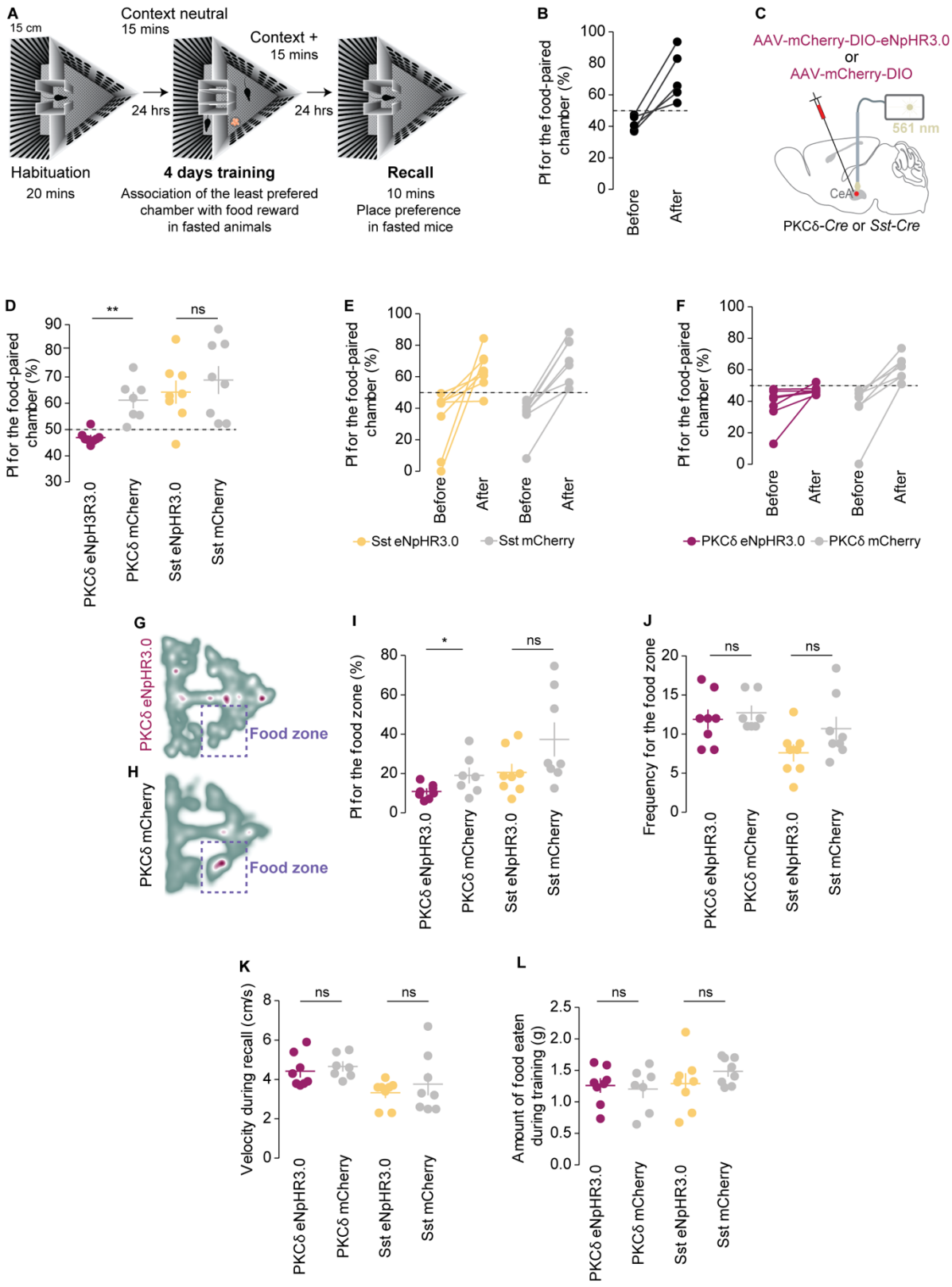
A
15 cm
Context neutral
15 mins
Context +
15 mins
24 hrs
24 hrs
Habituation
20 mins
4 days training
Association of the least prefered chamber with food reward in fasted animals
Recall
10 mins
Place preference in fasted mice
B
PI for the food-paired chamber (%)
Before
After
C
AAV-mCherry-DIO-eNpHR3.0
or
AAV-mCherry-DIO
561 nm
CeA
PKCδ-Cre or Sst-Cre
D
PI for the food-paired chamber (%)
**
ns
PKCδ eNpH3R3.0
PKCδ mCherry
Sst eNpHR3.0
Sst mCherry
E
PI for the food-paired chamber (%)
Before
After
Sst eNpHR3.0
Sst mCherry
F
PI for the food-paired chamber (%)
Before
After
PKCδ eNpHR3.0
PKCδ mCherry
G
PKCδ eNpHR3.0
Food zone
H
PKCδ mCherry
Food zone
I
PI for the food zone (%)
*
ns
PKCδ eNpHR3.0
PKCδ mCherry
Sst eNpHR3.0
Sst mCherry
J
Frequency for the food zone
ns
ns
PKCδ eNpHR3.0
PKCδ mCherry
Sst eNpHR3.0
Sst mCherry
K
Velocity during recall (cm/s)
ns
ns
PKCδ eNpHR3.0
PKCδ mCherry
Sst eNpHR3.0
Sst mCherry
L
Amount of food eaten during training (g)
ns
ns
PKCδ eNpHR3.0
PKCδ mCherry
Sst eNpHR3.0
Sst mCherry

Figure 3.1: Inhibition of CeA$^{PKC\delta}$ neurons during conditioning impairs contextual appetitive conditioning

(A) Conditioned place preference behavioural paradigm. After habituation, mice were conditioned for 4 days in the least preferred chamber where they had access to a food pellet. On the recall day, mice were tested again for preference. **(B)** Preference index (PI) for the context+ before and after conditioning for WT animals (n = 5 mice). **(C)** Optogenetic inhibition of CeA neurons. Cartoon showing the viruses injected in the CeA of PKCδ -*Cre* or Sst-*Cre* mice (AAV_5-Ef1a-DIO-eNpHR3.0-mCherry and the control AAV_5-Ef1a-DIO-mCherry) and the fibre placement. Neurons were photostimulated *in vivo* with constant yellow light. **(D)** PI for the food-paired chamber (context+) during recall after inhibition of CeA neurons during conditioning. PKCδ neuron inhibition impaired learning (for PKCδ CTRL versus eNpHR3.0: Mann-Whitney U test, $p = 0.0021$; for Sst CTRL versus eNpHR3.0: Mann-Whitney U test, $p = 0.7927$). **(E-F)** PI for the context+ before and after conditioning for PKCδ and Sst expressing eNpHR3.0 animals and control groups. **(G-H)** Representative heat maps of the behaviour of individual PKCδ-*Cre* mice expressing eNpHR3.0 or mCherry during recall. Green represents the minimum and purple the maximum per-pixel frequency. **(I)** PI for the food zone during recall (for PKCδ CTRL versus eNpHR3.0: Mann-Whitney U test, $p = 0.0489$; for Sst CTRL versus eNpHR3.0: Mann-Whitney U test, $p = 0.0650$). **(J)** No difference in the number of visits to the food zone during recall for all groups (for PKCδ CTRL versus eNpHR3.0: unpaired t test, $p = 0.5838$, $t = 0.5618$; for Sst CTRL versus eNpHR3.0: unpaired t test, $p = 0.0982$, $t = 1.772$). **(K)** No difference also in velocity during recall (for PKCδ CTRL versus eNpHR3.0: unpaired t test, $p = 0.5497$, $t = 0.6142$; for Sst CTRL versus eNpHR3.0: unpaired t test, $p = 0.4645$, $t = 0.7520$). **(L)** Total amount of food eaten during the four training days. Inhibition of PKCδ and Sst neurons did not modify food consumption compared to the controls (for PKCδ CTRL versus eNpHR3.0: unpaired t test, $p = 0.7394$, $t = 0.3398$; for Sst CTRL versus eNpHR3.0: unpaired t test, $p = 0.2730$, $t = 1.141$). Value = Mean± SEM, $*p < 0.05$, $**p < 0.01$. Experiments performed together with Dr. Marion Ponserre.

I next examined the role of PKCδ and Sst neurons during the retrieval test. Mice were subjected to a similar behaviour paradigm, with inhibition of PKCδ and Sst neurons during the recall phase. Compared with previous results, I found that inhibition of PKCδ, but not Sst, decreased the preference index of the inhibited animals for the context+ (Figure 3.2 A-C). However, no difference could be observed in the time spent in the food zone (Figure 3.2 D-F), nor in the frequency of visits (Figure 3.2 G). No significant difference in velocity during recall (Figure 3.2 H) and the amount of food eaten during conditioning (Figure 3.2 I) between groups was seen.

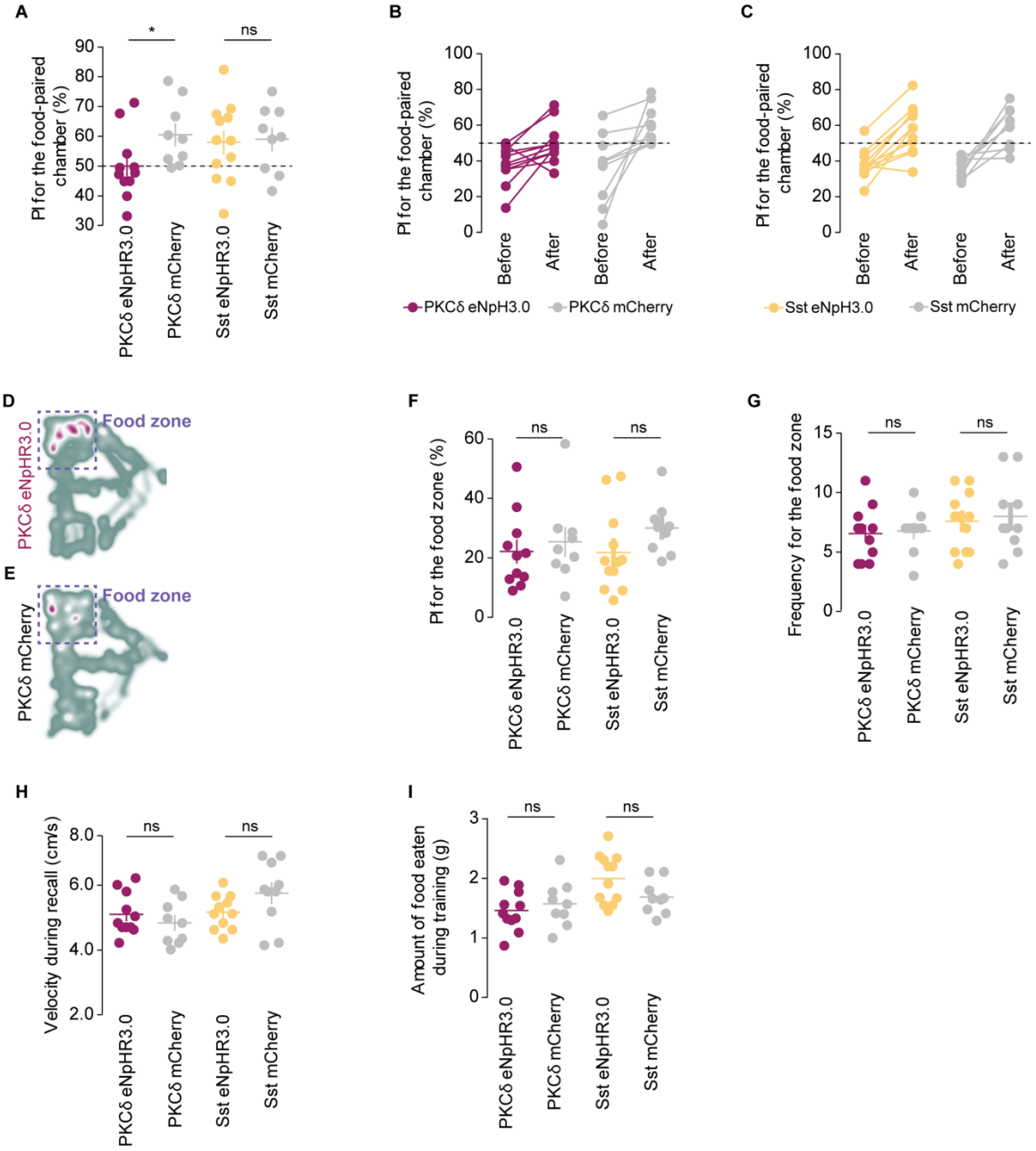

Figure 3.2: Inhibition of CeA$^{PKC\delta}$ neurons during the test impairs contextual appetitive conditioning

(A) PI for the food-paired chamber (context+) during recall while inhibiting CeA$^{PKC\delta}$ or CeA^{Sst} neurons. Inhibition of PKCδ neurons impaired the retrieval of contextual memory (for PKCδ CTRL versus eNpHR3.0: Mann-Whitney U test, $p = 0.0250$; for Sst CTRL versus eNpHR3.0: Mann-Whitney U test, $p = 0.07491$). **(B-C)** PI for the context+ before and after conditioning for PKCδ/Sst-*Cre* animals expressing eNpHR3.0 and controls. **(D-E)** Representative heat maps of the behaviour of individual mice during recall. Green represents the minimum and purple the maximum per-pixel frequency. **(F)** PI for the food zone during recall while mice were photoinhibited (for PKCδ CTRL versus eNpHR3.0: Mann-Whitney U test, $p = 0.4941$; for Sst CTRL versus eNpHR3.0: Mann-Whitney U test, $p = 0.0597$). **(G)** Analysis of the number of visits in the food zone during recall. The photoinhibited animals failed to

show differences with the control groups (for PKCδ CTRL versus eNpHR3.0: unpaired t test, p = 0.8094, t = 0.2447; for Sst CTRL versus eNpHR3.0: unpaired t test, p = 0.7251, t = 0.3566). **(H)** Analysis of velocity during recall did not show any effect due to inhibition of CeA neurons (for PKCδ CTRL versus eNpHR3.0: unpaired t test, p = 0.3849, t = 0.8922; for Sst CTRL versus eNpHR3.0: unpaired t test, p = 0.1041, t = 1.707). **(I)** Comparable amount of food consumed during the training by PKCδ-*Cre* and Sst-*Cre* animals expressing eNpHR3.0 and controls (for PKCδ CTRL versus eNpHR3.0: unpaired t test, p = 0.4806, t = 0.7204; for Sst CTRL versus eNpHR3.0: unpaired t test, p = 0.0686, t = 0.7520). Value = Mean± SEM, *$p < 0.05$, **$p < 0.01$.
Experiments performed together with Dr. Marion Ponserre.

To understand whether inhibition of PKCδ or Sst neurons would generalise anxiety behaviour, which might influence the results of the conditioning, I performed an open-field test. Mice were allowed to explore the arena for 10 min, receiving constant inhibition for the whole experiment. Since mice have a natural aversion to open areas, increased level of anxiety leads to decreased exploratory behaviour, calculated as less time spent in the centre zone. Photoinhibition did not lead to increased anxiety behaviour resulting in no differences in the duration or number of entries into the centre zone, nor the velocity between eNpHR3.0 expressing animals as compared to controls (Figure 3.3 A-G).
After behavioural tests, the injection site in the CeA and the placement of optic fibres were analysed (Figure 3.3 H-I). Mice were excluded from analysis if the virus was not bilaterally expressed in the CeA.

Overall, these results suggest that $CeA^{PKC\delta}$ neurons might play a role in forming and retrieving associations between contextual cues and food availability.

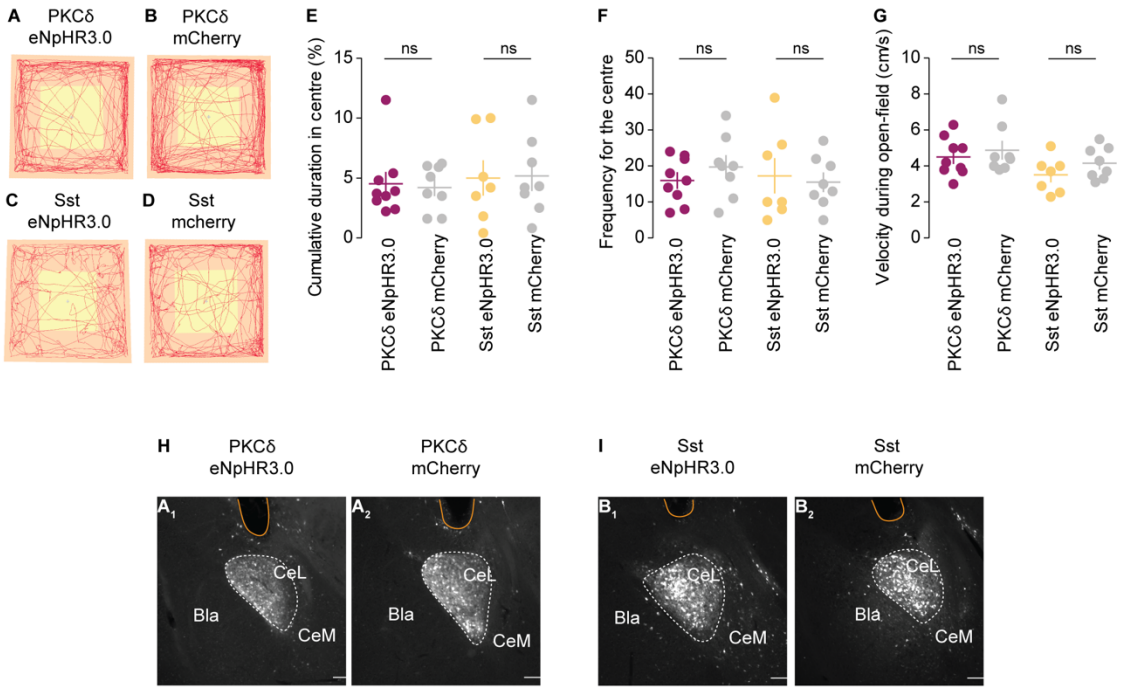

Figure 3.3: Inhibition of CeA$^{PKC\delta}$ and CeA^{Sst} neurons does not effect anxiety

(A-D) Representative traces (in red) of the behaviour of animals subjected to PKCδ or Sst neuron inhibition and relative controls. The yellow square represents the centre. **(E)** No photoinhibition effect for all the groups on the cumulative duration in centre during the openfield task (for PKCδ CTRL versus eNpHR3.0: Mann-Whitney U test, $p = 0.8096$; for Sst CTRL versus eNpHR3.0: Mann-Whitney U test, $p = 0.8168$), **(F)** the same is true for the number of visits in the centre (for PKCδ CTRL versus eNpHR3.0: unpaired t test, $p = 0.3181$, t = 1.033; for Sst CTRL versus eNpHR3.0: unpaired t test, $p = 0.7334$, t = 0.3481) and velocity **(G)** (for PKCδ CTRL versus eNpHR3.0: unpaired t test, $p = 0.5467$, t = 0.6166; for Sst CTRL versus eNpHR3.0: unpaired t test, $p = 0.2006$, t = 1.348). **(H-I)** Representative epifluorescent images of PKCδ-*Cre* and Sst-*Cre* mice injected in the CeA with an AAV_5-DIO-eNPHR3.0-mcherry or AAV_5-DIO-mcherry, showing the location of the optic fibre tract. Scale bars: 100 µm. Value = Mean± SEM, $*p < 0.05$, $**p < 0.01$.
Experiments performed together with Dr. Marion Ponserre.

3.1.2 *In vivo* recordings of $CeA^{PKC\delta}$ and CeA^{Sst} neuronal activity during appetitive conditioning

To better understand how $CeA^{PKC\delta}$ and CeA^{Sst} neuronal activity contributed to this behaviour, we performed *in vivo* calcium imaging. We injected the AAV_5-Syn.Flex.GCaMP6s virus, which expresses the calcium indicator GCaMP6s, in the CeA of PKCδ-*Cre* and Sst-*Cre* mice and a GRIN lens was implanted above the CeA (Figure 3.4 A-C). This allowed us to record the specific neuronal activity of PKCδ and Sst neurons with a miniscope during all phases of behaviour (Figure 3.4 D).

Mice underwent a similar behavioural paradigm with an additional step at the end of the 10 min recall: a food pellet was added in the context+ and recorded the behaviour for another 10 min, to make sure the 'food responsive' neurons could be functionally tagged. We recorded 202 cells in 5 PKCδ-*Cre* animals (24-61 cells per mouse) and 149 cells in 5 Sst-*Cre* mice (14-60 cells per mouse). The number of neurons that could be detected during the conditioning phase and recall was higher as compared to habituation for both Sst-*Cre* and PKCδ-*Cre* animals, probably due to the fact that investigation and food consumption recruited a new set of neurons (Figure 3.4 E). After aligning cell identities through all the different imaging sessions, around 10% of the cells could be detected for all four recording days (Figure 3.4 F-G), and 17% during conditioning and recall (Figure 3.4 F-G), suggesting that the neurons recorded in these two behavioural phases could be functionally more similar as compared to the ones activated during habituation. Five animals per genotype were tested, but only three per group had a PI during recall higher than 50% (Figure 3.4 H), probably due to the weight of the miniscope that made the movements more laborious. However two other animals, one per genotype, increased their preference for the context+ indicating a certain degree of learning (Figure 3.4 H). They were included in the analysis, resulting in four animals per group.

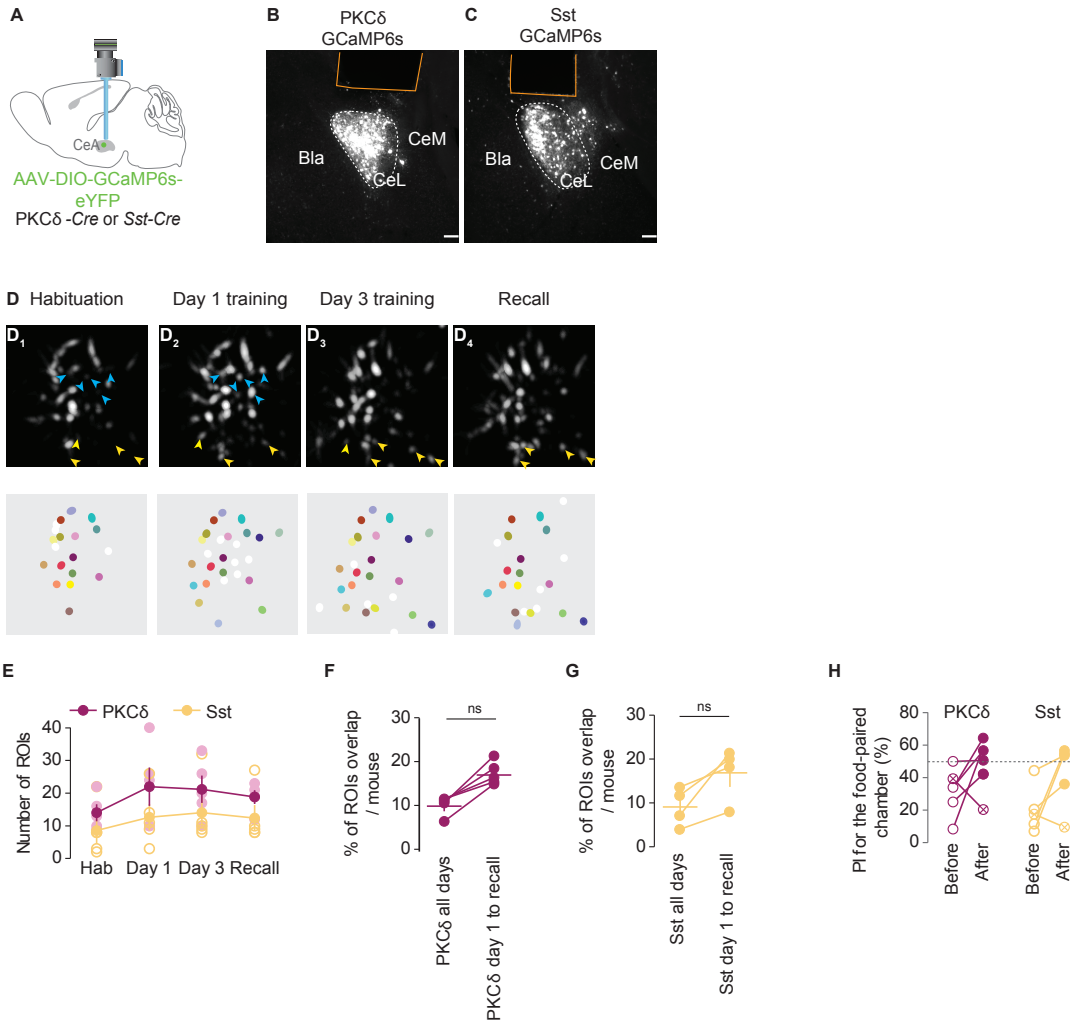

Figure 3.4: In vivo calcium imaging of CeA^{PKCδ} and CeA^{Sst} neurons

(A) Cartoon showing viral injection, and lens and miniscope placement. **(B-C)** Representative epifluorescent images of PKCδ-*Cre* and Sst-*Cre* mice injected in the CeA with an AAV_5-DIO-GCamp6s virus showing the location of the GRIN lens tract. Scale bars: 100 µm. **(D)** Maximum-projection images of PKCδ$^+$ GCaMP6s-expressing neurons from a representative recorded mouse during habituation (D_1), first (D_2) and third (D_3) days of training, as well as recall (D_4). Corresponding region-of-interests (ROIs) are depicted below each panel. ROIs identified over consecutive sessions are shown in identical colour. ROIs detected in only one session are shown in white. Blue arrowheads indicate neurons that appeared for the first time on day 1 of conditioning. Yellow arrowheads indicate neurons that were common between at least 2 out of 3 days of conditioning and recall and were not visible on habituation. **(E)** Numbers of detected ROIs during all four sessions (for PKCδ group comparisons: time, One-way ANOVA repeated measure, $F_{(3,4)}$ = 2.16, p=0.1458; for Sst group comparisons: time, One-way ANOVA repeated measure, $F_{(3,4)}$ = 3.98, p=0.0351). **(F-G)** Percentage of ROIs per PKCδ-*Cre* and Sst-*Cre* mouse that overlapped in all four recording sessions (from habituation to recall) or from day 1 of conditioning to recall (for PKCδ comparison: Wilcoxon signed-rank test, p=0.125; for Sst comparison: Wilcoxon signed-rank test, p=0.25). **(H)** PI for the context+ before and after conditioning for both PKCδ-*Cre* and Sst-*Cre* mice expressing GCaMP6s. Data points shown as

crossed circles represent mice that did not show an increase in learning after conditioning. Value = Mean± SEM, *$p < 0.05$, **$p < 0.01$. Experiments performed together with Dr. Marion Ponserre.

3.1.3 CeA encodes Pavlovian appetitive learning

With the *in vivo* calcium imaging experiments, we investigated whether CeA neurons, that fired during food intake, could specifically be active in the positive context after learning, being considered as memory cells. The positive context, which represents multisensory information, could become, after the learning process, a general predictor of food availability.

To study this aspect, we used a regression-based approach: we convolved the behavioural signal of the context+ with the kinetics of the calcium indicator to create a regressor of the context+. This can be simplified as a cell trace of a neuron perfectly active only in the positive context, and correlated across time with the activity of each CeA cell we recorded with the corresponding regressor[192]. For both PKCδ and Sst animals, we found that there was very little correlation with the positive context during habituation, but it was higher during recall (Figure 3.5 A-B). The curves of both neuronal subpopulations, indeed, shifted toward a more positive correlation during the test. To check the correlation between neuronal activity and the behaviour of each mouse, we randomly selected the 70% of the recall data and trained a logistic regression classifier (decoder). In this way we could verify if the location of the mice in the remaining 30% of the behavioural data could be accurately predicted using just the information of the PKCδ and Sst neuronal activity during that time. We used a decoder trained on temporally shuffled temporal data as a control. In all tested mice, we could consistently decode the position of the animals in the positive chamber (70.7±4.7% for $CeA^{PKC\delta}$ and 70±4.1% for the CeA^{Sst} recorded ensembles), while the accuracy decreased when we used the control decoder, indicating that the correct predictions were well above chance (Figure 3.5 C-E). When we tested the classifier on $CeA^{PKC\delta}$ and CeA^{Sst} population activity, excluding the four neurons showing the highest correlation to the positive context, we found a performance of around 60% (Figure 3.5 C-D), suggesting that at least a fraction of PKCδ and Sst neurons encoded essential information about the location of the animals in the context+ during recall. Aligning the neuronal activity of each neuron with the onset of the transition to the positive context and averaging the data (Figure 3.5 F-G), we found that a percentage of PKCδ and Sst neurons was specifically activated when the mouse was entering the context+ and that the activity remained high for the duration that the mouse was in the appetitive context, and preferentially within the

corner where the food was placed during training (Figure 3.5 H,J). We called the neurons that had a significant correlation to the positive context 'memory neurons': namely, 14.5% of the PKCδ and 8.7% of the Sst cells recorded during recall (Figure 3.5 I,K).

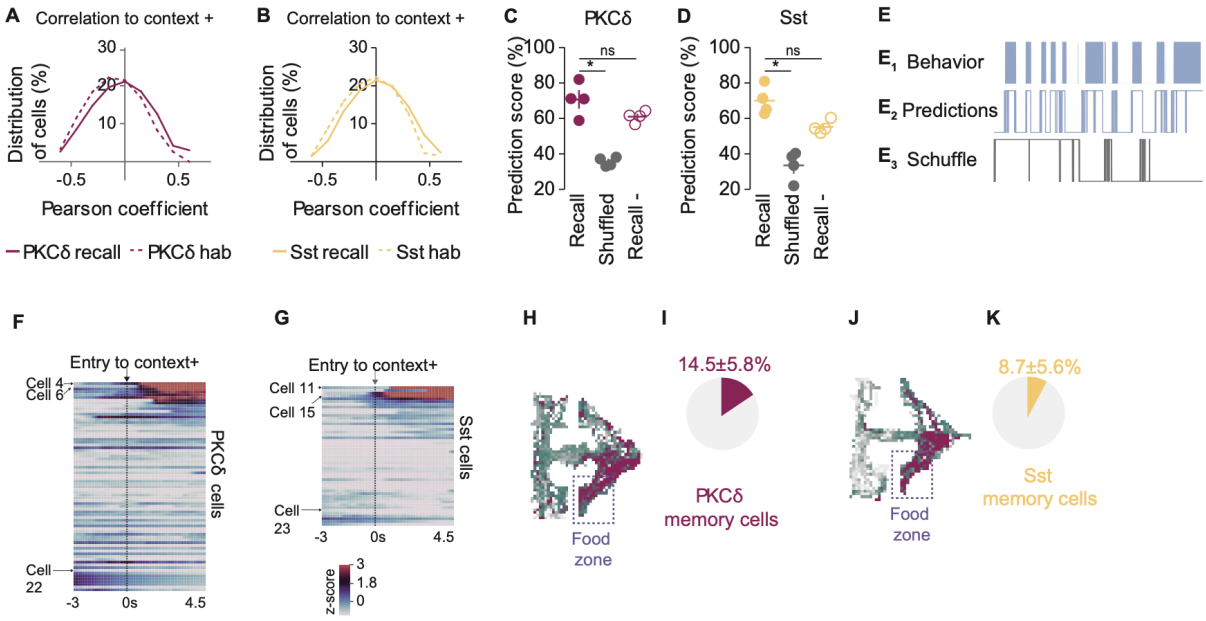

Figure 3.5: Central amygdala encoding of Pavlovian appetitive learning

(A-B) Frequency distribution of Pearson correlations to the positive context regressor in PKCδ **(A)** and Sst **(B)** calcium recorded neurons during habituation and recall. The correlation to the positive context was higher during recall. **(C-D)** Prediction scores of a logistic regression classifier of the locations of PKCδ-*Cre* **(C)** and Sst-*Cre* **(D)** animals in the positive context during recall, after temporally shuffling of behavioural data (shuffled), and after excluding 4 neurons per animal that exhibited the highest correlation value to the positive context regressor (recall -) (for PKCδ group: Friedman test with Dunn's Multiple Comparison, p=0.0062, F=9.9; for Sst group: Friedman test with Dunn's Multiple Comparison, p=0.0115, F=9.3, *P < 0.05). Bar graphs show mean +/- s.e.m and each dot is the quantification of a single animal. **(E)** Traces showing the behaviour of one representative animal in the positive context during recall **(E1)**, corresponding predictions by the logistic classifier **(E2)**, and corresponding predictions after randomly shuffling the behaviour data **(E3)**. **(F-G)** Heatmap of averaged z-scored calcium responses of PKCδ **(F)** and Sst **(G)** neurons following entry to the positive context (at 0 sec). Cells were sorted in descending order based on their activity response upon entry in the context+ (entries to the context+ varied from 6 to 14 times depending on the mice) (n = 75 PKCδ^{+} and 50 Sst^{+} neurons). **(H-J)** Heat maps showing the ΔF/F signal across the whole arena for one representative memory PKCδ **(H)** and Sst **(J)** cell. Green represents the minimum and purple the maximum per-pixel frequency. The activity was higher in the food zone. **(I)** Fraction of CeA^{PKCδ} memory neurons recorded during recall. **(K)** Fraction of CeA^{Sst} memory neurons recorded during recall. Analysis performed by Dr. Marion Ponserre.

Memory neurons were found in 4/4 PKCδ-*Cre* and 3/4 Sst-*Cre* mice analysed. Upon further investigation of the calcium traces of the memory neurons during recall, we found different patterns of activity, summarized by the following example cells (Figure 3.6 A): some neurons fired specifically upon transition to the positive context and food zone (Figure 3.6 A cells 1,2,3,4,5,6,7,12,13,14,15 and 3.6 C-D), and some were mostly active in the food zone (Figure 3.6 A cells 8,9,10,11). We also examined the pattern of activity of the unresponsive neurons in the positive context (9 PKCδ and 7 Sst neurons) (Figure 3.6 B): 6 of them showed significant activity in the neutral context, however none of them increased their activity upon transition to the neutral context (Figure 3.6 E-F). The non-memory neurons did not show any activity correlation with the positive context or food zone (Figure 3.6 cells 16,17,18,19,20,21). To analyse the activity of the memory neurons during the 10 min of recall with food, we generated a food regressor and correlated with it the activity of the neurons during the food consumption phase of the recall: we found that 6/10 PKCδ and 5/5 Sst memory neurons were significantly active during food consumption, demonstrating that some memory cells could be functionally tagged as food responsive (Figure 3.6 cells 1,2,3,4,5,7,11,12,13,14,15).

Examining the correlation between the number of memory neurons for each mouse and the behaviour learning index for the positive context during recall, we found that the animals that spent the highest percentage of time in the positive context (good learners) during the test, did not have more memory neurons compared to the ones that spent there less time (poor learners). We think that while the 'poor learners' could associate only the food zone with the reward, the 'good learners' could associate either the entire positive context or the entire arena with it, with neurons already firing when the animal recognized the whole arena. Memory neurons can still be found in these animals marked as 'poor learners', and we observed a negative correlation between the activity of the neurons in the food zone and the PI for the positive context (Figure 3.6 G). Moreover, the accuracy of the logistic classifier decreased with higher learning performances (Figure 3.6 H), not being able to find a good representation of the positive context in the neuronal activity of the 'best learners' and supporting our hypothesis that the mice that learned best, generalised the representation of the context+ with the entire arena. Together these data suggest that a subgroup of PKCδ and Sst neurons in the CeA are involved in the learning process through which they associate contextual information of the positive chamber with food delivery.

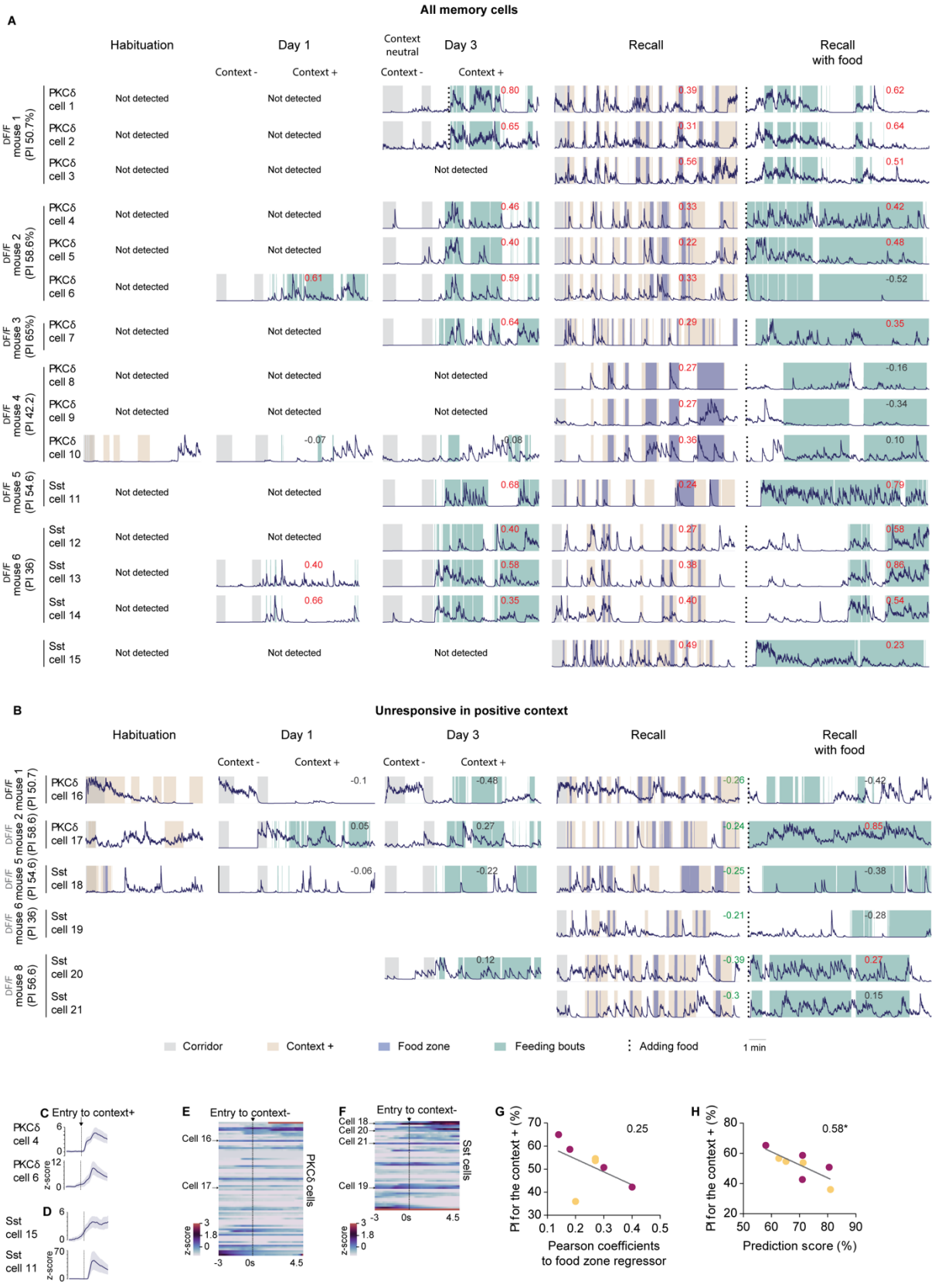
A
All memory cells
Habituation
Day 1
Context neutral
Day 3
Recall
Recall with food
Context -
Context +
PKCδ cell 1
PKCδ cell 2
PKCδ cell 3
PKCδ cell 4
PKCδ cell 5
PKCδ cell 6
PKCδ cell 7
PKCδ cell 8
PKCδ cell 9
PKCδ cell 10
Sst cell 11
Sst cell 12
Sst cell 13
Sst cell 14
Sst cell 15
DF/F mouse 1 (PI 50.7%)
DF/F mouse 2 (PI 58.6%)
DF/F mouse 3 (PI 65%)
DF/F mouse 4 (PI 42.2)
DF/F mouse 5 (PI 54.6)
DF/F mouse 6 (PI 36)
Not detected
B
Unresponsive in positive context
PKCδ cell 16
PKCδ cell 17
Sst cell 18
Sst cell 19
Sst cell 20
Sst cell 21
DF/F mouse 1 (PI 50.7)
DF/F mouse 2 (PI 58.6)
DF/F mouse 5 (PI 54.6)
DF/F mouse 6 (PI 36)
DF/F mouse 8 (PI 56.6)
Corridor
Context +
Food zone
Feeding bouts
Adding food
1 min
C Entry to context+
D
E Entry to context-
F Entry to context-
PKCδ cells
Sst cells
z-score
G
PI for the context + (%)
Pearson coefficients to food zone regressor
0.25
H
Prediction score (%)
0.58*

Figure 3.6: Representative traces of memory neurons and positive context unresponsive cells

(A) Calcium traces of all PKCδ and Sst identified memory neurons during each step of the behaviour. Values during recall indicate the Pearson coefficients of each cell to its corresponding memory regressor. Values during day 1, day 3, and recall with food indicate the Pearson coefficients of each cell to its corresponding feeding bouts regressor. Values in red indicate a significant correlation. Each ΔF/F trace was normalised to its maximum value. **(B)** Calcium traces of the 6 PKCδ and Sst cells that showed both a significant negative correlation to the positive context regressor and a significant positive correlation to the neutral context regressor. Values during recall indicate the Pearson coefficients of each cell to its corresponding memory regressor. Values in green indicate a significant negative correlation. Values during day 1, day 3, and recall with food indicate the Pearson coefficients of each cell to its corresponding feeding bouts regressor. Values in red indicate a significant positive correlation. Each ΔF/F trace was normalised to its maximum value. **(C-D)** Average traces of PKCδ **(C)** and Sst **(D)** neurons following entry to the positive context (at 0 sec). Cells 4, 6, 15 and 11, are 4 representative memory neurons. Shaded areas represent s.e.m. **(E-F)** Heatmap of average z-scored calcium responses of PKCδ (E) and Sst (F) neurons following entry to the neutral context (context- at 0 sec). ΔF/F transients were z-scored with the baseline calculated from time points when the animals were in the positive context. Cells were sorted in descending order based on their activity response upon entry in the context- (n = 75 $PKC\delta^+$ and 50 Sst^+ neurons). **(G)** PI in the positive context on test day in function of the averaged value of all Pearson correlation coefficients to the food zone regressor for all identified memory neurons in a given mouse. Each dot is the quantification of a single PKCδ-*Cre* (purple) or Sst-*Cre* (yellow) animal. Values shown are R square. **(H)** Prediction score of the logistic regression classifier in function of the PI of the animal on recall day. Each dot is the quantification of a single PKCδ-*Cre* (purple) or Sst-*Cre* (yellow) animal. Values shown are R square. *$p < 0.05$.
Analysis performed by Dr. Marion Ponserre.

3.1.4 Differences in calcium activity patterns between CeA $^{PKC\delta}$ and CeA ^{Sst} neurons

We next tried to identify possible differences in the activity of PKCδ and Sst neurons examining cell traces of all five PKCδ-*Cre* and Sst-*Cre* recorded animals. On training days one and three, we found that a large portion of both PKCδ and Sst neurons strongly increased their activity when the mice were in the context+ (Figure 3.7 A-D cells A-B-C-D-E-F). On day one, we identified the 30.9±10.3% of PKCδ and the 31.1±7.3% of Sst cells active in the positive context, while on day three their proportions increased to 41.7±6.7% and 58.3±7.8%, respectively (Figure 3.7 E). To investigate the correlation of the neuronal activity with the food consumption, we calculated the Pearson correlation of each cell to its corresponding feeding regressor. We observed that while CeA^{Sst} neurons increased their activity at the onset of each feeding bout (Figure 3.6 F), the $CeA^{PKC\delta}$ cells did not always fire systematically at the beginning of the food consumption (Figure 3.7 C). On day one and three, CeA^{Sst} neurons showed a stronger positive correlation to the feeding regressor compared to $CeA^{PKC\delta}$ (Figure 3.7 F,G) with a higher proportion of food responsive cells (Figure 3.7 H). However, there was no significant difference in the number of neurons active in the positive context during training

between PKCδ and Sst populations (Figure 3.7 E), suggesting that the activity of the Sst neurons may be more closely related to food consumption, while the PKCδ cells could be activated by the salience of the food reward, and not the consumption itself. This phenotype was independent from the time spent eating during the training, since it was comparable for both PKCδ-*Cre* and Sst-*Cre* animals (Figure 3.7 I). Moreover, there was no positive correlation between time and proportion of food responsive cells during day three (Figure 3.7 J). Tracking the food responsive cells over these days, we observed that the majority of them conserved the significant correlation to the feeding regressor (Figure 3.7 C,D cells B,D,E,F,). Additionally, when looking at PKCδ and Sst neurons, classified as food responsive during recall, we found that the 83% were also food responsive on day three, and 22% of the PKCδ and the 50% of the Sst during day one (Figure 3.7 K,M). The majority of these cells were also significantly active in the context+ during training and were not detected during habituation (Figure 3.7 C-D cells B,C,D,E,F, 3.7L-N). Furthermore, the majority of the non-food responsive cells during recall, were non-responsive as well during the training days (Figure 3.7 K-M), showing the functional selectivity maintained by the neurons during the behavioural paradigm.

In conclusion, these data suggest that CeA^{Sst} neurons may be important to link environmental information with the physical properties of food, while $CeA^{PKC\delta}$ may rather form associations between environmental information and the salience of the food reward.

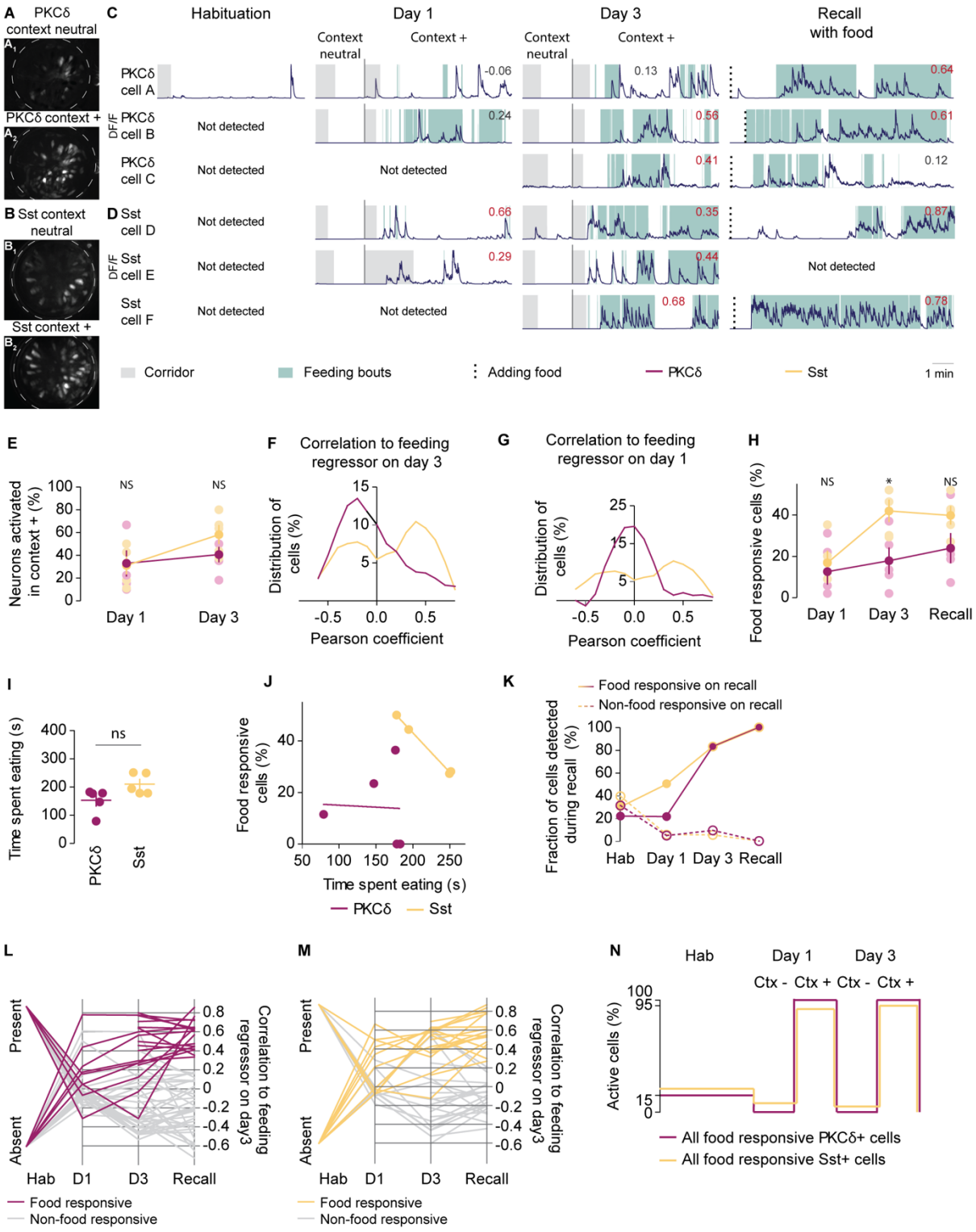

Figure 3.7: Differences in calcium activity patterns between CeA $^{PKC\delta}$ and CeA^{Sst} neurons

(A-B) Maximum-projection representative images of the field of view of recorded PKCδ^{+} **(A)** and Sst^{+} **(B)** GCaMP6s-expressing neurons during day 3 of conditioning in the neutral and positive context. **(C-D)** Representative calcium traces of PKCδ^{+} **(C)** and Sst^{+} **(D)** recorded neurons during habituation, day

1, day 3 of conditioning, and recall with food. The coloured background represents the location of the mouse in the corridor (grey), or on top of the food (green). The values indicate the Pearson coefficients of each cell to its corresponding feeding bout regressor. Values in red indicate a significant correlation. Each ΔF/F trace was normalised to its maximum value. **(E)** Proportion of neurons per mouse significantly active in context+ compared to neutral context on day 1 and 3 of conditioning. (for PKCδ versus Sst on day1: Mann-Whitney U test, $p = 0.8413$; for PKCδ versus Sst on day3: Mann-Whitney U test, $p = 0.2045$). **(F)** Frequency distribution of Pearson correlations to the feeding bout regressor in all PKCδ and Sst recorded neurons during day 3 of conditioning. **(G)** Frequency distribution of Pearson correlations to the feeding regressor in all PKCδ and Sst recorded neurons during day 1. **(H)** Proportion of food responsive neurons on day 1, day 3, and recall (for PKCδ versus Sst on day1: Mann Whitney U test, $p = 0.6723$; for PKCδ versus Sst on day3: Mann-Whitney U test, $p = 0.0362$; for PKCδ versus Sst on recall: Mann-Whitney U test, $p = 0.0952$). **(I)** Time spent eating during day 3 for PKCδ and Sst mice (for PKCδ versus Sst: unpaired t test, $p = 0.552$, $t = 2.242$). Bar graphs show mean +/- s.e.m and each dot is the quantification of a single animal. **(J)** Proportion of food responsive PKCδ$^+$ and Sst$^+$ cells as a function of the time spent eating on day 3. **(K)** Fraction of food responsive (solid lines) and non-food responsive (dotted lines) cells detected during recall that were tagged as food responsive on day 3 and 1 of conditioning, and present during habituation. **(L-M)** Food responsive PKCδ$^+$ (purple lines, E) and Sst$^+$ (yellow lines, F) cells and non-food responsive cells (gray lines) detected during recall and traced back to day 3 and day 1 and habituation. Each line represents a cell and its correlation value to the feeding regressor on recall, day 3, and day 1 of conditioning, as well as whether it was present or not during habituation. Values above 0.25 represent a significant positive correlation to the feeding regressor (n = 92 PKCδ$^+$ and 59 Sst$^+$ neurons). **(N)** Proportion of food responsive PKCδ$^+$ and Sst$^+$ neurons that were active during habituation and that were significantly active in the neutral context or the context+ during day 1 and day 3 of conditioning (n = 40 PKCδ$^+$ and 39 Sst$^+$ neurons). Analysis performed by Dr. Marion Ponserre.

3.2 A role for neurons of the medial division of the central amygdala in appetitive behaviours.

The central amygdala (CeA), with its lateral (CeL) and medial (CeM) divisions, orchestrates a wide range of behaviours, including defensive and appetitive responses[3]. The CeA is composed of many different GABAergic neuronal subpopulations that are marked by expression of specific neuropeptides, receptors and kinases, and elicits distinct, sometimes opposite, behavioural phenotypes ranging from fear and anxiety to consummatory and rewarding behaviours[3] . The relative contributions of subpopulations in the CeL versus CeM is, however, not completely understood.

Moreover, there is currently no method that allows us to specifically manipulate only the CeL or the CeM subregion *in vivo* in order to study their contribution to CeA related behaviours. Here, I took advantage of an intersectional genetic approach to investigate how neurons marked by expression of serotonin receptor 2a (Htr2a) or somatostatin (Sst), located in either the CeL or CeM subdivisions, regulate feeding, drinking, and promote positive reinforcement. The Htr2a and Sst neurons partially overlap in the CeA: approximately 50% of Htr2a neurons are also Sst positive. Previous work in the lab suggested that the two subpopulations can share some similarities in terms of behaviour. For example, their activation overrides the reduced consumption of bitter food, but also the peculiarity of Htr2a neurons is that they promote feeding in satiated animals. In this work, I focussed on both subpopulations to try to dissect their involvement in appetitive behaviours in more detail.

3.2.1 Characterization of Htr2a and Sst neurons in the CeL

Our lab recently generated a Wfs1-*FlpoER* mouse line in which the Flp recombinase is conditionally expressed only in Wfs1 (Wolframin1) positive cells after tamoxifen injection. Wfs1 is a specific CeL marker that co-localises with Htr2a and Sst positive cells in the CeL. Crossing Htr2a-*Cre* and Wfs1-*FlpoER* mice generated double transgenic 'intersectional' mice (Htr2a-*Cre*::Wfs1-*FlpoER* and Sst-*Cre*::Wfs1-*FlpoER*), in which the CeL^{Htr2a} and CeL^{Sst} positive cells were both Cre and Flp positive, while the CeM^{Htr2a} and CeM^{Sst} positive cells were only Cre positive.

In order to examine the percentage of co-localisation between Htr2a/Sst and Wfs1 cells, both Htr2a-*Cre* and Sst-*Cre* mice were crossed to a reporter tdTomato mouse line that allows us to specifically mark the Htr2a and Sst cells with tdTomato expression (Figures 3.8 A,D and 3.9 A,D). Subsequent immunostaining of brain sections with a Wfs1 antibody (Figures 3.8 B,E and 3.9 B,E) confirmed that Wfs1 expression is mainly restricted to the CeL and showed that 46±1.19% of the Wfs1 positive cells were Htr2a positive and 56±1.89 were Sst positive (Figures 3.8 F,G and 3.9 C,F,G). 96% of double Htr2a (±1.27) and Sst (±1.27) positive cells co-localised with Wfs1 in the CeL (Figures 3.8 H and 3.9 H).

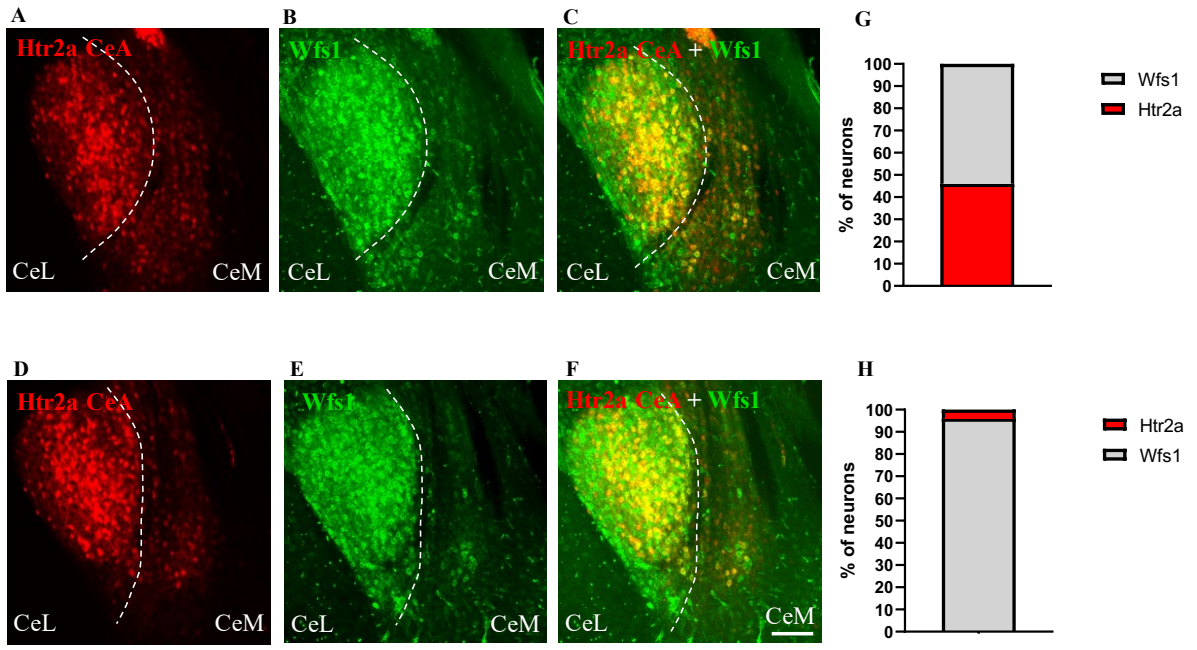

Figure 3.8: Co-localisation of Htr2a and Wfs1 in the CeL

(A,D) Htr2a expression in the CeA of Htr2a-*Cre*::TdTomato mice. **(B,E)** Wfs1 antibody staining revealed expression of this marker mainly in the CeL. **(C,F)** Co-localisation analysis between Wfs1 and Htr2a in the CeL showed that 46±1.19% of the Wfs1 positive cells expresses Htr2a **(G)**. **(H)** 96±1.27% of Htr2a cells co-localise with Wfs1 in CeL. (n=3 brains, 3 sections per mouse). Value = Mean ± SEM. Scale bar: 115 µm.

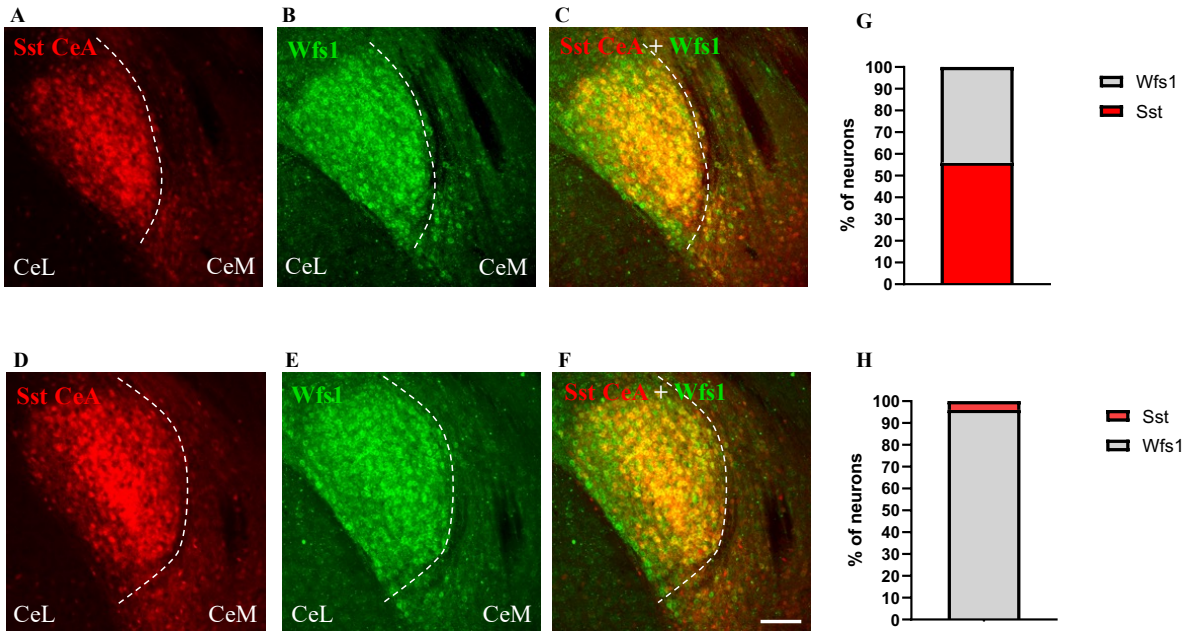

Figure 3.9: Co-localisation of Sst and Wfs1 in the CeL

(A,D) Sst expression in the CeA of Sst-*Cre*::TdTomato mice. **(B,E)** Wfs1 antibody staining. **(C,F)** Co-localisation analysis between Wfs1 and Sst in the CeL showed that 56±1.27% of Wfs1 positive cells express Sst **(G)** and 96±1.27% of Sst cells co-localise with Wfs1 in CeL **(H)**. (n=3 brains, 3 sections per mouse). Value = Mean ± SEM. Scale bar: 115 µm.

3.2.2 Characterisation of the Wfs1-*FlpoER* mouse line

The pattern of expression of the protein encoded by the Wfs1 gene indicated that this is a specific CeL marker[193]. In order to elucidate the accuracy of the Wfs1 pattern of expression in our transgenic line, Wfs1-*FlpoER* mice were crossed with FPDI reporter mice[188] so that in the resulting Wfs1-*FlpoER*::FPDI, only *Flp*-positive cells were marked with mCherry (Figure 3.10 A,D). A protocol of three consecutive days of tamoxifen (intraperitoneal injection 200mg/kg)[194] followed. The results show that Wfs1 expression is mostly limited to the CeL (Figure 3.10 A-F). Co-localisation analysis revealed that 65±1.2% of Wfs1 positive cells are mCherry positive (Figure 3.10 C,F,G) and that there is 10.6±0.7% of ectopic Wfs1 expression in the CeM (Figure 3.10 H). Since the technology used to generate the transgenic mouse line is based on the random integration of the exogenous DNA into the genome, the lower percentage of expression of the transgene, compared to the endogenous one, could be

dependent on the site of integration and the copy number of the transgenic DNA. The transgene expression, in fact, could be perturbed by endogenous neighbouring genes or promoters.

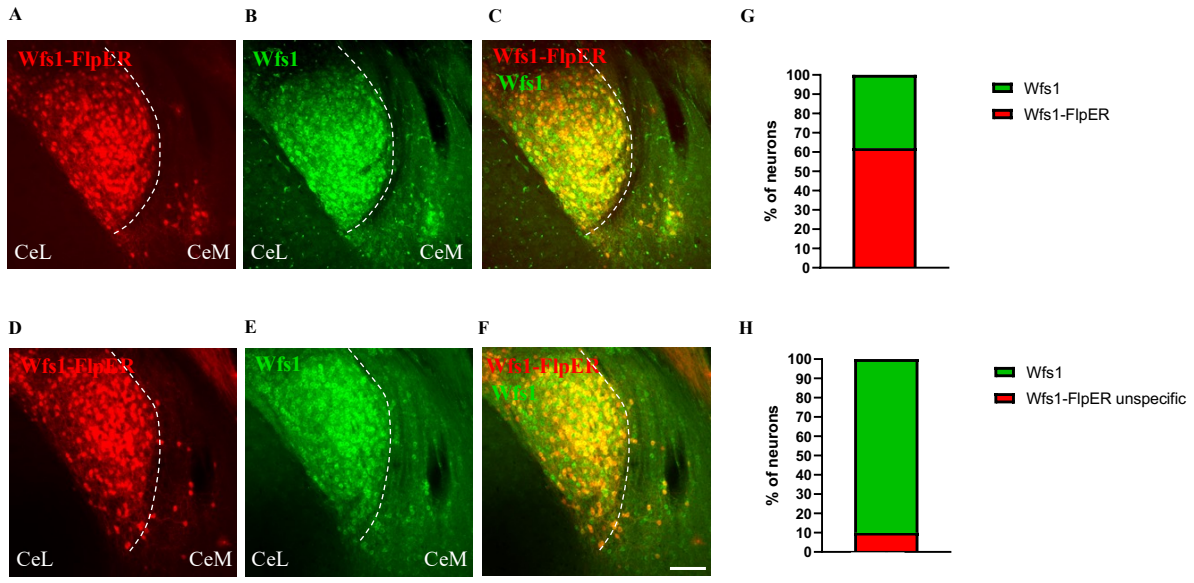

Figure 3.10: Characterisation of the Wfs1-*FlpoER* transgenic line

(A,D) Expression of the transgenic Wfs1 in the CeA of Wfs1-*FlpoER*::FPDi mice, marked with mCherry. **(B,E)** Wfs1 antibody staining showing endogenous Wfs1 expression. **(C,F)** Co-localisation analysis of Wfs1 and mCherry (transgenic Wfs1) in the CeL showed that 65±1.2% of the Wfs1 positive cells express mCherry **(G)**. In the CeM, the transgene has an ectopic expression of the 10.6±0.7% as compared to the Wfs1 positive cells (n=2 brains, 3 sections per mouse). Value = Mean± SEM. Scale bar: 115 µm.

To test the co-localisation between Htr2a and Sst neurons with the Wfs1 positive cells of our transgenic line, I crossed Htr2a-*Cre*::Wfs1-*FlpoER* and Sst-*Cre*::Wfs1-*FlpoER* with the reporter line FL-hM3Dq[189]. Immunostaining of the brain sections allowed us to see the expression of the transgenic Wfs1 in green (*Flp* positive cells) (Figures 3.11 A,D and 3.12 A,D), and the cells that are both Flp and Cre positive in red (Figures 3.11 B,E and 3.12 B,E); in other words the Htr2a and Sst populations in the CeL. Results showed that the expression of the transgenic Wfs1 compared to the same endogenous protein is 77±2.25% for the Htr2a-*Cre*::Wfs1-*FlpoER*::FL-hM3Dq (Figure 3.11 A-G), and 80% for the Sst-*Cre*::Wfs1-*FlpoER*::FL-hM3Dq (3.12 A-G). The percentage of expression of the transgene in Htr2a-*Cre*::Wfs1-*FlpoER*::FL-hM3Dq (77±2.25%) and Sst-*Cre*::Wfs1-*FlpoER*::FL-hM3Dq (80%)

differs from that previously shown in the Wfs1-*FlpoER*::FPDI (65±1.2%). One explanation could be that the Flp recombinase is tamoxifen inducible and the different reporter used genes may vary in stability, signal intensity and fluorescence, being more or less favourable for a specific application.

The expression of the double positive Htr2a and transgenic Wfs1 was 33±5.55% (Figure 3.11 G) and 24% for Sst and transgenic Wfs1 (Figure 3.12 G), compared to the total Wfs1 positive neurons in the CeL. These results are lower compared to the co-localisation between Htr2a/Sst and endogenous Wfs1 (Figures 3.8 F,G and 3.9 C,F,G), mainly due to the reduced expression of the transgenic Wfs1.

Together, these data demonstrate the specificity of our Wfs1-*FlpoER* mouse line and confirm its suitability as a genetic tool to study neuronal CeA populations exclusively in the CeL.

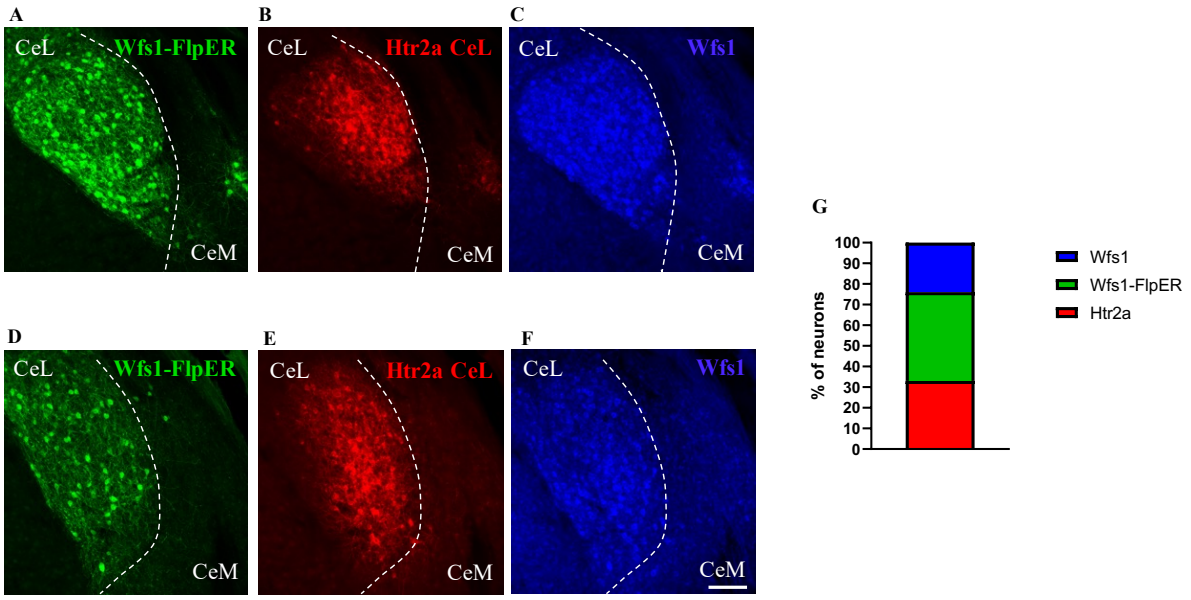

Figure 3.11: Characterisation of CeL^{Htr2a} expression in Htr2a-*Cre*::Wfs1-*FlpoER*::FL-hM3Dq mice

(A,D) Expression of the transgenic Wfs1 in Htr2a-*Cre*::Wfs1-*FlpoER*::FL-hM3Dq. The Flp positive cells are marked in green. **(B,E)** Expression of the Htr2a cells co-localising with the transgenic Wfs1. The Cre and Flp positive cells are marked in red. **(C,F)** Wfs1 antibody staining showing endogenous Wfs1 expression. **(G)** Co-localisation analysis showed that the transgenic Wfs1 marked 77±2.25% of the cells expressing the endogenous Wfs1, and 33±5.55% of the transgenic Wfs1 cells in the CeL are Htr2a positive (n=2 brains, 3 sections per mouse). Value = Mean± SEM. Scale bar: 115 µm.

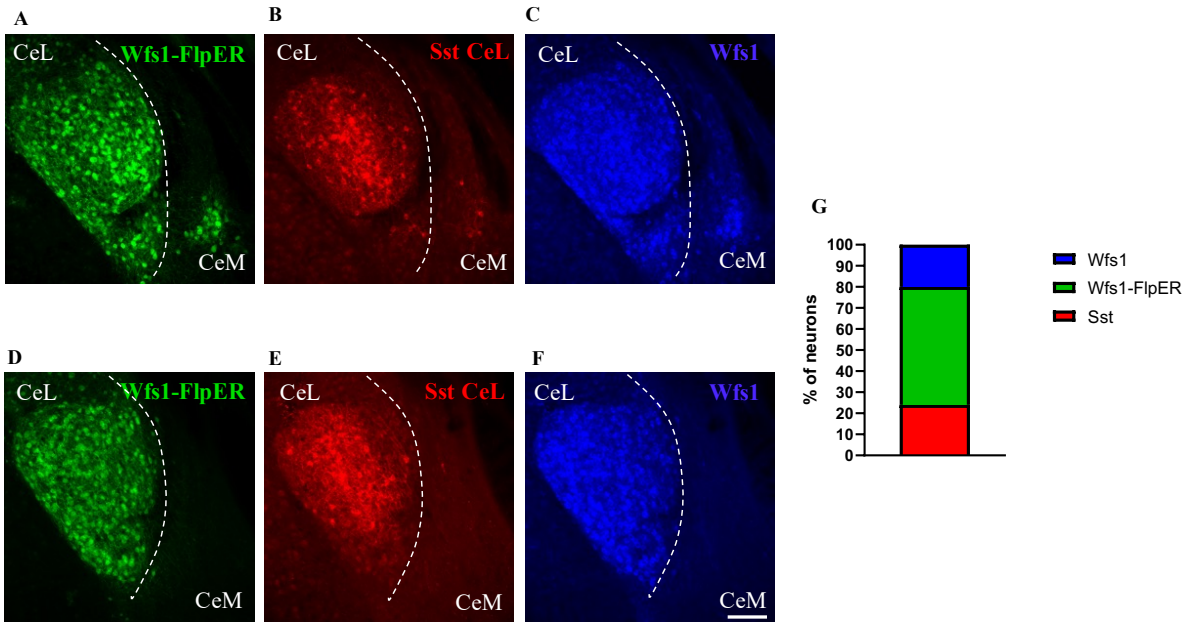

Figure 3.12. Characterisation of CeL^{Sst} expression in Sst-*Cre*::Wfs1-*FlpoER*::FL-hM3Dq mice

(A,D) Expression of transgenic Wfs1 in Sst-*Cre*::Wfs1-*FlpoER*::FL-hM3Dq. The cells marked in green are *Flp* positive cells. **(B,E)** Expression of the Sst cells co localising with the transgenic Wfs1. The *Cre* and *Flp* positive cells are marked in red. **(C,F)** Wfs1 antibody staining showing endogenous Wfs1 expression. **(G)** Co-localisation analysis showed that the transgenic Wfs1 marked 80% of the cells expressing endogenous Wfs1, and 24% of the transgenic Wfs1 cells in the CeL are Sst positive (n=1 brain, 3 sections per mouse). Scale bar: 115 µm.

3.2.3 Validation of optogenetic tools

After characterising the Wfs1-*FlpoER* line, the different roles of CeL$^{Htr2a/Sst}$ and CeM$^{Htr2a/Sst}$ in rewarding and consummatory behaviours could be further investigated. Intersectional optogenetic viruses injected in the CeA of Htr2a-*Cre*::Wfs1-*FlpoER* and Sst-*Cre*::Wfs1-*FlpoER* animals allowed us to specifically and independently manipulate either the CeL or the CeM. The AAV-hSyn-Con/Fon hChR2(H134R)-EYFP-WPRE and the control AAV-hSyn-Con/Fon EYFP-WPRE (CreOn/FlpOn viruses), were expressed in the CeL$^{Htr2a/Sst}$ (cells both Wfs1-*FlpoER* and Htr2a(Sst)-*Cre* positive), the AAV-hSyn-Con/Foff hChR2(H134R)-EYFP-WPRE and control AAV-hSyn-Con/Foff EYFP-WPRE (CreOn/FlpOff viruses), were expressed in the CeM$^{Htr2a/Sst}$ (cells Htr2a(Sst)-*Cre* positive but Wfs1-*FlpoER* negative).

To validate the specificity of expression of the virus in the CeL, I co-injected the control AAV_5-hSyn-Con/Fon EYFP-WPRE together with the AAV_5-Ef1a-DIO-mCherry, in the CeA of Htr2a-*Cre*::Wfs1-*FlpoER* mice. In this way, I could observe the Htr2a neurons in red in the entire CeA (Figure 3.13 A,C,D) while in green, I saw the Htr2a cells in the CeL (Figure 3.13 B,E). Results showed that the CreOn/FlpOn virus specifically expressed in 60% of the CeL^{Htr2a} neurons (Figure 3.13 F). There was 10% of ectopic expression in the CeM (Figure 3.13 G). I am currently analysing more brains and I am repeating the same experiment with Sst-*Cre*::Wfs1-*FlpoER* mice.

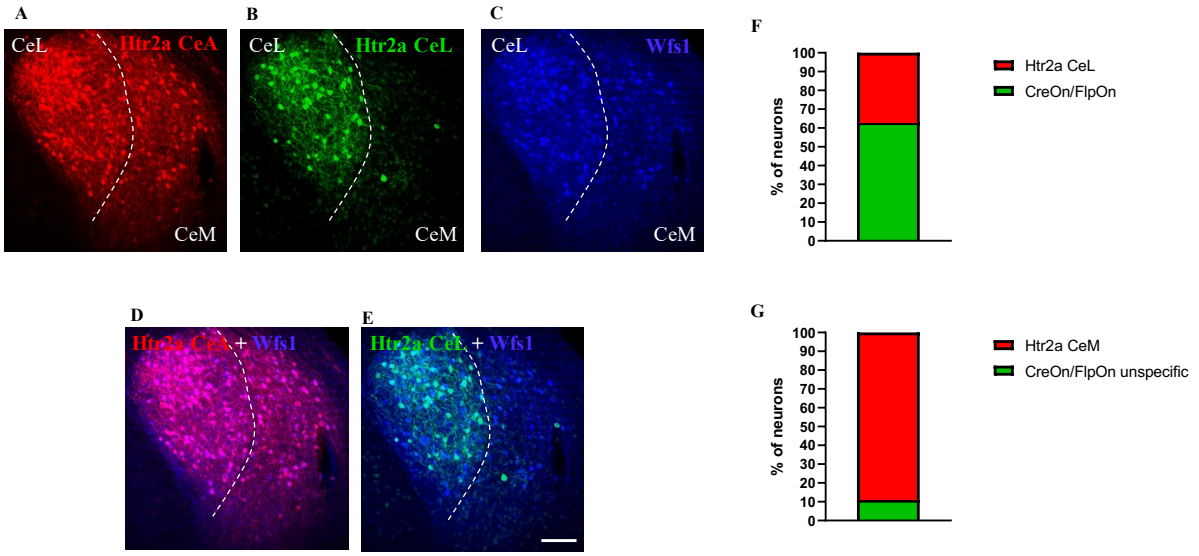

Figure 3.13: Validation of AAV-hSyn-Con/Fon EYFP-WPRE expression in the CeL of Htr2a-*Cre*::Wfs1-*FlpoER* mice

(A) Expression of AAV_5-Ef1a-DIO-mCherry in CeA^{Htr2a} positive cells (CeL and CeM) of Htr2a-*Cre*::Wfs1-*FlpoER* mice**. (B)** Specific viral expression of AAV-hSyn-Con/Fon EYFP-WPRE in CeL^{Htr2a} neurons. **(C)** Wfs1 antibody staining showing endogenous Wfs1 expression. **(D)** Co-localisation between CeA^{Htr2a} neurons and Wfs1. **(E)** Co-localisation between CeL^{Htr2a} neurons and Wfs1. **(F)** Analysis showed that AAV-hSyn-Con/Fon EYFP-WPRE is expressed in 60% of the Htr2a neurons in the CeL. **(G)** The AAV-hSyn-Con/Fon EYFP-WPRE virus has an ectopic expression in the CeM, expressing in 10% of the total CeM^{Htr2a}. (n=1 brain, 3 sections per mouse). Scale bar: 115 µm.

To analyse viral expression in the CeM, I co-injected the control AAV_5-hSyn-Con/Foff EYFP-WPRE together with the AAV_5-Ef1a-DIO-mCherry in the CeA of Htr2a-*Cre*::Wfs1-*FlpoER* mice. I could mark in red the entire population of Htr2a neurons (Figure 3.14 A,C,D), and in

green, the Htr2a neurons in the CeM (Figure 3.14 B,C,E). In this case, the intersectional virus was expressed in 60% of the cells in the CeM (Figure 3.14 F), with 30% ectopic expression in the CeL (Figure 3.14 G). The 30% of ectopic expression in the CeL could be due to the fact that the transgenic Wfs1 is expressed in around the 60% of the Wfs1 positive neurons with a resulting reduction in the co-localisation between the cells expressing the Cre and FlpER recombinases. Since the virus is CreOn/FlpOff, it has to be 'switched off' in the cells that express the FlpER, which are induced by the tamoxifen injections, while the Cre recombinase is constitutively active. A small delay in the FlpER activation, compared to the Cre, could contribute to the ectopic viral expression.

The same experiment is at the moment in progress with Sst-*Cre*::Wfs1-*FlpoER* mice.

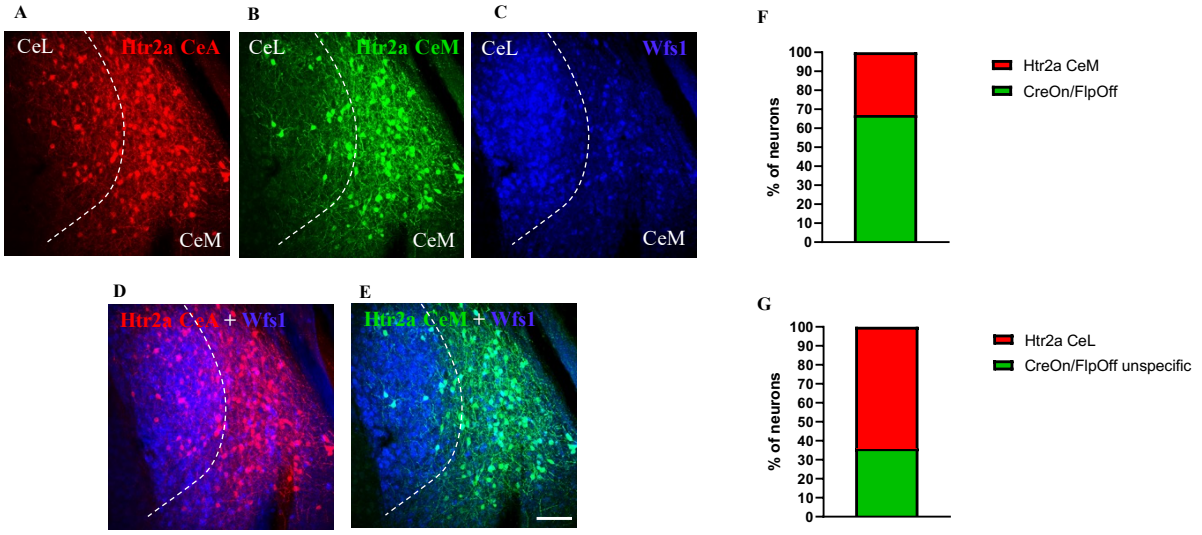

Figure 3.14: Validation of AAV-hSyn-Con/Foff EYFP-WPRE expression in the CeM of Htr2a-*Cre*::Wfs1-*FlpoER* mice

(A) Expression of AAV_5-Ef1a-DIO-mCherry in CeA^{Htr2a} positive cells (CeL and CeM) of Htr2a-*Cre*::Wfs1-*FlpoER* mice**. (B)** Specific viral expression of AAV_5-hSyn-Con/Foff EYFP-WPRE in CeM^{Htr2a} neurons. **(C)** Wfs1 antibody staining showing endogenous Wfs1 expression. **(D)** Co-localisation between CeA^{Htr2a} neurons and Wfs1. **(E)** Co-localisation between CeM^{Htr2a} neurons and Wfs1. **(F)** Analysis showing that AAV_5-hSyn-Con/Foff EYFP-WPRE is expressed in 67% of the Htr2a neurons in the CeM. **(G)** The AAV-hSyn-Con/Foff EYFP-WPRE virus had ectopic expression in the CeL, expressing in 36% of the total CeL^{Htr2a}. (n=1 brain, 3 sections per mouse). Scale bar: 115 µm.

Once the specificity of the viral tools was verified, the different roles of Htr2a and Sst neurons in the CeL and CeM could be further investigated using various behavioural paradigms.

3.2.4 Activation of CeA and CeM Htr2a neurons, but not CeL, promotes drinking behaviour in water deprived as well as fully hydrated mice

To investigate the role of Htr2a neurons in drinking behaviour, I targeted either the entire CeA population or the CeL and CeM populations separately. To target the entire CeA population, I bilaterally injected a Cre-dependent ChR2 virus (AAV_5-hSyn-DIO-hChR2(H134R)-EYFP) and respective control (AAV_5-hSyn-DIO-EYFP) in the CeA of Htr2a-*Cre* mice. To target the CeM population, I injected AAV5-hSyn-Con/Foff-hChR2(H134R)-EYFP in Wfs1-*FlpoER*::Htr2a-*Cre* animals and to target the CeL, I injected AAV_5-hSyn-Con/Fon-hChR2(H134R)-EYFP in the CeL of Htr2a-*Cre*::Wfs1-*FlpoER* animals. Drinking behaviour was analysed for 180 min in water-deprived animals. Briefly, the test started without light stimulation (OFF) for 10 min, followed by 10 min of light (ON, 473 nm, 20 Hz, 10mW). I repeated this cycle three times. To check the effect of a longer and sustained photostimulation on water intake, immediately after the 10 min OFF/ON series, I started a 30 min "light ON" followed by 30 min "light OFF" sequence (30 ON/OFF). This was then repeated twice.

The data showed that during the first 10 min (OFF period), ChR2 expressing animals and controls drank a comparable amount of water (Figure 3.15 A). During this time, we could observe that while the control group was slowly satiated and the water consumption decreased independently of whether the light was ON or OFF, activation of Htr2a neurons in the CeA increased water consumption in every ON period (Figures 3.15 A). In the 30 min ON/OFF paradigm, while the control group was satiated and drank only a very small amount of water during both the ON and OFF periods, activation of CeA^{Htr2a} neurons was sufficient to make the animals consume a significantly greater volume of water (Figure 3.15 B). If we consider the total amount of water consumed during the 10 min OFF/ON (Figure 3.15 C), 30 min ON/OFF paradigm (Figure 3.15 D), as well as the entire behaviour (Figure 3.15 E), we observe that photostimulation of Htr2a neurons in the CeA was sufficient to promote water intake in water deprived animals.

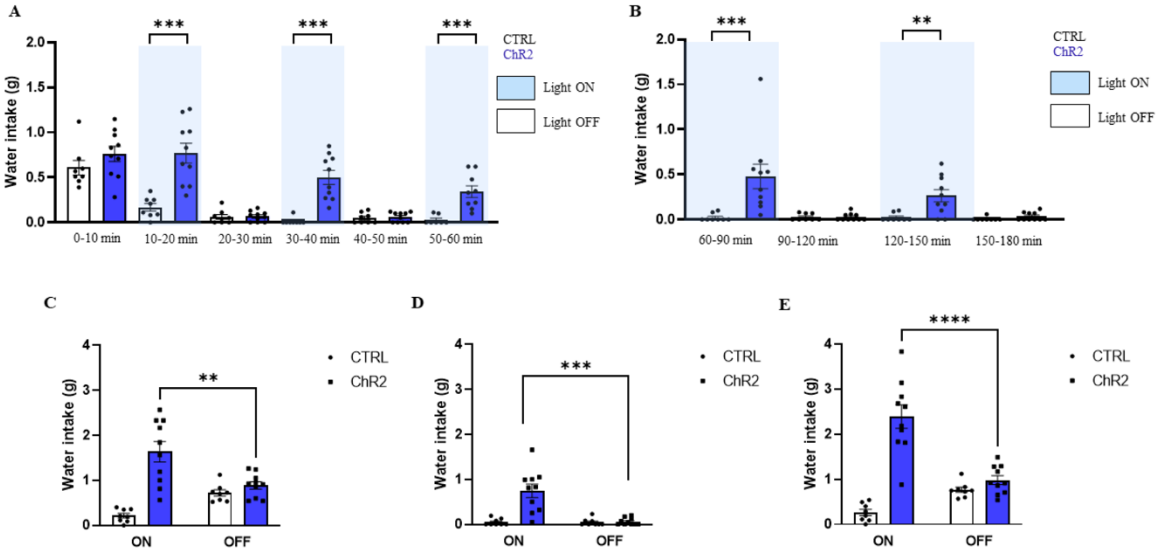

Figure 3.15: Activation of Htr2a neurons increases water intake in water-deprived animals

(A) Htr2a animals expressing either ChR2 or eYFP were subjected to a protocol of 10 min no light stimulation (OFF) and 10 min light stimulation (ON). ChR2 expressing animals showed an increase in water intake during the ON phases as compared to controls (10-20 min, unpaired t test p=0.0003, t=4.655; 30-40 min, Mann-Whitney U test p<0.0001; 50-60 min, Mann-Whitney U test p=0.0001). Control animals mainly drank during the first 10 min (laser OFF). **(B)** The 30 min ON/OFF paradigm showed that the ChR2 expressing animals have increased water intake during the ON phase (60-90 min, Mann-Whitney U test, p=0.002; 120-150 min, Mann-Whitney U test, p=0.0052). **(C)** Total amount of water intake in the 10 OFF/ON paradigm, ChR2 expressing mice consumed more water during the ON period compared to control (interaction, Two-way ANOVA, $F_{(1,32)}$ =19.79, p<0.0001; ChR2, Two-way ANOVA, $F_{(1,32)}$ =31.84, p<0.0001). **(D)** CeA^{Htr2a} neuronal photostimulation induced significantly more drinking in the ON period during 30 min ON/OFF stimulation (for ChR2 ON versus ChR2 OFF, Mann-Whitney U test, p=0.0001). **(E)** The total amount of water consumed during the entire behaviour showed a significant increase in drinking behaviour when the animals expressing ChR2 were photostimulated as compared to controls (interaction, Two-way ANOVA, $F_{(1,32)}$ =35.10, p<0.0001; light, Two-way ANOVA, $F_{(1,32)}$ =7.866, p=0.0085; ChR2, Two-way ANOVA, $F_{(1,32)}$ =52.76, p<0.0001). Value = Mean± SEM, *p < 0.05, **p < 0. 01.

Activation of CeM^{Htr2a} showed comparable results to those of CeA^{Htr2a}. In the 10 min OFF/ON paradigm, the ChR2 expressing mice drank every time the light was ON (Figure 3.16 A). In the 30 min ON/OFF phase, while the control group consumed only a limited amount of water during both ON and OFF period, the ChR2 expressing animals drank only during the 'light ON' phase (Figure 3.16 B). The effect of photostimulation of CeM^{Htr2a} in promoting water intake in water-deprived mice is evident in the 10 min OFF/ON (Figure 3.16 C), 30 min ON/OFF paradigm (Figure 3.16 D), as well as the entire behaviour (Figure 3.16 E).

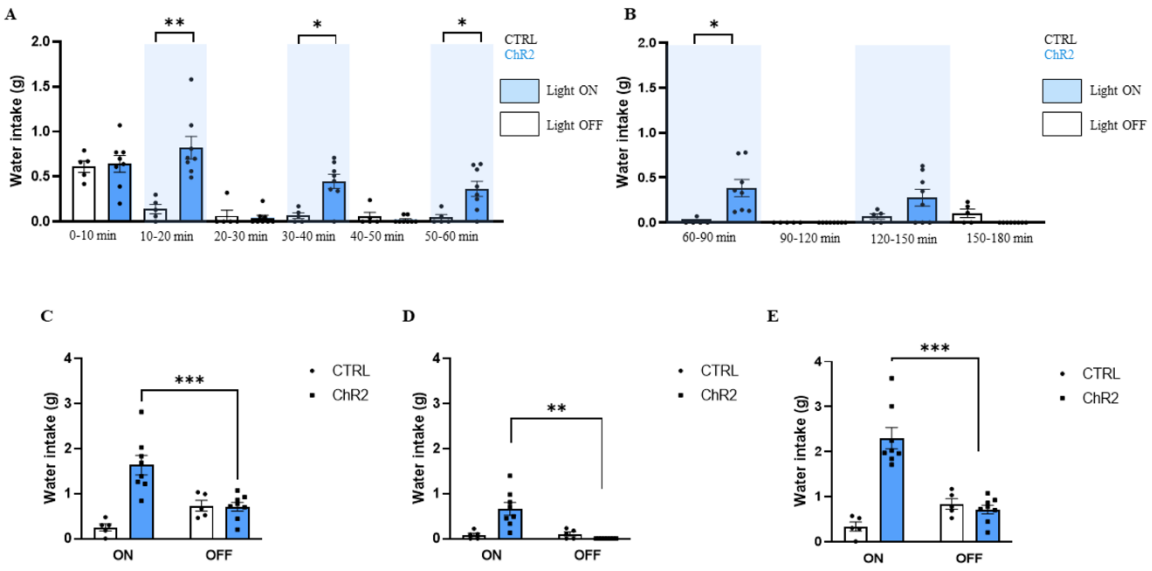

Figure 3.16: Activation of CeM^{Htr2a} neurons increases drinking behaviour in water-deprived mice

(A) Stimulation of CeM^{Htr2a} neurons using a protocol of 10 min OFF and 10 min ON increased drinking behaviour during the ON phase in animals expressing ChR2 (10-20 min, unpaired t test p=0.0017, t=4.128; 30-40 min, unpaired t test p=0.0038, t=3.657; 50-60 min Mann-Whitney U test p=0.0194). **(B)** 30 min light ON stimulated drinking (60-90 min, Mann-Whitney U test p=0.0016,). **(C)** In the 10 min OFF/ON paradigm, activation of CeM^{Htr2a} cells increased water intake (interaction, Two-way ANOVA, $F_{1,22}$ =18.85, p=0.003; ChR2, Two-way ANOVA, $F_{1,22}$ =17.69, p=0.0004) **(D)** The 30 min ON/OFF series increased water intake in animals expressing ChR2 during light ON (for ChR2 ON versus ChR2 OFF: Wilcoxon signed-rank test p=0.0078). **(E)** Light effect of CeM^{Htr2a} cells stimulation in promoting total drinking behaviour (for ChR2 ON versus ChR2 OFF: Mann-Whitney U test p=0.0002). Value = Mean± SEM, *$p < 0.05$, **$p < 0.01$.

Activation of CeL^{Htr2a} was insufficient to stimulate drinking behaviour. The ChR2-expressing CeL animals and the control group showed, in fact, the same trend in the amount of water consumed over time, with the majority of it drank during the first 10 min (OFF period) (Figure 3.17 A,B). Looking at the water consumption during the 10 min OFF/ON paradigm, there is a significant difference of water intake between the ON and OFF periods, both for ChR2 and control animals, however, unlike with the CeM^{Htr2a} neurons, the greatest amount was consumed during the OFF period (Figure 3.17 C). The same results were also seen regarding total water intake (Figure 3.17 E). In the 30 min ON/OFF paradigm both groups, at this point satiated, consumed a limited amount of water, with no light effect (Figure 3.17 D).

The CeL^{Htr2a} behavioural outcome can be explained by the fact that both groups, being water-deprived, drank the majority of the water in the first 10 min (OFF) of the behaviour experiment. The two water consumption graphs then have the same progress, that is, slowly going to zero, as the animals become satiated. In the CeA and CeM ChR2 groups instead, every photostimulation was able to increase the water intake.

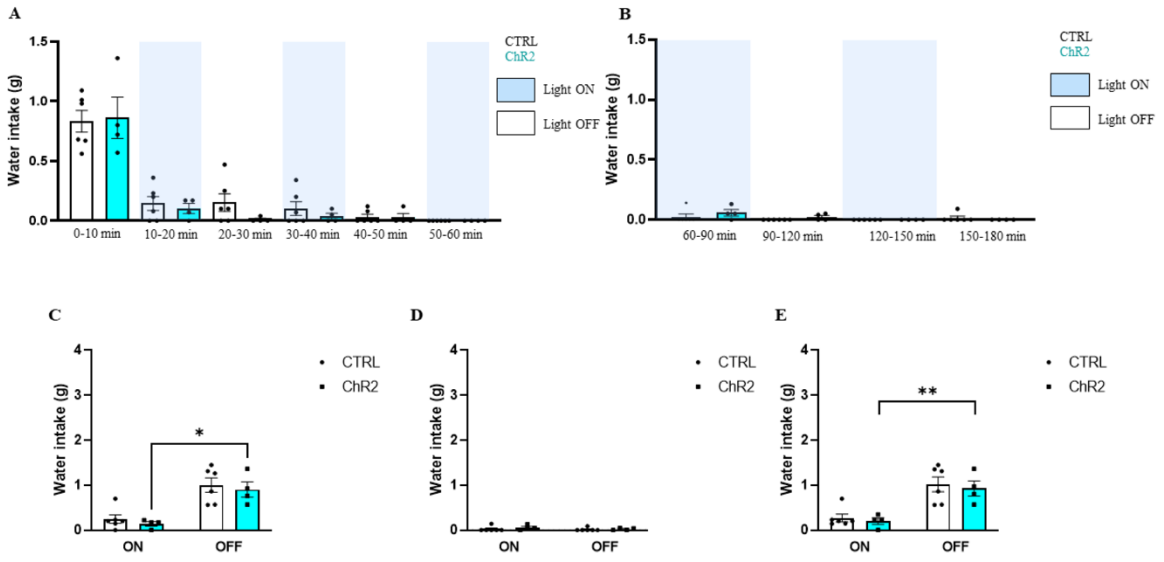

Figure 3.17: Activation of CeL^{Htr2a} failed to elicit drinking behaviour

(A) No difference was seen in the drinking behaviour between ChR2 expressing animals in the CeL and controls (10-20 min, unpaired t test p=0.6105, t=0.5301; 30-40 min, unpaired t test p=0.4116, t=0.8662; 50-60 min, Wilcoxon signed-rank test samples with equal values). **(B)** No light effect during the 30 min light ON period (60-90 min, Mann-Whitney U test p=0.1905). **(C)** In the 10 min OFF/ON paradigm mice drank more during the OFF period (interaction, Two-way ANOVA, $F_{1,16}$ =0.0008, p=0.9783; ChR2, Two-way ANOVA, $F_{1,16}$ =0.5757, p=0.4590). **(D)** Very limited water consumption for ChR2 expressing animals and controls in the 30 min ON/OFF phase (for ChR2 ON versus ChR2 OFF: unpaired t test p=0.2866, t=1.169). **(E)** In the total behaviour, a greater volume of water was consumed during the OFF period for the ChR2 expressing mice (for ChR2 ON versus ChR2 OFF: Mann-Whitney U test p=0.0286). Value = Mean± SEM, *$p < 0.05$, **$p < 0.01$.

To understand whether activation of Htr2a cells in the CeA and CeM is sufficient to promote drinking of hydrated mice, I performed the same behavioural paradigm, 10 min OFF/ON followed by 30 min ON/OFF, with the same mice expressing ChR2 specifically in either the CeA or CeM, having *ad libitum* water in their cage until the behaviour started.

The results of the CeA^{Htr2a} activation, showed that the control group consumed a very limited amount of water during the entire behavioural paradigm (Figure 3.18 A,B), while photostimulation of CeA^{Htr2a} cells induced drinking behaviour in a significant way whenever the laser was ON (Figure 3.18 A,B). The effect of Htr2a neuronal activation in promoting drinking is observable considering the total amount of water consumed by the animals expressing ChR2 in the CeA^{Htr2a} cells, in the 10 min OFF/ON (Figure 3.18 C), 30 min ON/OFF (Figure 3.18 D) series and the entire behaviour (Figure 3.18 E). Mice were actively drinking only during the light ON phases, showing instead, during the OFF phases, the same behaviour as the control group.

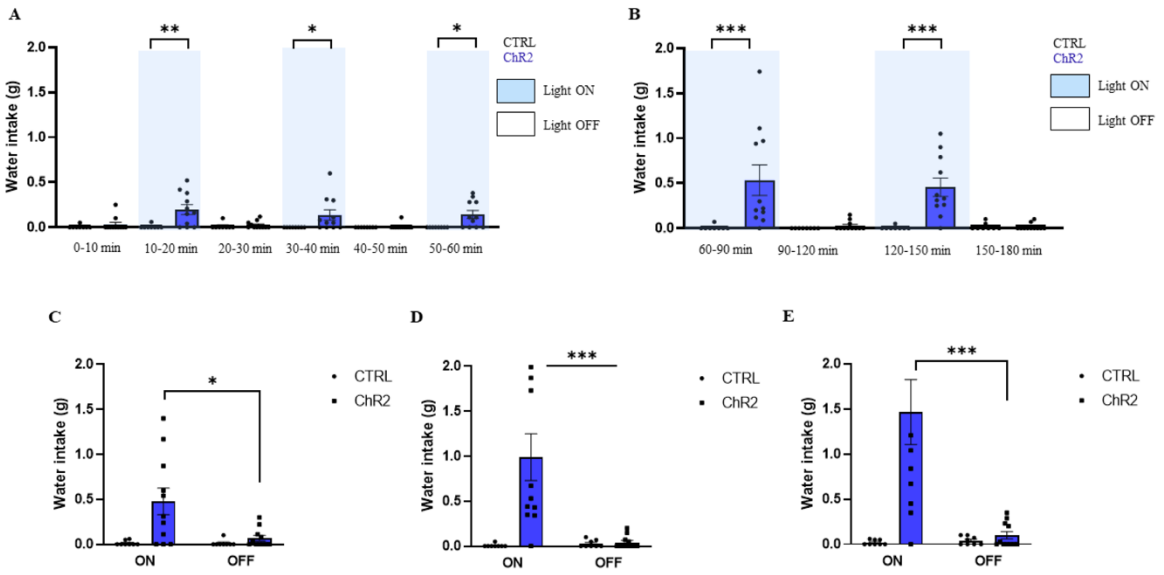

Figure 3.18: Activation of CeA^{Htr2a} neurons promotes drinking behaviour in mice under normal conditions

(A) ChR2 expressing animals in the CeA^{Htr2a} cells, subjected to a protocol of 10 min no light stimulation (OFF) and 10 min light stimulation (ON) in the presence of water, showed drinking behaviour during the ON phase (10-20 min, Mann-Whitney U test p=0.0077; 30-40 min, Wilcoxon signed-rank test t p=0.0156; 50-60 min, Wilcoxon signed-rank test t p=0.0156) as compared to the controls. **(B)** The results of the 30 ON/OFF phase showed drinking behaviour only for the ChR2 animals and not the controls (60-90 min, Mann-Whitney U test p=0.0003; 120-150 min, Mann-Whitney U test p=0.0003). **(C)** In the 10 min OFF/ON paradigm, ChR2 expressing animals consumed water only during the ON period (for ChR2 ON versus ChR2 OFF: Mann-Whitney U test p=0.0241). **(D)** In the 30 min ON/OFF paradigm, ChR2 expressing animals drank only during light ON (for ChR2 ON versus ChR2 OFF: Mann-Whitney U test p=0.0001). **(E)** In the entire behavioural paradigm, while for the controls the light activation had no effect, in the ChR2 expressing animals it significantly promoted drinking behaviour

(for ChR2 ON versus ChR2 OFF: Mann-Whitney U test p=0.0002). Value = Mean± SEM, *$p < 0.05$, **$p < 0.01$.

Activation of CeM^{Htr2a} neurons was sufficient to stimulate drinking behaviour in ChR2 expressing animals in both the 10 min OFF/ON (Figure 3.19 A) and in the 30 min ON/OFF (Figure 3.19 B) phases. Very limited water intake was seen in the control group throughout the entire paradigm (Figure 3.19 A,B). The difference in drinking between the photostimulated and control groups is visible with regard to the total amount of water consumed in the 10 min OFF/ON (Figure 3.19 C), 30 min ON/OFF (Figure 3.19 D) series, as well as the total amount consumed (Figure 3.19 E). It can thus be clearly stated that activation of CeM^{Htr2a} cells promoted drinking in all the ON phases.

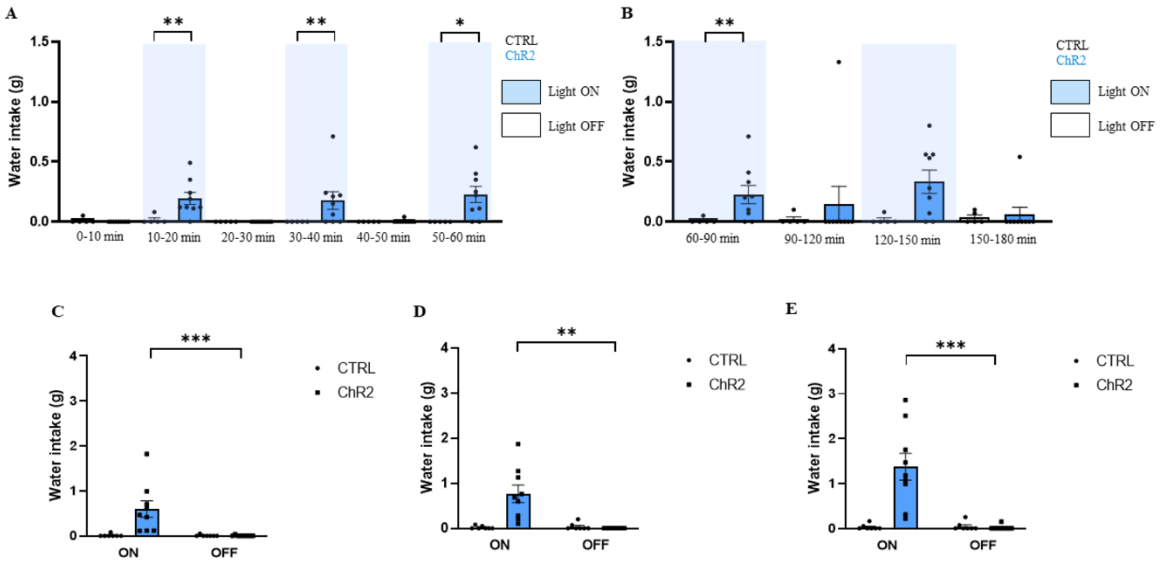

Figure 3.19: Activation of CeM^{Htr2a} neurons promotes drinking in hydrated mice

(A) Optogenetic activation of CeM^{Htr2a} neurons, during a protocol of 10 min OFF and 10 min ON, stimulated drinking only during the ON phase (10-20 min, Mann-Whitney U test p=0.0065; 30-40 min, Wilcoxon signed-rank test t p=0.0313; 50-60 min, Wilcoxon signed-rank test p=0.0156). **(B)** During the first 30 min light ON period, animals expressing ChR2 consumed much more water in contrast to the control group (60-90 min, Mann-Whitney U test p=0.0215; 60-90 min, Mann-Whitney U test p=0.0340). **(C)** In the 10 min OFF/ON paradigm, activation of CeM^{Htr2a} cells increased the total amount of water intake (for ChR2 ON versus ChR2 OFF: Mann-Whitney U test p<0.0001)). **(D)** In the 30 min ON/OFF paradigm, photostimulation of CeM^{Htr2a} cells increased water intake (for ChR2 ON versus ChR2 OFF: Wilcoxon signed-rank test p=0.0039). **(E)** The effect of CeM stimulation in promoting drinking behaviour is visible with regard to the total amount of water consumed during the entire behaviour (for ChR2 ON versus ChR2 OFF: Mann-Whitney U test p<0.0001). Value = Mean± SEM, *$p < 0.05$, **$p < 0.01$.

Together these data show that Htr2a neurons are sufficient to promote drinking behaviour in thirsty and hydrated mice and demonstrates that within the CeA, the subregion responsible for this behaviour is the CeM.

3.2.5 CeM^{Sst} neurons promote drinking behaviour in water deprived and hydrated mice

To study the effect of Sst activation on drinking behaviour, I targeted the CeA^{Sst} population by injecting a Cre-dependent ChR2 virus (AAV_5-hSyn-DIO-hChR2(H134R)-EYFP) or corresponding control (AAV_5-hSyn-DIO-EYFP) in Sst-*Cre* mice, and the CeM^{Sst} population by injecting AAV_5-hSyn-Con/Foff-hChR2(H134R)-EYFP or the control virus AAV_5-hSyn-Con/Foff-EYFP in Sst-*Cre*::Wfs1-*FlpoER*. I therefore applied the same 10 min OFF/ON and 30 min ON/OFF behavioural paradigm that I had used to test water deprivation in Htr2a mice. The results show that photostimulation of CeA^{Sst} cells during the 10 min OFF/ON (Figure 3.20 A) and 30 min ON/OFF (Figure 3.20 B) paradigms promoted water intake in ChR2 expressing animals as compared to the control group. While for the controls, the amount of consumed water gradually diminished after the first 10 min and was close to zero in the 30 min ON/OFF paradigm, neuronal activation promoted drinking every interval the light was ON in ChR2 expressing animals (Figure 3.20 A-B). The effect of increased water intake is recapitulated in the graphs showing the total amount of water drank in the 10 min OFF/ON (Figure 3.20 C), 30 min ON/OFF (Figure 3.20 D), as well as in the total behaviour (Figure 3.20 E).

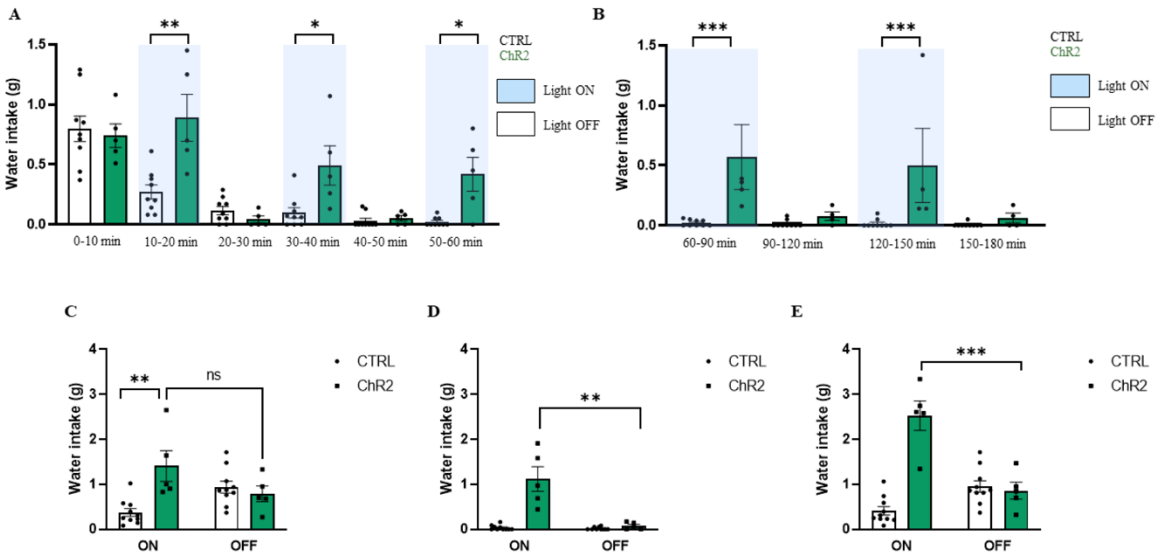

Figure 3.20: CeA^{Sst} photostimulation promotes drinking in water deprivation

(A) Optogenetic activation of CeA^{Sst} cells during a protocol of 10 min OFF and 10 min ON promoted water consumption during the ON phase (10-20 min, unpaired t test p=0.0026, t=3.791; 30-40 min, Mann-Whitney U test p=0.0115; 50-60 min, Mann-Whitney U test p=0.0215). **(B)** An increase in drinking for the ChR2 expressing animals is visible during the 30 min light ON period compared to the controls (60-90 min, Mann-Whitney U test p=0.00010; 120-150 min, Mann-Whitney U test p=0.0005). **(C)** In the 10 min OFF/ON paradigm, activation of CeA^{Sst} cells increased water intake (interaction, Two-way ANOVA, $F_{1,24}$ =10.34, p=0.0037; light, Two-way ANOVA, $F_{1,24}$ =0.0315, p=0.8606; ChR2, Two-way ANOVA, $F_{1,24}$ =5.502, p=0.0276). **(D)** In the 30 min ON/OFF paradigm, ChR2 expressing animals drank significantly more with light ON (for ChR2 ON versus ChR2 OFF: unpaired t test p=0.0054, t=3.781). **(E)** During the entire behaviour, activation of Sst neurons promoted drinking (interaction, Two-way ANOVA, $F_{1,24}$ =37.23, p<0.001; light, Two-way ANOVA, $F_{1,24}$ =9.799, p=0.0045; ChR2, Two-way ANOVA, $F_{1,24}$ =30.37, p<0.0001). Value = Mean± SEM, *p < 0.05, **p < 0. 01.

Preliminary results (experiments to increase the 'n' number are ongoing) showed a similar effect also due to activation of CeM^{Sst} cells. During the first photostimulation (10-20 min), ChR2 expressing animals drank significantly more than the controls (Figure 3.21 A). Currently, there is a tendency to an increased water consumption during activation between 30-40 min and 50-60 min, but the difference is not significant (Figure 3.21 A). In the 30 min ON/OFF paradigm, I did not observe a significant increase in water consumption in the first 30 min, nor between 120 and 150 min (Figure 3.21 B). Considering the total amount of water intake, rather than distinct time points, in the 10 min OFF/ON, 30 min ON/OFF and the total behaviour, the Sst animals expressing ChR2 in the CeM drank significantly more when photostimulated than

without stimulation (Figure 3.21 C-E). Together these results show an involvement of Sst neurons in drinking with the CeM as the responsible CeA subregion.

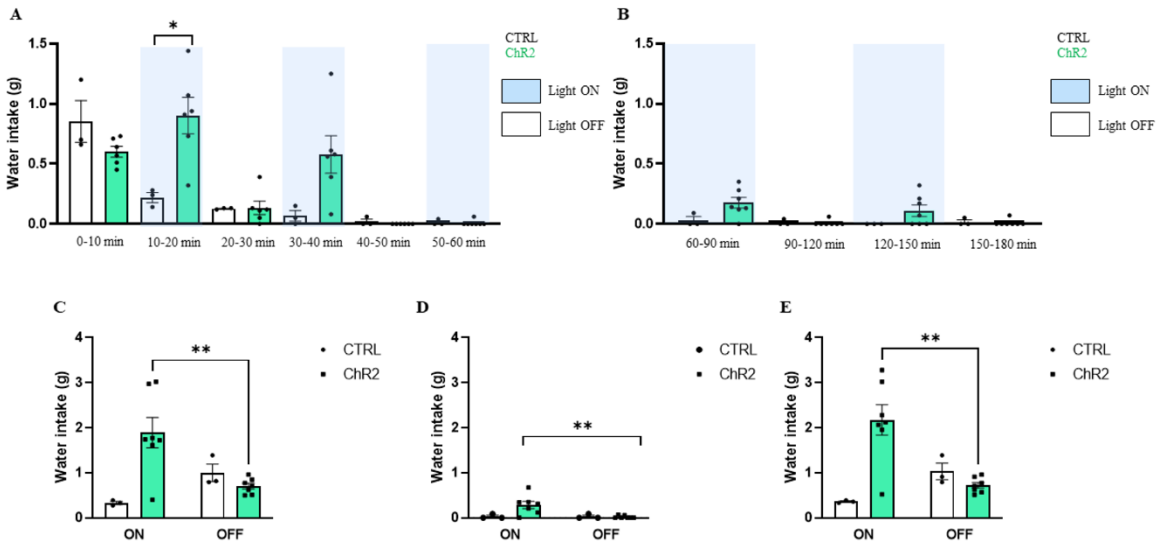

Figure 3.21: Activation of CeM^{Sst} neurons increases water intake in water deprived mice

(A) Optogenetic activation of CeM^{Sst} neurons during a protocol of 10 min OFF/ON significantly promoted drinking in ChR2 expressing animals as compared to the control only in the first 'light ON' period (10-20 min, unpaired t test p=0.0185, t=3,053; 30-40 min, unpaired t test p=0.0625, t=2.214; 50-60 min, unpaired t test p=0.0832, t=2.019). **(B)** No significant effect on drinking during the 30 min light ON period (60-90 min, Mann-Whitney U test p=0.0667, 120-150 min, Wilcoxon signed-rank test p=0.1250). **(C)** Activation of CeM^{Sst} cells increased water intake in the 10 OFF/ON paradigm (interaction, Two-way ANOVA, $F_{1,16}$ =11.10, p=0.0042; light, Two-way ANOVA, $F_{1,16}$ =0.8606, p=0.3674; ChR2, Two-way ANOVA, $F_{1,16}$ =5.132, p=0.0377), **(D)** and in the 30 ON/OFF paradigm (for ChR2 ON versus ChR2 OFF: Mann-Whitney U test p=0.0064). **(E)** The effect of CeM stimulation in promoting drinking behaviour is visible considering the total amount of water consumed during the entire behaviour (interaction, Two-way ANOVA, $F_{1,16}$ =14.78, p=0.0014; light, Two-way ANOVA, $F_{1,16}$ =2.015, p=0.1749; ChR2, Two-way ANOVA, $F_{1,16}$ =7.441, p 0=0.0149). Value = Mean± SEM, *p < 0.05, **p < 0.01.

To test whether activation of Sst neurons is sufficient to promote drinking behaviour, I repeated the same behavioural paradigm with the same animals (10 min OFF/ON, 30 min ON/OFF), but in this case, without water deprivation, in an *ad libitum* water condition. Preliminary results showed that activation of CeA^{Sst} neurons failed to elicit any perturbation in drinking behaviour: no significant effect between ChR2 expressing animals and controls during photostimulation

either in the 10 min OFF/ON (Figure 3.22 A) or 30 min ON/OFF paradigm (Figure 3.22 B). In addition, no effect was seen with regard to the total amount of water drank during the 10 min OFF/ON behaviour, where both ChR2 and control animals drank very little amount of water (Figure 3.22 C). Only two ChR2 animals out of six consumed around 0.5g of water with light ON in the 30 min ON/OFF phase (Figure 3.22 D), not enough for the effect to be statistically significant. This non statistically significant effect was also present in the last graph, with regard to the total amount of water consumed in the entire behaviour (Figure 3.22 E).

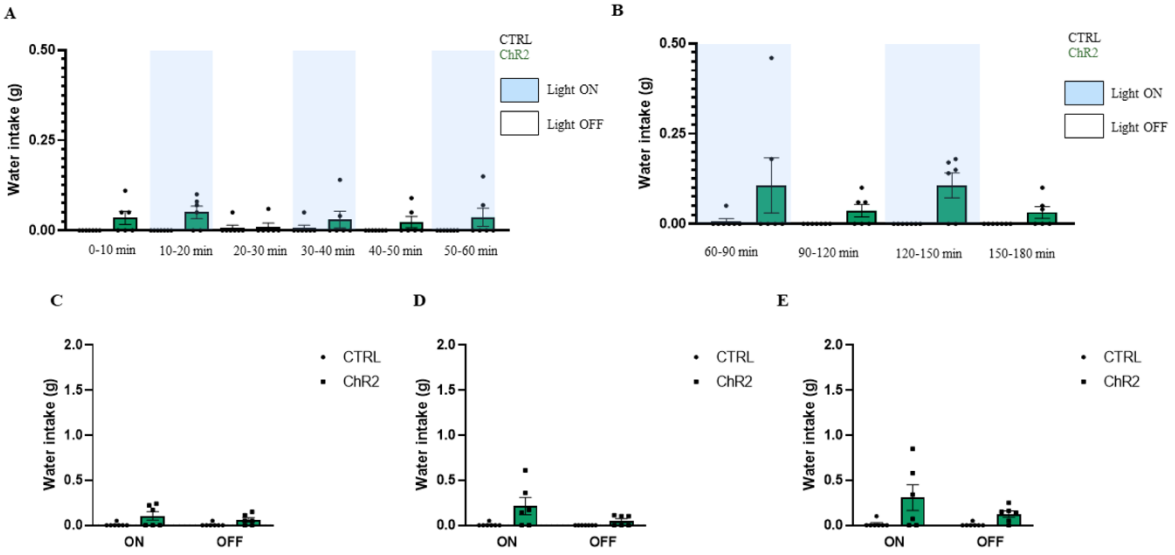

Figure 3.22: Photostimulation of CeA^{Sst} cells does not promote water consumption in hydrated mice

(A) Optogenetic activation of CeA^{Sst} neurons during a protocol of 10 min OFF/ON did not increase drinking significantly during the ON phase in the ChR2 expressing animals compared to the controls (10-20 min, Wilcoxon signed-rank test p=0.1250; 30-40 min, Mann-Whitney U test p=0.4371; 50-60 min, Wilcoxon signed-rank test p=0.5). **(B)** No significant effect of light stimulation during the 30 min light ON period (60-90 min, Mann-Whitney U test p=0.3147; 120-150 min, Wilcoxon signed-rank test p=0.1250). **(C)** No significant increase in water intake in ChR2 expressing animals in the 10 OFF/ON paradigm (for ChR2 ON versus ChR2 OFF: Mann-Whitney U test p=0.6537), **(D)** as well as in the 30 ON/OFF paradigm (for ChR2 ON versus ChR2 OFF: Mann-Whitney U test p=0.1558). **(E)** No effect of light stimulation in drinking between ChR2 expressing animals and controls in the entire behaviour (for ChR2 ON versus ChR2 OFF: Mann-Whitney U test p=0.6991). Value = Mean± SEM, *$p < 0.05$, **$p < 0.01$.

Preliminary results obtained by activating the CeM^{Sst} neurons showed an involvement of this CeM subpopulation in promoting drinking under normal conditions. Looking at the overall water consumption in the 10 (Figure 3.23 C) and 30 min (Figure 3.23 D) ON/OFF paradigms, as well as in the complete behaviour (Figure 3.23 E), photostimulation of Sst neurons in the CeM elicited drinking in the ChR2 animals that during the OFF phase did not show any water intake. The control group did not consume water during the entire paradigm (Figure 3.23 C-E). During the behaviour, every time the laser was ON for 10 min it generated an increase in the water consumption for the ChR2 animals, although currently, this finding is not statistically significant (Figure 3.23 A). With the light ON for 30 min, it is instead possible to observe a significant effect in the first 30 min of the experiment (Figure 3.23 B). Additional animals are currently being tested to confirm the data.

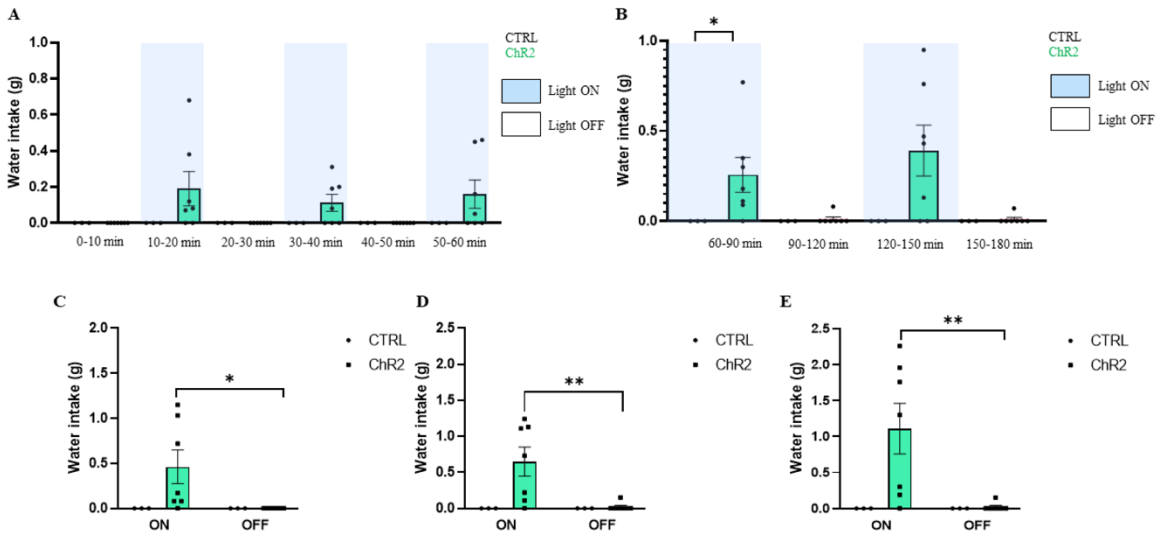

Figure 3.23: Activation of CeM^{Sst} neurons promotes water consumption in mice under normal conditions

(A) Preliminary results of optogenetic activation of CeM^{Sst} neurons during a 10 min OFF/ON behaviour showed an increase in drinking for the ChR2 expressing animals when the light was ON but not in a significant way (10-20 min, Wilcoxon signed-rank test p=0.0625; 30-40 min, Wilcoxon signed-rank test p=0.1250; 50-60 min, Wilcoxon signed-rank test p=0.1250). **(B)** During the first 30 min of the 30 light ON/OFF paradigm there was a significant effect on drinking in ChR2 expressing animals (60-90 min, Wilcoxon signed-rank test p=0.0313; 120-150 min Wilcoxon signed-rank test p=0.0625). **(C)** Activation of CeM^{Htr2a} cells increased water intake during the 10 OFF/ON paradigm (for ChR2 ON versus ChR2 OFF: Wilcoxon signed-rank test p=0.0313), **(D)** as well as in the 30 ON/OFF paradigm (for ChR2 ON versus ChR2 OFF: Mann-Whitney U test p=0.0087). **(E)** The effect of CeM stimulation in promoting drinking behaviour is visible when considering the total amount of water consumed during

the entire behaviour (for ChR2 ON versus ChR2 OFF: Mann-Whitney U test p=0.0047). Value = Mean± SEM, *$p < 0.05$, **$p < 0.01$.

To summarise, the data show an involvement of the Sst population in drinking, with the CeM subregion being chiefly responsible for the behaviour. While the CeM population was able to promote drinking in water deprived animals but also under *ad libitum* conditions, the CeA showed an effect only in thirsty animals. Further experiments to increase the number of animals of both groups and to test the involvement of the CeL^{Sst} neurons are underway.

3.2.6 Effect of Htr2a and Sst neuronal activation in the CeA and its subregions on drinking behaviour.

In my previous results, I tested the involvement of Htr2a and Sst neurons in the CeA and its subregions using a behaviour where I alternated phases of photostimulation with phases of light off. Moreover, I also tested the effect of brief neuronal activation (10 min), as well as a more sustained one (30 min), repeating them several times during the same behavioural paradigm to check if the effect of optogenetic stimulation had a comparable effect in every reiteration. In order to have a 'screenshot' of the result of Htr2a and Sst cells activation in drinking behaviour in a limited time, I tested Htr2a-*Cre* and Sst-*Cre* mice expressing Chr2 in the CeA and Htr2a-*Cre*::Wfs1-*FlpoER* and Sst-*Cre*::Wfs1-*FlpoER* expressing ChR2 in the CeM or CeL in a shorter behavioural paradigm in which thirsty mice were exposed to water for 30 min while being photostimulated for the whole time. I also repeated the same experiment with mice under normal conditions. The results were similar to those from the experiments conducted alternating light ON and OFF. Activation of Htr2a neurons in the CeA and CeM was sufficient to stimulate drinking behaviour both in water deprived and hydrated animals (Figures 3.24 A-B, 3.25 A-B). Light stimulation of CeL^{Htr2a} neurons failed to promote drinking (Figure 3.24 C). For the Sst groups, preliminary results suggest that CeM^{Sst} neurons are those mainly responsible for triggering water consumption under normal and water deprived conditions (Figures 3.24 E, 3.25 D). In this 30 min behaviour, in contrast to the previous results, activation of CeA^{Sst} neurons failed to induce drinking in water deprived animals, suggesting perhaps, the need of sustained and repeated neuronal activation (Figure 3.24 D). No effect on drinking was seen also for activation of CeA^{Sst} cells in mice under normal condition (Figure 3.25 C), as previously described.

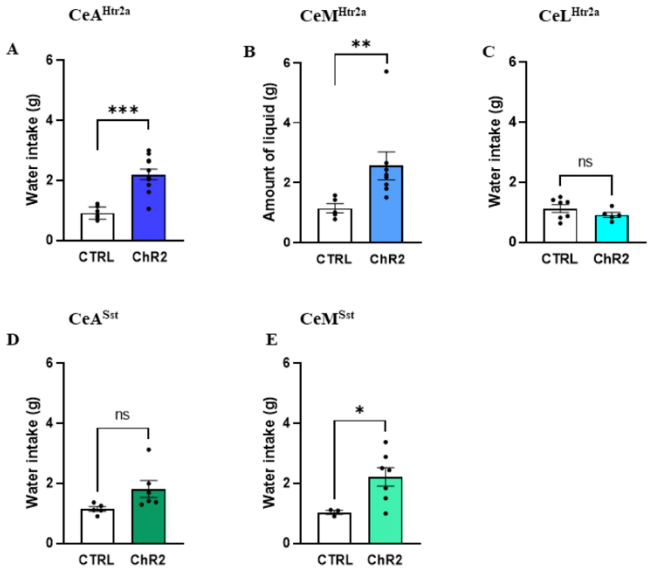

Figure 3.24: Activation of Htr2a and Sst neurons in the CeA and CeM promotes drinking behaviour in water deprived animals

(A) Activation of CeA^{Htr2a} neurons significantly increased water consumption when compared to control animals (unpaired t test $p<0.0001$, t=5.585). **(B)** A significant effect in drinking could be observed upon activation of CeM^{Htr2a} neurons (Mann-Whitney U test $p=0.0031$), **(C)** while no difference was seen between animals expressing ChR2 in the CeL and relative controls in the total amount of water consumed (unpaired t test $p=0.2373$, t=1.257). **(D)** Activation of CeA^{Sst} cells was not sufficient to drive drinking behaviour (unpaired t test $p=0.0663$, t=2.089). **(E)** A significant increase in water intake followed CeM^{Sst} neuron stimulation (unpaired t test $p=0.0431$, t=2.401). Value = Mean± SEM, $*p < 0.05$, $**p < 0.01$.

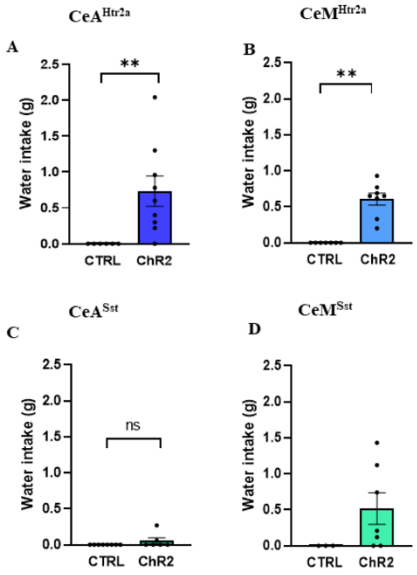

Figure 3.25: Activation of Htr2a in the CeA and Htr2a and Sst neurons in the CeM promotes drinking behaviour in hydrated animals

(A) Activation of Htr2a neurons in CeA stimulated drinking (Wilcoxon signed-rank test p=0.0078). **(B)** CeM^{Htr2a} neuron photostimulation induced drinking behaviour compared to controls (Wilcoxon signed-rank test p=0.0078). **(C)** No difference in water consumption between mice expressing ChR2 in CeA^{Sst} neurons and controls (Wilcoxon signed-rank test p=0.5). **(D)** Preliminary results of activation of CeM^{Sst} cells showed a positive trend in promoting water intake (Wilcoxon signed-rank test p=0.0625). Value = Mean± SEM, *$p < 0.05$, **$p < 0.01$.

3.2.7 PKCδ neuron activation inhibits drinking in water deprived animals

In the CeA, Htr2a and PKCδ neurons modulate eating behaviour with a local circuit mechanism: the anorexigenic PKCδ cells inhibit feeding via local inhibition of the rewarding Htr2a neurons[2]. Thus, two different and not overlapping CeA subpopulations control antagonistic consummatory behaviour (feeding) via reciprocal inhibitory connections. Because of this, after demonstrating the involvement of Htr2a neurons in drinking, an additional consummatory behaviour to feeding, I decided to investigate the role of the PKCδ neurons and a possible local circuit mechanism regulating drinking within the CeA. I bilaterally injected AAV$_5$-hSyn-DIO-hChR2(H134R)-EYFP and the respective control AAV$_5$-hSyn-DIO-EYFP in PKCδ-*Cre* mice to analyse the effect of PKCδ cell activation during drinking behaviour in water deprived animals.

The mice underwent a protocol of 10 min ON/OFF and 30 min OFF/ON, similar to the protocol described previously. However, in this case the laser was ON during the first 10 min. Results showed that while the controls drank the majority of the volume during the first 10 min, activation of PKCδ neurons completely stopped drinking behaviour during this time (Figure 3.26 A). In the controls, the amount of water consumed gradually diminished with time as the mice became satiated, independently of the light phase. The ChR2 expressing animals, instead, consumed water only during the OFF phases (Figure 3.26 A). During the 30 min OFF/ON paradigm, the control group consumed a very little amount of water during the entire experiment, while the ChR2 expressing animals drank significantly more when the light was OFF, between 120 and 150 min (Figure 3.26 B). The strong reduction in drinking behaviour, due to PKCδ neuronal photostimulation, is observable in the graphs that summarize the behavioural paradigm (Figure 3.26 C-E): PKCδ-*Cre* animals expressing ChR2 drank most exclusively during the light OFF period.

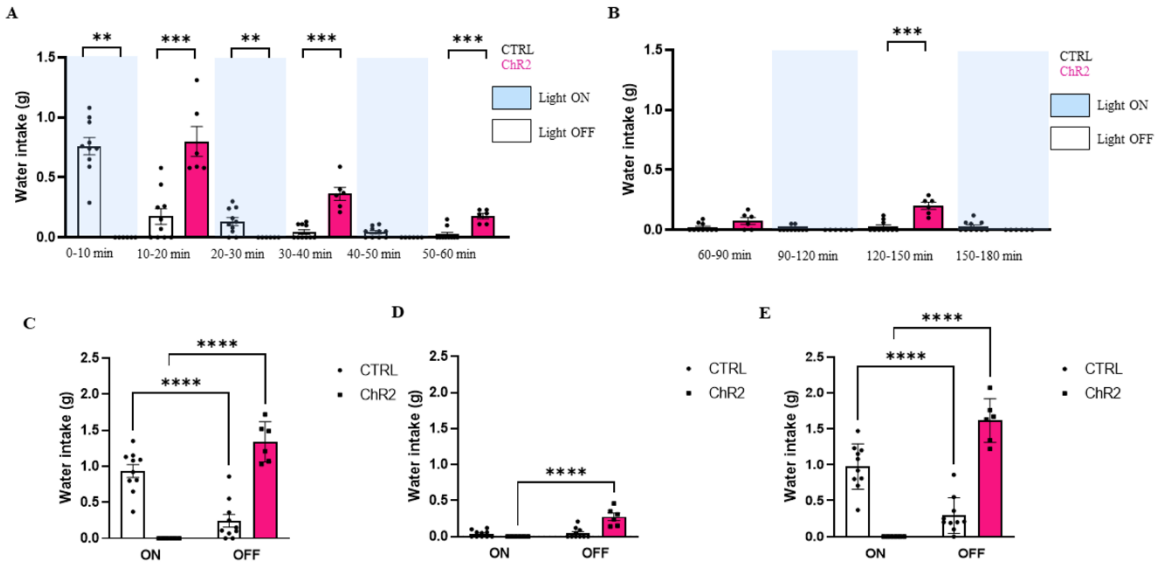

Figure 3.26: CeA$^{PKC\delta}$ neurons negatively modulate drinking behaviour in water deprived animals

(A) PKCδ::ChR2 and PKCδ::YFP mice, water deprived, were exposed to water in a 10 min ON/OFF behavioural paradigm. While photostimulation of ChR2 expressing animals drastically diminished drinking behaviour, control mice were not affected by the light stimulation, drinking the majority of the water during light ON (0-10 min Wilcoxon signed-rank test p=0,0020; 10-20 min Mann-Whitney U test p=0,0006; 20-30 min Wilcoxon signed-rank test p=0,0078; 30-40 min Mann-Whitney U test

p=0,0002; 50-60 min Mann-Whitney U test *p*=0,0005). **(B)** During the 30 OFF/ON paradigm control mice drank a very limited amount of water independently of the light, while ChR2 expressing mice drank significantly more during the OFF phase (60-90 min Wilcoxon signed-rank test *p*=0,0002). The strong effect of PKCδ neuronal activation on reducing drinking behaviour is visible in the graphs summarising the total amount of water consumed in the 10 min ON/OFF paradigm **(C)** (for CTRL ON versus CTRL OFF: Mann-Whitney U test *p*=0,0002; for ChR2 ON versus ChR2 ON: Wilcoxon signed-rank test *p*=0,0313), 30 min OFF/ON **(D)** (for ChR2 ON versus ChR2 ON: Wilcoxon signed-rank test *p*=0,0313) and the entire behaviour **(E)** (for CTRL ON versus CTRL OFF: Mann-Whitney U test *p*=0,0002; for ChR2 ON versus ChR2 ON: Wilcoxon signed-rank test *p*=0,0313). Value = Mean± SEM, **p* < 0.05, ***p* < 0.01.

To further analyse the effect of PKCδ neuronal photostimulation, I tested the same animals using a simpler behavioural paradigm: PKCδ-*Cre* mice expressing ChR2, or eYFP as controls, were water deprived and allowed to drink for 30 min while optogenetically photostimulated for the duration (Figure 3.27). The result clearly shows that the activation of PKCδ cells ablated water consumption, suggesting that an intra-CeA circuit modulates drinking behaviour.

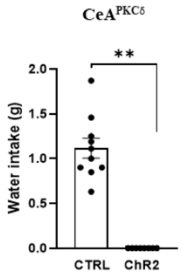

Figure 3.27: CeA$^{PKC\delta}$ neuron activation drastically reduces drinking behaviour in water deprived animals

Activation of PKCδ neurons in the CeA for 30 min completely ablates drinking (Wilcoxon signed-rank test *p*=0.0020). Value = Mean± SEM, **p* < 0.05, ***p* < 0.01.

3.2.8 Activation of Htr2a but not Sst neurons promotes food consumption

To test the role of Htr2a and Sst neurons in feeding behaviour, I injected a Cre-dependent ChR2 virus (AAV_5-hSyn-DIO-hChR2(H134R)-EYFP) and respective control (AAV_5-hSyn-DIO-EYFP) in Htr2a-*Cre* and Sst-*Cre* mice to target the CeA, while to target the CeM population, I injected AAV_5-hSyn-Con/Foff-hChR2(H134R)-EYFP in Htr2a-*Cre*::Wfs1-*FlpoER* mice.

The animals were photostimulated at 20 Hz with 473nm light pulses for 40 min in an arena containing two plastic cups in opposite corners - one with precision pre-weighed food pellets (20 mg each), and one empty. Experiments with Htr2a-*Cre* mice confirmed already published data[2], which highlights the role of Htr2a neurons in promoting feeding in satiated animals (Figure 3.28 A). To investigate which CeA subregion is responsible for the food consumption, I tested feeding in Htr2a-*Cre*::Wfs1-*FlpoER* animals expressing ChR2 in the CeM^{Htr2a} cells (Figure 3.28 B). I found a result very similar to that seen when CeA^{Htr2a} cells were activated, indicating that feeding behaviour is driven by CeM^{Htr2a} neurons. Experiments to verify a possible involvement of CeL^{Htr2a} are planned. Activation of CeA^{Sst} neurons failed to elicit feeding behaviour with neither ChR2 animals nor control group showing consummatory behaviour (Figure 3.28 C).

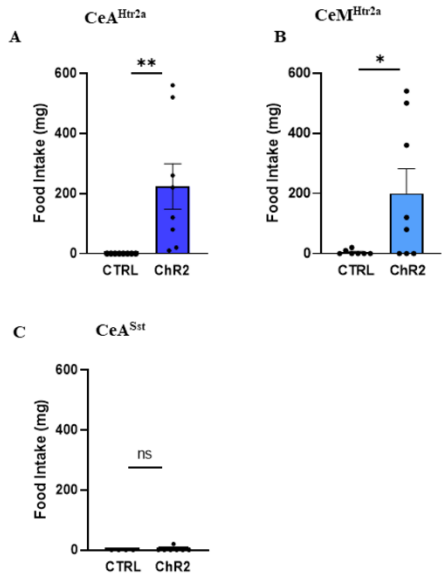

Figure 3.28: CeA and CeM Htr2a neuronal activation promotes food intake in satiated animals

(A) Activation of CeA^{Htr2a} neurons promoted food consumption (Wilcoxon signed-rank test p=0.0078). **(B)** CeM^{Htr2a} neuron photostimulation increased food intake (Mann-Whitney U test p=0.0710). **(C)** No difference between the Sst-*Cre* expressing ChR2 animals and controls (Wilcoxon signed-rank test p>0.999). Value = Mean± SEM, *p < 0.05, **p < 0.01.

3.2.9 Htr2a and Sst neuronal activity is positively reinforcing

Since Htr2a and Sst neurons in the CeA and CeM promote drinking, and Htr2a cells in the CeA and CeM promote feeding, I hypothesised they may potentiate these behaviours through a positively reinforcing mechanism. It is possible that, being involved in consummatory behaviours, the activity of Htr2a and Sst neurons reinforce ongoing consumption, contributing to the rewarding properties of what is consumed, whether it is food or water. It has already been published that mice engage in behaviours that lead to artificial activation of Htr2a[2] and Sst[3] neurons in the CeA. To demonstrate this, a real time place preference (RTPP) behavioural paradigm was used: Htr2a and Sst animals expressing ChR2 or eYFP in the CeA were able to explore a two-chamber arena with one compartment paired with laser photostimulation. Animals expressing ChR2 spent more time in the photostimulated side as compared to the controls, exhibiting a significant preference for it[2,3].

Both feeding and drinking experiments showed that the subregion of the CeA responsible for these two rewarding behaviours is the CeM. To test whether Htr2a and Sst neurons in the CeM are accordingly engaged in self-reward behaviour, I repeated the RTPP experiment, this time, in addition to using mice expressing ChR2 in CeA^{Htr2a} and CeA^{Sst} cells and relative controls expressing eYFP, I also expressed ChR2 specifically in the $CeM^{Htr2a/Sst}$ and $CeL^{Htr2a/Sst}$ neurons of Htr2a-*Cre*::Wfs1-*FlpER* and Sst-*Cre*::Wfs1-*FlpER* mice. The results confirmed the positively reinforcing effect due to the activation of the entire CeA for Htr2a neurons (Figure 3.29 A), and also showed the same effect in the CeM (Figure 3.29 B). Preliminary results highlighted an involvement also for the CeL^{Htr2a} (Figure 3.29 C), but more animals are currently being tested to confirm the data.

Preliminary results seem to confirm the role Sst cells in the CeA in rewarding behaviour, with animals expressing ChR2 having a preference for the photostimulated chamber for more than 60% (Figure 3.29 D). Control animals still need to be added, but will be subjected to the same behaviour in the future. Preliminary results also show a preference for the light-paired chamber upon activation of CeM^{Sst} cells (Figure 3.29 E). More animals are being tested to confirm the data.

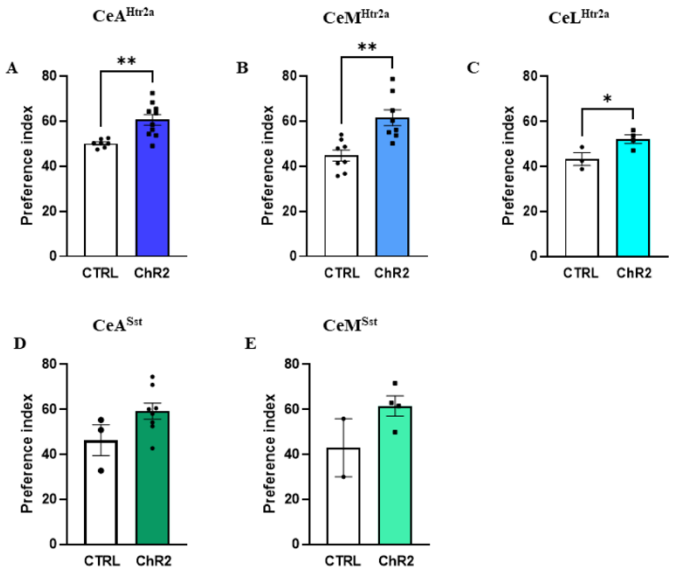

Figure 3.29: Activation of Htr2a and Sst neurons promotes real-time place preference

During RTPP, optic fibre-tethered mice were allowed to explore a two-chambered arena: one side was paired with a 473 nm pulse intracranial stimulation. The behaviour was repeated for two consecutive days and the stimulated chamber was switched on the second day. The values represent the average of the preference index for the stimulated chamber for each animal during the two days. **(A)** Photostimulation of CeA^{Htr2a} cells (unpaired t test p=0.0024, t=3.638) and CeM^{Htr2a} cells **(B)** (unpaired t test p=0.0016, t=3.893) had a rewarding effect and the animals spent the majority of the time in the stimulated chamber. **(C)** Preliminary results showed a preference for the stimulated chamber for mice expressing ChR2 in CeL^{Htr2a} neurons (unpaired t test p=0.0437, t=2.682). A tendency was seen for CeA^{Sst} (unpaired t test p=0.0630, t=2.278) **(D)** and CeM^{Sst} cell **(E)** (Mann-Whitney U test p=0.2667) activation to promote self-reward behaviour, as the ChR2 expressing animals spent in the photostimulated chamber more than 60% of the time. Value = Mean± SEM, *$p < 0.05$, **$p < 0.01$.

3.2.10 Htr2a and Sst neurons condition taste preference

The place preference results confirmed that Htr2a and Sst neurons elicit positive reinforcement. Since Htr2a and Sst cells are involved in drinking behaviour, I then investigated whether activation of Htr2a and Sst neurons could increase the rewarding properties of a consumed liquid and promote its consumption. To do this, I performed a taste preference test. Mice expressing ChR2 in Htr2a or Sst neurons in either the CeA/CeM/CeL were water deprived and exposed to two non-nutritive liquids for two consecutive days: one with grape, and the other with strawberry flavour. After identifying the favourite taste, the preferred one was consumed

for four days in the absence of photostimulation, while the other was paired with optogenetic activation. After conditioning, the flavour preference of the mice was tested. Activation of Htr2a neurons in the CeA and CeM (Figure 3.30 A-C) reversed the preference of the animals, making the less preferred taste the most preferred one. During conditioning, the two groups of animals consumed a significantly higher amount of the taste that was paired with light stimulation (Figure 3.30 B-D). Preliminary results of CeL^{Htr2a} cell activation did not show a change of taste preference for all animals, although some of them reversed their choice (Figure 3.30 E). Moreover, CeL^{Htr2a} neuronal activation did not promote more liquid consumption (Figure 3.30 F). More animals are being tested to clarify the involvement of CeL^{Htr2a} cells in this behaviour.

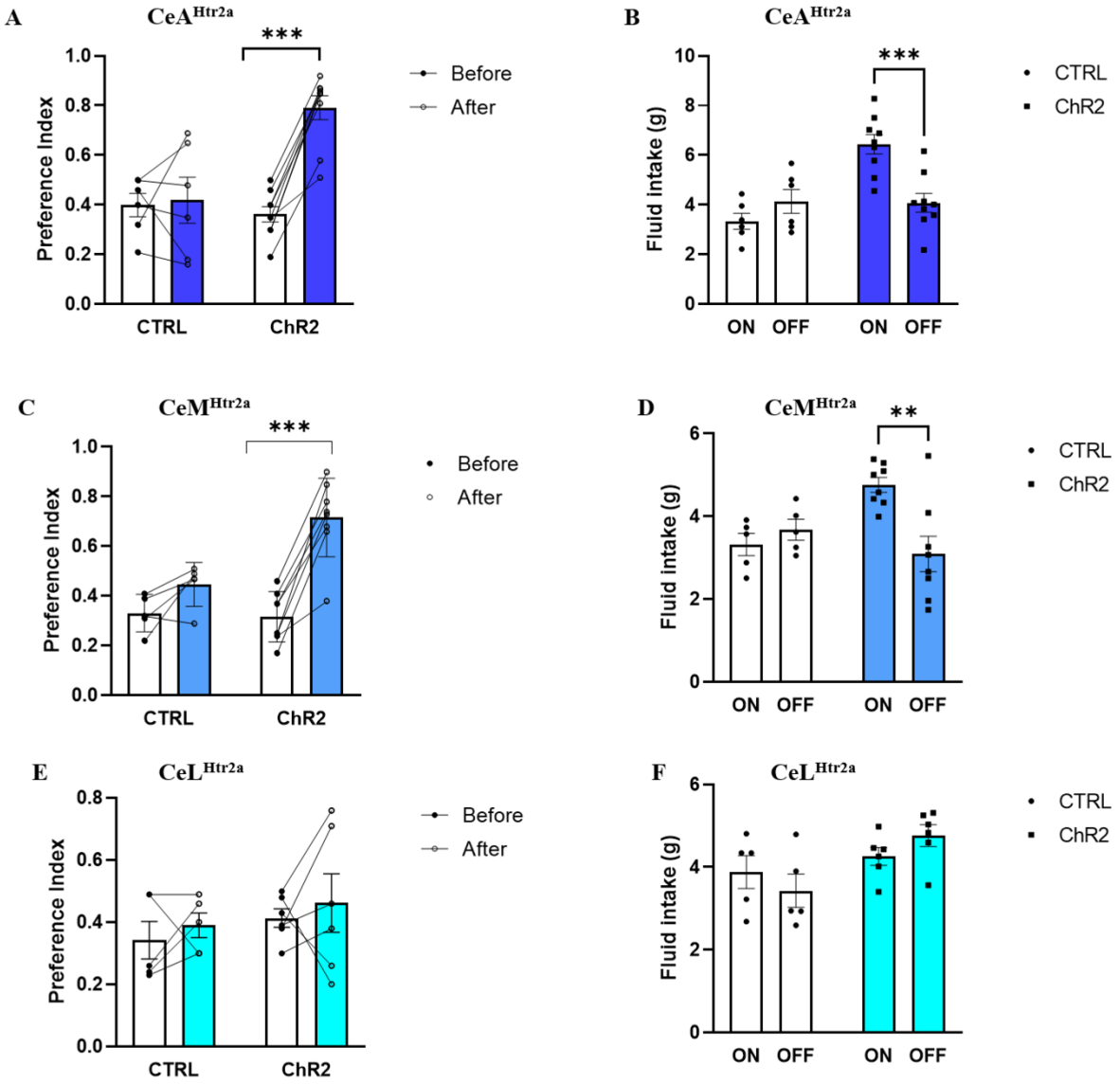

Figure 3.30: Activation of Htr2a neurons reverses taste preference

(A) Optogenetic activation of CeA^{Htr2a} neurons changed the taste preference for the ChR2 expressing animals but not for the control group (for ChR2 before versus ChR2 after: Mann-Whitney U test $p<0.0001$). **(B)** CeA^{Htr2a} cell stimulation induced more consumption of flavoured water during the "light ON" period (interaction, Two-way ANOVA, $F_{1,26}=15.07$, $p=0{,}0006$; light, Two-way ANOVA, $F_{1,26}=3.679$, $p=0.0661$; ChR2, Two-way ANOVA, $F_{1,26}=13.97$, $p\ 0=0.0009$). **(C)** CeM^{Htr2a} cell activation reversed the taste preference (for ChR2 before versus ChR2 after: unpaired t test $p<0.0001$, t=6.045) and increased fluid intake **(D)** (interaction, Two-way ANOVA, $F_{1,22}=9.431$, $p=0.0056$; light, Two-way ANOVA, $F_{1,22}=3.990$, $p=0.0583$; ChR2, Two-way ANOVA, $F_{1,22}=1.700$, $p\ 0=0.2058$). No effect was seen for CeL^{Htr2a} neuronal stimulation both for taste preference **(E)** (for ChR2 before versus ChR2 after: unpaired t test $p=0.6355$, t=0.4889) and for the amount of fluid intake **(F)** (interaction, Two-way ANOVA, $F_{1,18}=2.243$, $p=0.1515$; light, Two-way ANOVA, $F_{1,18}=0.0076$, $p=0.9315$; ChR2, Two-way ANOVA, $F_{1,18}=7.264$, $p\ 0=0.0148$). Value = Mean± SEM, $*p<0.05$, $**p<0.01$.

Photostimulation of Sst neurons in both the CeA and CeM positively conditioned taste preference (Figure 3.31 A-C), stimulating drinking of the light-paired taste (Figure 3.31 B-D). Together these results suggest that the Htr2a and Sst neurons in the CeM are responsible for reinforcing the rewarding properties of the consumed nutrient.

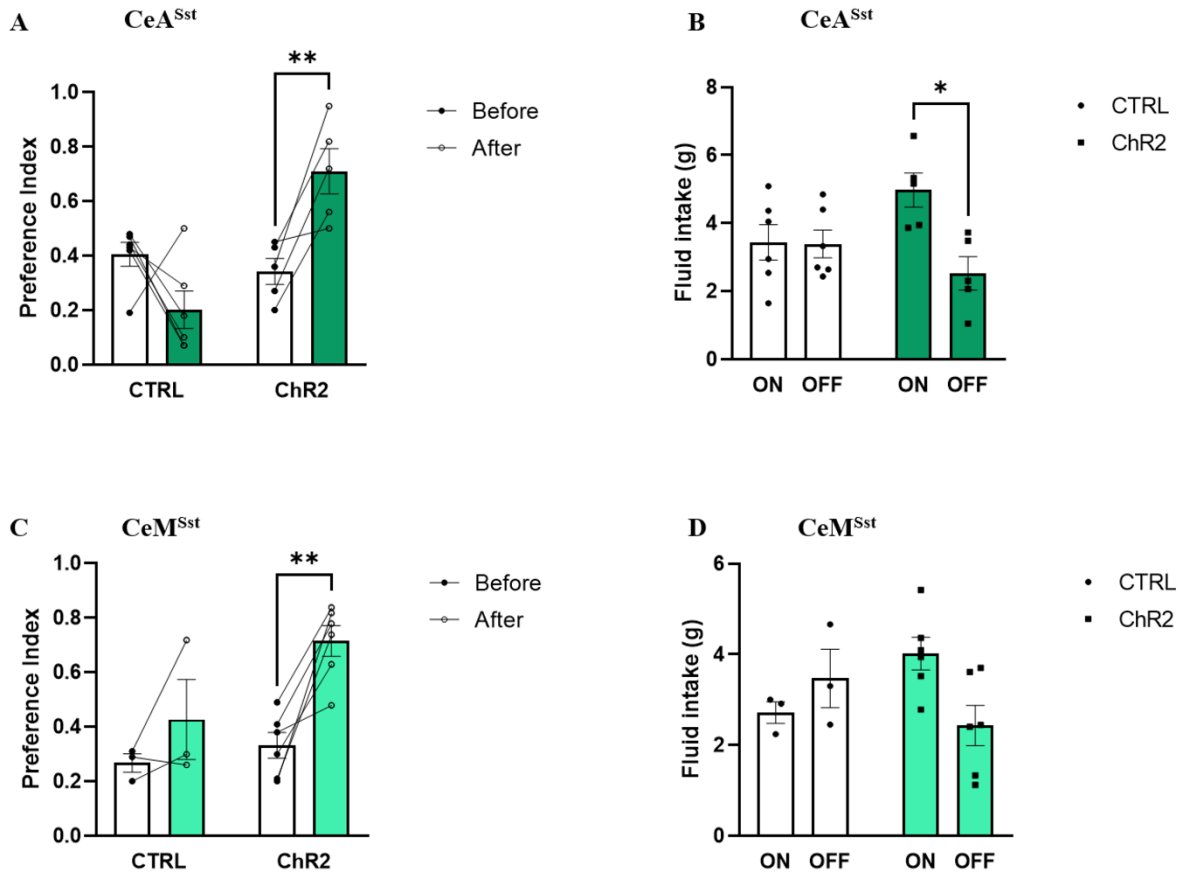

Figure 3.31: Activation of Sst neurons in both the CeA and CeM conditions flavour preference

(A) Optogenetic activation of CeA^{Sst} neurons reversed the less preferred taste to the most preferred one (for ChR2 before versus ChR2 after: unpaired t test p=0.0048, t=3.863). **(B)** Animals expressing ChR2 in CeA^{Sst} neurons consumed more of the taste paired with the photostimulation (interaction, Two-way ANOVA, $F_{1,18}$ =6.134, p=0.0234; light, Two-way ANOVA, $F_{1,18}$ =6.637, p=0.0190; ChR2, Two-way ANOVA, $F_{1,18}$ =0.4788, p=0.4978). **(C)** The same effect of reversing preference was caused by CeM^{Sst} neuronal activation (interaction, Two-way ANOVA, $F_{1,14}$ =2.348, p=0.1477; light, Two-way ANOVA, $F_{1,14}$ =5.878, p=0.0295; ChR2, Two-way ANOVA, $F_{1,14}$ =13.90, p=0.0022). **(D)** No significant effect in the amount of flavour drank with "light ON" for the animals expressing ChR2 in CeM^{Sst} cells (interaction, Two-way ANOVA, $F_{1,14}$ =6.058, p=0.0274; light, Two-way ANOVA, $F_{1,14}$ =0.7663, p=0.3961; ChR2, Two-way ANOVA, $F_{1,14}$ =0.778, p=0.7844). Value = Mean± SEM, *p < 0.05, **p < 0.01.

3.2.11 Inhibition of Htr2a and Sst neurons decreases water consumption in water deprived mice

Gain of function experiments highlighted an involvement of Htr2a and Sst neurons in positively promoting water consumption. To further demonstrate the function of these two amygdala subpopulations in drinking behaviour, I tested the effect of inhibiting Sst cells in the CeA and Htr2a cells in the CeA and CeM. Htr2a-*Cre* and Sst-*Cre* mice, injected with AAV_5-Ef1a-DIO-eNpHR3.0-mCherry and the control AAV_5-Ef1a-DIO-mCherry, and Htr2a-*Cre*::Wfs1-*FlpER*, with AAV_8-nEF-Con/Foff iC++-EYFP and the control AAV_8-nEF-Con/Foff-EYFP, were water deprived and tested for water consumption for 30 min while constantly photoinhibited.

Inhibition of CeA Htr2a and Sst cells significantly decreased water intake as compared to the controls (Figure 3.32 A-C). Preliminary results also showed a reduction in drinking due to the inhibition of CeM^{Htr2a} neurons (Figure 3.32 B). Experiments to confirm the data and to test the effect of CeM^{Sst} neuronal inhibition are already planned. To summarise, these data are in line with experiments previously shown and corroborate the role of CeM^{Htr2a} and CeA^{Sst} neurons in drinking behaviour.

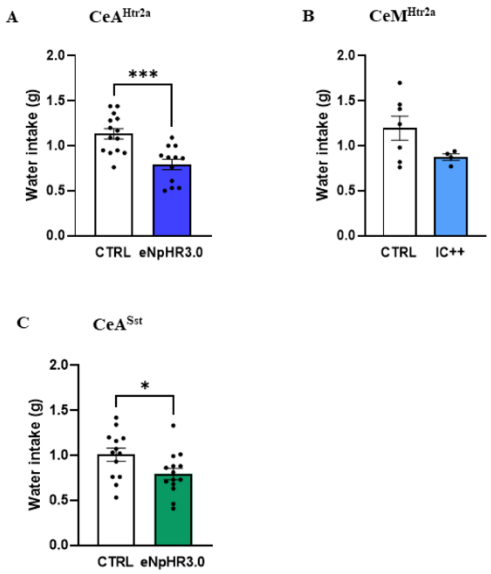

Figure 3.32: CeA and CeM Ht2a and Sst neuron inhibition decreases water intake

(A) Inhibition of Htr2a neurons in the CeA decreased drinking (unpaired t test p=0.0004, t=4.126). **(B)** Preliminary results showed a similar effect for CeM^{Htr2a} neurons (unpaired t test p=0.1109, t=1.768). **(C)** A reduction in water intake also resulted after inhibition of CeA^{Sst} neurons (unpaired t test p=0.0363, t=2.213). Value = Mean± SEM, *$p < 0.05$, **$p < 0.01$.

3.2.12 Inhibition of PKCδ neurons increases water intake in water deprived mice

Activation of PKCδ neurons generated a very strong reduction in water intake for thirsty animals, exhibiting an opposite effect compared to the Htr2a and Sst populations, and drawing my attention to a possible CeA internal circuit modulating drinking behaviour. To further confirm the role of PKCδ neurons, I injected the AAV_5-Ef1a-DIO-eNpHR3.0-mCherry virus in the CeA of PKCδ-*Cre* animals and exposed them to 30 min photoinhibition in the presence of water. As hypothesized, the animals drank significantly more compared to the control group (Figure 3.33), showing a complementary effect to the Htr2a and Sst neurons.

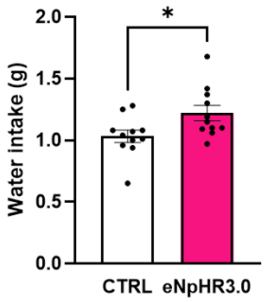

Figure 3.33: CeA$^{PKC\delta}$ neurons inhibition increases drinking behaviour in water deprived animals

Inhibition of PKCδ neurons in the CeA significantly increased drinking compared to the control group (unpaired t test p=0.0282, t=2.365). Value = Mean± SEM, *$p < 0.05$, **$p < 0.01$.

3.2.13 Inhibition of Htr2a and Sst neurons decreases palatable liquid consumption

The role of Htr2a neurons in promoting food intake and their modulation of reward suggested that inhibition of the same cells could weaken rewarding properties of a consumed substance with a consequent reduction of consummatory behaviour. To test whether inhibition of Htr2a neurons reduces palatable reward consumption when it is driven not by a homeostatic need but exclusively by the rewarding properties of the substance, I performed the following experiment: I injected an AAV_5-Ef1a-DIO-eNpHR3.0-mCherry or relative control AAV_5-Ef1a-DIO-mCherry in the CeA of Htr2a-*Cre* mice, an AAV_8-nEF-Con/Foff iC++-EYFP and the control AAV_8-nEF-Con/Foff-EYFP (to specifically inhibit the CeM) in Htr2a-*Cre*::Wfs1-FlpER. After 16h of food deprivation, mice were allowed to consume a palatable reward solution (Fresubin, 2kcal/ml) for 30-45 min. The animals then went back to *ad libitum* food and the following day were tested for Fresubin consumption for 30 min with constant photoinhibition (561nm, 10mW) for the animals expressing eNpHR3.0, and with 20 Hz 473nm photostimulation for the animals expressing IC++. Results showed that inhibition of Htr2a neurons in the CeA and CeM significantly reduced the consumption of the palatable liquid reward compared to the controls (Figure 3.34 A-B). I also tested Sst-*Cre* mice expressing eNpHR3.0 in the CeA, but inhibition did not have any effect (Figure 3.34 C). This result confirmed the outcome obtained with the gain of function experiments, showing that Sst neurons are not involved in consummatory behaviour. The Htr2a data, instead, support their role in modulating the rewarding properties of a palatable liquid.

.

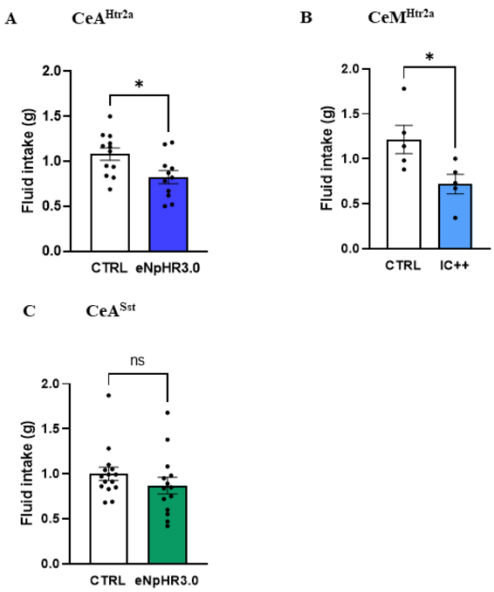

Figure 3.34: Inhibition of Htr2a neurons, but not Sst, in the CeA and CeM decreases food intake

(A) Inhibition of Htr2a neurons in the CeA (unpaired t test p=0.0170, t=2.593), and CeM **(B)** decreased feeding (unpaired t test p=0.0327, t=2.578). **(C)** No effect on consumption for CeA^{Sst} neurons (Mann-Whitney U test p=0.1365) compared to controls was seen. Value = Mean± SEM, *$p < 0.05$, **$p < 0.01$.

4. Discussion

The amygdala has long been known to be an integrative brain centre for emotions and motivation, playing an essential role in processing both fearful and rewarding environmental stimuli. Recent technological advances in optogenetic and chemogenetic techniques that are able to be combined with various transgenic mouse lines, provide the possibility to map the complex anatomical connections of the amygdala onto behavioural functions. The most recent publications in the field have highlighted the importance of functionally manipulating the activity of defined neuronal subpopulations and, taking into consideration the input and output brain regions of the main target of this study, to dissect complex behaviours. Importantly, recent studies seem to suggest that optogenetic manipulations of the same, or overlapping, cell populations can give rise to distinct, or sometimes even opposite, behavioural phenotypes[2,3,52,53].

The purpose of this thesis work is to provide new insights into the functional organisation of amygdala neural circuits: in particular, I investigated the role of different central amygdala subpopulations in encoding contextual appetitive memories and rewarding behaviours, focusing my attention on three subsets of neurons - PKCδ, Sst and Htr2a.

4.1 The CeA and learning: from a serial to a parallel model

The ultimate goal of an organism is to survive and transfer its genome to the progeny. Wild animals must constantly weigh environmental stimuli and determine whether these predict a threat or an opportunity. Every time an animal is engaged in foraging, it needs to balance the possibility of finding food with the risk of being predated by other animals. Being able to rapidly learn to identify potentially dangerous environmental features can lead to a much more successful achievement of the goal.

The amygdala is a fast detector of aversive environmental stimuli, producing affective or behavioural states as adaptive responses to potential threats[1,32]. The amygdala's central role in emotional learning and memory has been well developed, starting from classical Pavlovian fear conditioning[34]. Until recently, the generally accepted model proposed that the formation of associations between sensory or perceptual cues and events takes place in the LA, where pathways carrying this information converge and are enhanced through a Hebbian plasticity mechanism. In addition, the performance of different defensive responses proceeds through the

CeA to hypothalamic, midbrain and medullary nuclei[70]. This model suggests that emotional processing in the amygdala progresses in a serial manner from the LA to the CeA.

Recent evidence from appetitive conditioning experiments suggests that the BLA and the CeA operate in parallel to mediate distinct incentive behaviours. For instance, the BLA encodes emotional events with reference to their sensory features, while the CeA encodes motivational or affective significance[70].

This thesis tries to highlight the role of the CeA, particularly of different and exclusive neuronal subtypes, in a contextual appetitive learning paradigm. Following this direction, I showed that two distinct subpopulations of neurons in the CeA, PKCδ^{+} and Sst^{+}, can encode contextual appetitive memories in line with a Hebbian plasticity mechanism.

To show this, I used a behavioural paradigm, the conditioned place preference. On the first day, mice were allowed to freely explore an arena composed of two chambers with different shapes, floor textures, and wall patterns. The chamber in which the mice spent the majority of the time was defined as the preferred one. For four consecutive days, the animals, under food restriction, were sequestered for the first fifteen minutes in the preferred chamber and for the following fifteen in the other one (positive context) where there was a pellet of food available. On the test day, the mice were allowed to explore both chambers, without the presence of the food. Results showed naive animals, after training, strongly preferred the positive context, the chamber that had previously been paired with food.
In order to investigate the involvement of the two distinct CeA neuron subpopulations in this learning paradigm, I optogenetically inhibited PKCδ and Sst neurons, either during the learning phase or during the retrieval test. The results showed that inhibition of PKCδ neurons, but not Sst, in both conditions, decreased the preference of mice toward the positive context, suggesting that PKCδ cells are involved in the formation and presentation of reward memory. The outcome of this experiment was independent of the amount of food consumed during the behavioural task, since we found that inhibition of PKCδ and Sst neurons did not promote or suppress food consumption as compared to the controls.

To test the Hebbian model of appetitive conditioning, I performed *in vivo* calcium imaging experiments to record calcium activity in PKCδ and Sst neurons during all phases of behaviour.

One of the main reasons for conducting this experiment was to analyse whether I could observe PKCδ or Sst neurons being activated in the positive context during training, with food presented, or in the positive context, during the test, without the presence of food. I wanted to investigate if CeA neurons could acquire a specific response to the positive context after learning, thus acting as a hub for memory storage.

We found that a specific group of PKCδ and Sst neurons had a context-specific high activity, particularly in the food zone. These neurons were activated upon transition in the positive context. Within the neurons that presented memory, some were preferentially active in the food zone, some in the positive context, and some did not show specific preference toward the positive context or the food zone. Interestingly, the mice that had a stronger preference for the positive context were the ones with less specificity of neuronal activity toward the food zone, while in the animals that had less preference, the neuronal activity was highly correlated with the food zone.

Our hypothesis is that during the test, mice with a stronger preference to the positive context associated the entire arena or the entire positive context as a predictor of food availability, while the others associated the reward strictly to the food zone. Together, these results demonstrate that the positive context can be a predictor of food availability and the CeA encodes Pavlovian appetitive learning. This work is in line with the most recent amygdala parallel model used to explain Pavlovian conditioning[70].

By using different tracing methods, it is clear that the CeA receives all the necessary connections for CS-US association: gustatory and visceral information from the IC and thalamus[195,196], visceral and nociceptive from the PBN[197-183], olfactory from the piriform cortex[198], auditory and visual from the thalamic nuclei[27], and contextual from the hippocampus[199]. The CeL undergoes experience dependent potentiation during fear conditioning and its inhibition prevents fear acquisition and excitatory synaptic enhancement [1,91]. Projections from the IC to the CeA are important in establishing appropriate behavioural responses to taste-predicting cues, mediating learning that an auditory cue anticipates an unpleasant tastant. IC-CeA projections seem to be critical for generating appropriate behavioural responses during foraging when facing different choices[200]. Moreover, mice trained in a place preference test where they were supposed to associate sweet water with a

specific corner of the cage resulted in high c-Fos expression specifically in the CeM, supporting the hypothesis that the CeA is particularly involved in appetitively motivated learning processes[201].

4.2 Differences between PKCδ and Sst neurons during contextual appetitive learning

The calcium recording performed in appetitive contextual behaviour showed memory neurons in both PKCδ-*Cre* and Sst-*Cre* animals. However, only inhibition of PKCδ neurons but not Sst impaired contextual learning, therefore we investigated possible differences in the calcium activity of these two neuronal subpopulations.

During training, a large percentage of both neurons was active in the positive context during the presence of food, maintaining this functional tag over four days. The majority of these cells was not active during habituation probably meaning that they were recruited during the learning phase. During the last training day, a higher number of Sst neurons showed a significantly stronger activity while the mice were eating in the positive context compared to the PKCδ-expressing neurons. Moreover, the activity of Sst cells was locked in time to the onset of the feeding bouts of the animal, while for PKCδ cells we found a different pattern of activation, sometimes before approaching the food and sometimes with a delay during consumption. This effect was not due to the amount of food the mice ate, since the two groups of mice consumed a comparable quantity. Interestingly, there was no difference in the total number of cells activated during training in the positive context for both lines. These results suggested that Sst cells might be involved in correlating the physical properties of food, such as texture and taste with the environment. However, PKCδ neurons could instead link the salience of the food reward with its physical properties. PKCδ cells were in fact activated upon food delivery in the chamber and may associate the context with the general affective properties of the food.

The role of the CeA in controlling distinct aspects of emotional learning was already hypothesised several years ago during different studies about the involvement of the BLA and the CeA in a parallel way in Pavlovian conditioning[70]. While the BLA mediates associations between predictive stimuli and the sensory properties of biologically events, the CeA mediates the association of predictive stimuli with the affective and emotional properties of those events, establishing the general affective response that underlies their effect[70]. Thus, in the behavioural

paradigm I performed, PKCδ neurons could be the CeA population resembling the characteristics just described, explaining why their inhibition impairs the formation of the contextual food memory. However, the experiments I performed don't allow a complete understanding of the role of the expectation of the animal in this behaviour. It would be very important to understand if the animal's expectation of the food pellet in the positive context could modulate the activity of the CeA cells following the classical reward prediction error theory. That is, a reward that is better than predicted elicits activation (positive prediction error response), a fully predicted reward draws no response, and a reward that is worse than predicted induces a depression (negative error response)[202].

We found at least two memory cells, showing reduced activation upon food consumption when I added a new food pellet to the positive context after the retrieval test, suggesting that expectation could reduce or inhibit neuronal activity for the fully predicted reward (food pellet) after learning. In line with this concept, it would be interesting to investigate the motivation of the animal to perform the behaviour and reach the food in the arena. Both the behaviour and the calcium imaging experiments are not enough to fully clarify whether the outcome of the training is due to a learning process, or whether a motivational component is also involved. Pairing with laser activation of the CeA has been demonstrated to amplify the motivational attractiveness or the incentive value of its associatively paired reward representation[66]. Studies based on anatomical perspectives have suggested that the CeA occupies a unique striatal-level within cortical-striatal-pallidal levels of forebrain organization, whereas the BLA occupies a more cortical-level role[203]. Other striatal-level structures, such as the nucleus accumbens, are known to generate intense incentive motivational states[204-206] and the CeA may also contribute to the generation of motivational signals[70,207]. Although a role for the CeA in motivation seems to be generally quite clear, the specific contribution of different CeA neuron subpopulations is still largely unknown and would be worth further investigation.

4.3 PKCδ neurons: aversive or rewarding?

The role of PKCδ neurons in Pavlovian appetitive learning seems to go against the previous functional description of this subpopulation, that had previously been characterized in different publications as general aversive[104,129].

PKCδ neurons are located in the capsular and lateral part of the CeA and have been studied in a broad variety of behaviours from eating, to fear, and pain modulation. They are triggered by multiple anorexigenic signals *in vivo,* and robustly inhibit food intake via optogenetic-based activation, constituting an important role in the integration and processing of appetite suppressing signals[104]. Apart from feeding, activation of PKCδ neurons inhibits drinking behaviour, as showed in the experiments I previously described. The role of PKCδ neurons is very well explained in the context of fear conditioning. Within the CeL, two different subpopulations of neurons have been shown to exert opposing functions and to have distinct genetic markers. One of them is inhibited in response to the CS (CeL^{OFF} cells), and the other one is instead excited by the CS (CeL^{ON} cells)[1]. CeL^{OFF} and CeL^{ON} cells reciprocally inhibit one another and send projections to the CeM[88,90]. CeL^{ON} neurons respond to the CS before the CeL^{OFF}, suggesting that activation of CeL^{ON} cells inhibits CeL^{OFF} neurons projecting to CeM output neurons, promoting freezing through disinhibition[90,88]. The CeL^{OFF} cells were identified as PKCδ-expressing neurons.

The role of these neurons in fear conditioning has been very well examined, showing that they are essential for the synaptic plasticity underlying learning in the LA, conveying information about the US to the lateral nucleus during fear conditioning[208]. Inhibition of PKCδ neurons completely abolishes the synaptic strengthening in the LA and impairs conditioned freezing. During fear conditioning, the convergence of sound (CS) and shock (US) in LA neurons is necessary for these neurons to undergo synaptic plasticity and be involved in the learning process. The sound usually reaches the LA via the auditory thalamus and cortex, but the pathway through which the shock information is transmitted remains unclear. PKCδ neurons might be a key component in the regulation of this process since they are a postsynaptic target of the PBN, a structure that provides nociceptive signals, and activation of PKCδ neurons is sufficient to relay the US information and drive aversive learning. To illustrate this hypothesis, PKCδ neurons were inhibited during the US presentation period, showing that this

manipulation is sufficient to impair the formation of fear memory[208]. Inhibition of PKCδ neurons reduced reactions of animals to electrical shocks, carrying negative emotional valence and processing the affective component of the US. Activation of PKCδ neurons in a real time place preference assay resulted in mice avoiding the chamber paired with the light, giving a further indication that PKCδ neurons drive aversive learning[208]. These results highlight the role of PKCδ neurons in transmitting information about the US to the LA during fear conditioning.

In addition to fear and feeding, PKCδ neurons play a role in pain as well: they receive excitatory inputs from the PBN and are sensitized by nerve injury, increasing and amplifying pain related responses through their activation[129]. Considering these publications, one could think that PKCδ neurons form a broad aversive population related to pain, anorexia, and threat, but not reward stimuli[104].

The first publication suggesting a possible function of PKCδ in non-aversive behaviours identified a subset of PKCδ neurons as part of a CeA general anaesthesia GABAergic population activated by different anaesthesia drugs. These cells, when optogenetically stimulated, suppress pain-elicited reflexive behaviour and pain induced mechanical sensitivity, while their inhibition exacerbates pain and is able to revoke the analgesic effect of ketamine[130]. The summary of previous publications, together with our findings that PKCδ neurons are responsible for Pavlovian learning in appetitive conditioning, suggest that PKCδ neurons cannot be simply described as a 'broad aversive' population but might have more general functions and, depending on stimuli and context, select defensive or appetitive responses. Further studies to identify differences between the subset of PKCδ neurons in the CeC and the CeL, as well as dissimilarities within the PKCδ neurons due to different inputs received or different outputs these neurons project to, will clarify the numerous roles of PKCδ neurons, a very heterogeneous CeA population.

4.4 CeL and CeM: connectivity and function

The CeA is divided into the lateral (CeL) and the medial (CeM) parts, which differ in the composition of their neuronal subpopulations, connectivity, and function. Gene expression studies have shown a wide variety of genetic markers expressed in the CeA[209-212]. Recently, single-molecule fluorescence *in situ* hybridization revealed some markers that were expressed

specifically in the CeL and the CeM[3]. Crh, Htr2a, Nts, PKCδ, Sst, and Tac2 were found in the CeL; Htr2a, Nts, Sst, and Tac2 in the CeM. The majority of neurons in the CeL and the CeM are GABAergic. PKCδ positive cells are only present in the CeL and the CeC, Crh on the other hand mainly expresses in the CeL.

The first evidence that the same CeA neuronal subpopulations could be involved in different functions depending on their location in either the CeL or the CeM, come from fear conditioning studies[90,91]. The CeL, in fact, is the main CeA site assigned to learning processes and comprehends PKCδ (CeL^{OFF}) neurons, which are inhibited in response to the CS and Sst neurons (CeL^{ON}), which are activated. The crosstalk between these two CeL distinct neuronal subpopulations activates the CeM output neurons, promoting freezing[88,90]. CeL^{Sst} neurons are particularly important for the acquisition of CS-US association and their inhibition during the learning phase prevents fear acquisition and excitatory synaptic enhancement. Moreover, they directly project to both the PAG[91] and the PVT[92], bypassing the CeM.

CeL, as well as CeM, projections contribute to the expression of fear. Interestingly, genetically distinct CeA populations in the CeL or the CeM drive appetitive responses, despite their function in defensive behaviour. To further investigate the properties of different CeA neurons, different neurons were activated or inhibited in the CeL or CeM subregion during feeding, drinking and freezing behaviour[3]. In an optogenetic-based self-stimulation test, activation of CeL Sst, Crh, and Tac2, and CeM Nts, Sst, and Tac2 neurons resulted in an effect similar to rewarding. Inhibition of PKCδ neurons in the CeL increased drinking in water deprived animals and inhibition of Sst, Crh, Nts, and Tac2 neurons in the CeL decreased drinking. No effect was seen in all the other combinations compared to the control groups[3].

Although in the Kim *et al* paper, *in vivo* neuronal manipulations specifically in the CeL and the CeM, were simply provided by viral stereotactic brain injections[3], the accuracy of this approach may be low. This approach, in fact, has great technical difficulties: it is very hard to inject virus exclusively into the CeC, CeL or CeM without affecting the nearby structures with an unspecific viral expression. In this thesis work, I propose a new method to precisely and consistently manipulate defined CeA subpopulations of neurons (Htr2a and Sst) in either the CeL or CeM. The strategy adopted employs a new approach based on the use of intersectional genetics. To do so, we generated the new Wfs1-*FlpoER*^{T2} mouse line, in which the specific

marker Wfs1 (Wolframin1) drives the expression of the Flp recombinase only in the CeL after tamoxifen administration[193]. After crossing with a Cre driver line (in this case Sst-*Cre* or Htr2a-*Cre*), the double transgenic Htr2a-*Cre*::Wfs1-*FlpoER* or Sst-*Cre*::Wfs1-*FlpoER* animals will have Htr2a/Sst positive cells in the CeL expressing both Cre and Flp (all the Htr2a and Sst cells in the CeL coexpress Wfs1), while Htr2a/Sst neurons in the CeM will only express the Cre recombinase.

It is possible to independently modulate Htr2a/Sst positive neurons in only the CeM or CeL, analysing the involvement of these neurons during different behavioural paradigms, due to the availability of such intersectional optogenetic-based tools, which allow us to manipulate neurons expressing Cre or Flp alone, as well as neurons expressing both recombinases. I tested Htr2a-*Cre*::Wfs1-*FlpoER* and Sst-*Cre*::Wfs1-*FlpoER* animals in drinking, feeding and rewarding behaviours. The role of the CeA^{Htr2a} neurons in feeding and reward had already been characterized in the lab, as activation of Htr2a neurons positively modulates food consumption and promotes positive reinforcement[2], but no distinction between the role of Htr2a neurons in the CeL and the CeM had been done. The CeL/CeM Sst neurons were shown to promote reward behaviour and the inhibition of the CeL to stimulate drinking[3].

My results indicate that stimulation of both Htr2a and Sst in the CeA promotes drinking behaviour in water deprived animals, and activation of these neurons induces self-reward behaviour. Activation of Htr2a and Sst neurons in the CeM, but not CeL, results in a similar outcome to activation of Htr2a and Sst neurons in the CeA. Interestingly, Htr2a neurons seem to be the only population involved in feeding behaviour. Activation of Htr2a neurons in the CeA and the CeM of satiated animals promotes food pellet consumption, while activation of the Sst neurons does not have the same outcome. This is quite interesting, since approximately 50% of Htr2a neurons co-express Sst, but they maintain this unique feature. The CeM subregion, for both neuronal types, seems to be responsible for the reward effect because animals undergoing RTPP prefer the chamber where the Htr2a/Sst CeM neurons are stimulated. To investigate whether activation of Htr2a and Sst neurons can condition a preference for a specific flavour, I performed a test in which mice were allowed to consume two different flavours, and then were conditioned for four consecutive days, pairing the least preferred flavour with neuronal photostimulation. On the last day, the mice were able to freely choose between the two tastes again. The results show that activation of Htr2a and Sst in the CeA is enough to positively change the preference of the animals and, also in this case, the CeM seems

to be the main CeA subregion contributing to this effect. In addition, I inhibited the CeA and the CeM of Htr2a-*Cre* and Sst-*Cre* animals during drinking and feeding. The results showed a reduction of water consumption for both neuronal subtypes and reduction of food consumption with inhibition of Htr2a alone, supporting the previous results.

The involvement of the internal CeA microcircuit in the regulation of consummatory behaviour through reciprocal inhibitory connections within different CeA populations[2,104], was analysed with the description of the anorexigenic role of PKCδ cells, performed via local inhibition of PKCδ negative neurons (Htr2a positive)[104]. Here I show that PKCδ neurons exert an opposite function compared to Htr2a and Sst cells, also in drinking behaviour, since their activation completely blocks water intake in thirsty animals. To prove that PKCδ neurons can inhibit Htr2a and Sst in the CeM (the main area responsible for consummatory behaviours in the CeA), electrophysiological experiments are currently being conducted. By using an intersectional approach, Htr2a/Sst neurons in the CeM were recorded in PKCδ-*Flp*::Htr2a-*Cre*::TdTomato or PKCδ-*Flp*::Sst-*Cre*::TdTomato slices, which had been transduced with a Flp dependent ChR2 virus. Preliminary results reveal a monosynaptic connection from the PKCδ to the CeM Htr2a/Sst neurons. The opposite role of PKCδ and Htr2a/Sst neurons in feeding and drinking might explain the microcircuit in the CeA. However, it is important to take into consideration the inputs and outputs of the neurons as well. Input of Htr2a and Sst neurons in the CeA has been previously described[2,52], unfortunately, intersectional rabies viruses that would allow us to specifically target either the CeL or the CeM subregions are not currently available. Regarding the outputs, while experiments to map the differences between the CeL and the CeM are on-going (result not shown), I have started to focus my attention on one region that receives projections from Htr2a and Sst neurons, and is already known to process gustatory and sensory signals and to be a key regulator of fluid homeostasis[2,148]: the PBN. The involvement of CeA^{Htr2a} projections to the PBN in feeding indicates that their activation is rewarding and promotes food consumption[2]. Since the CeM is the subregion of the CeA responsible for consummatory behaviours, I will manipulate Htr2a/Sst CeM projections to the PBN during drinking and feeding to understand their specific contribution to different appetitive behaviours. It would be interesting to investigate the identity of the PBN target cells which have not yet been described.

The role of CeL^{Htr2a} and CeL^{Sst} cells is still not completely understood. CeA^{Sst} neurons are involved in the acquisition of CS-US association during fear conditioning and their inhibition during the learning phase prevents fear acquisition[91,92]. However, previous results were not obtained using precise intersectional tools to manipulate the CeL. Inhibition of Htr2a cells in the CeA increased innate freezing and regulated the hierarchical relationship between the innate and learned freezing response, in which the first predominates[117]. One could speculate that, similarly to Sst neurons, the CeL^{Htr2a} neurons may be involved in defensive behaviour, while the CeM^{Htr2a} modulate reward and feeding. A deeper investigation of the role of the CeL^{Sst} and CeL^{Htr2a} in fear conditioning and defensive behaviour, using intersectional genetics, would clarify their function.

4.5 Htr2a and Sst: so close yet so far

Htr2a and Sst neurons are two CeA subpopulations, corresponding to almost 50% of the neurons, involved in defensive and appetitive behaviours at the same time. However, these two subtypes promote behaviour in a different way. In particular, Htr2a neurons are a hierarchy fear generator, prioritising innate over learned fear. Their inactivation in fact, upregulates innate-freezing responses and downregulates learned-freezing[117]. Innate and learned fear were already described as having different neuronal pathways[116] and the CeA was thought to be the region that separates the information into different downstream pathways to generate distinct behavioural responses[116]. For the first time a specific subpopulation of CeA, the Htr2a positive neurons, has been proposed to integrate both sets of information and regulate responses in opposite directions that contribute to establishing a hierarchical relationship in which innate fear responses predominate over the learned ones[117].

The role of Sst neurons was instead clarified only in learned fear. In the CeL, Sst neurons are excited by the CS during fear conditioning[88,90] and their inactivation downregulates learned freezing behaviour[91]. This suggests that suppression of learned freezing by the Htr2a could be mediated by the neurons that overlapped with the Sst neurons. Apart from generation of defensive behaviours[53,92], Sst neurons are also involved in rewarding behaviours as well as Htr2a neurons. Both subpopulations promote drinking behaviour, and activation of these neurons is positively reinforcing for the animal[2,3]. An important difference between the two populations is related to feeding behaviour, since this consummatory behaviour is promoted by

activation of Htr2a [2] but not Sst neurons. However, during *in vivo* calcium imaging experiments performed using a paradigm of appetitive conditioning in which mice forage for food, we found that Sst neurons increase their activity at the onset of feeding bouts while the animal is eating. This result is very similar to what has been previously described for the Htr2a neurons, which, during a feeding task, showed an increase in activity at each eating bout[2].

Since it is only possible to record a limited number of cells per animal during *in vivo* calcium imaging experiments, it could be that the small fraction of Sst neurons that show activity during feeding also co-express Htr2a. However, optogenetic manipulation of the entire Sst population, comprising both Htr2a positive and negative neurons, is not sufficient to promote feeding behaviour. Alternatively, the activity of the Sst neurons we showed could be related to the particular learning behavioural paradigm and put in evidence their role in linking environmental information to the physical properties of the food, and not in a simple consummatory behaviour where no learning and association is needed. Further experiments to better understand the role of Sst neurons in feeding behaviour would be of great interest. It currently is clear that Htr2a and Sst neurons, although having common features, present unique characteristics and, depending on stimuli and context, can be selected to initiate the appropriate defensive or appetitive behaviour.

4.6 Outlook

The aim of this thesis work was to provide a further insight into the CeA circuit in appetite behaviours.

In the first project, in particular, I investigated how specific activity patterns of CeA subpopulations guide optimal choices in foraging. In a conditioned place preference behavioural paradigm, where mice associate food-reward consumption with the environment, I found that both PKCδ and Sst neurons can assign motivational properties to the surrounding signals. Only the PKCδ population, however, is required for learning of contextual food cues, probably incorporating environmental features and stimulus salience to encode memory to the goal location. Previous works showed a role of PKCδ neurons in inhibiting appetitive behaviour in response to satiety[104], in promoting pain-related responses[90], and in the expression of aversive memories[129]. Our work, instead, highlights a 'positive' role of the same neuronal population in the formation of contextual food memories. Because of this, we can hypothesise

that PKCδ neurons represent a general encoding population selecting defensive and appetitive responses depending on circumstances or context. To prove this hypothesis, calcium imaging experiments recording PKCδ cells in the same animal undergoing defensive versus appetitive behaviour would be of great interest. In this way, we could understand if the same cells respond to opposite stimuli, or if different clusters of neurons are involved in opposite behaviours.

The loss of function experiments, which led us to conclude that inhibiting the formation of memory could impair the animal's ability to prefer the location of the food reward, were performed by inhibiting the entire PKCδ population, while with the *in vivo* recordings we analysed the activity only of a subset of cells. It is therefore possible that the specific inhibition of the memory neurons could lead to a different phenotype. However, it is technically very complex to record and manipulate neurons at single cell resolution. One possibility would be to co-express an opsin and a genetically encoded calcium indicator in the same cell, while simultaneously doing optogenetic inhibition and calcium imaging recording. Nevertheless, it would be of extreme interest to further investigate the heterogeneity of the genetic markers that the PKCδ neurons express, based on their location in the CeL or the CeC, for example by performing single nuclei RNA-sequencing. After a further subdivision, one could examine the neuronal function manipulating specifically subclusters of PKCδ cells at the time.

In my second project, I was able to dissect the role of the Htr2a and Sst neurons in the two main CeA subregions, the CeL and CeM, using an intersectional approach. I particularly focused on rewarding and consummatory behaviours and found that while both populations promote drinking, only Htr2a neurons promote food consumption. Surprisingly, we observed that optogenetic activation of the CeM population is sufficient to mediate appetitive responses. A complete examination of the circuit in which Htr2a and Sst function will be very important to understand their role in modulating rewarding behaviours. Preliminary results (data not shown), highlighted a possible role for the CeM projections to the PBN, an important brain region that processes gustatory signals[2], in drinking and feeding behaviour. Since the Htr2a and the Sst populations partially overlap, but only Htr2a neurons activation promotes feeding, it is critical to determine the identity of the PBN neurons that receive CeM^{Htr2a} and CeM^{Sst} projections, and to underline possible distinctions that could explain their different involvement in feeding behaviour. Moreover, since both CeL and CeM Htr2a and Sst neurons project to the PBN, it would be interesting to investigate the specific PBN targets, which could be responsible

for the of the incapacity of the CeL to elicit appetitive behaviour. One possibility to answer these questions would be to apply new spatial transcriptomic techniques: spatially mapping the complete set of RNA expression on brain slices of the PBN cells that receive Htr2a and Sst projections. This would allow us to understand the difference of the targeted PBN cells in both their molecular profile and location.
Additionally, a further investigation of the role of CeL^{Sst} and CeL^{Htr2a}, possibly in fear conditioning, would complete the picture of understanding the function of these two neuronal subpopulations in the CeA.

In conclusion, my findings provide a new insight into the heterogeneity of function of CeA neuronal subpopulations and provide a new method to dissect the CeA based on its spatial subdivisions.

5. References

1 Janak, P. H. & Tye, K. M. From circuits to behaviour in the amygdala. *Nature* **517**, 284-292, doi:10.1038/nature14188 (2015).

2 Douglass, A. M. *et al.* Central amygdala circuits modulate food consumption through a positive-valence mechanism. *Nat Neurosci* **20**, 1384-1394, doi:10.1038/nn.4623 (2017).

3 Kim, J., Zhang, X., Muralidhar, S., LeBlanc, S. A. & Tonegawa, S. Basolateral to Central Amygdala Neural Circuits for Appetitive Behaviors. *Neuron* **93**, 1464-1479.e1465, doi:10.1016/j.neuron.2017.02.034 (2017).

4 Pitkänen, A., Savander, V. & LeDoux, J. E. Organization of intra-amygdaloid circuitries in the rat: an emerging framework for understanding functions of the amygdala. *Trends Neurosci* **20**, 517-523, doi:10.1016/s0166-2236(97)01125-9 (1997).

5 Sah, P., Faber, E. S., Lopez De Armentia, M. & Power, J. The amygdaloid complex: anatomy and physiology. *Physiol Rev* **83**, 803-834, doi:10.1152/physrev.00002.2003 (2003).

6 Dumont, E. C., Martina, M., Samson, R. D., Drolet, G. & Paré, D. Physiological properties of central amygdala neurons: species differences. *Eur J Neurosci* **15**, 545-552, doi:10.1046/j.0953-816x.2001.01879.x (2002).

7 Chieng, B. C., Christie, M. J. & Osborne, P. B. Characterization of neurons in the rat central nucleus of the amygdala: cellular physiology, morphology, and opioid sensitivity. *J Comp Neurol* **497**, 910-927, doi:10.1002/cne.21025 (2006).

8 Krettek, J. E. & Price, J. L. A description of the amygdaloid complex in the rat and cat with observations on intra-amygdaloid axonal connections. *J Comp Neurol* **178**, 255-280, doi:10.1002/cne.901780205 (1978).

9 McDonald, A. J. Coexistence of somatostatin with neuropeptide Y, but not with cholecystokinin or vasoactive intestinal peptide, in neurons of the rat amygdala. *Brain Res* **500**, 37-45, doi:10.1016/0006-8993(89)90297-7 (1989).

10 Shimada, S. *et al.* Coexistence of peptides (corticotropin releasing factor/neurotensin and substance P/somatostatin) in the bed nucleus of the stria terminalis and central amygdaloid nucleus of the rat. *Neuroscience* **30**, 377-383, doi:10.1016/0306-4522(89)90259-5 (1989).

11 Veening, J. G., Swanson, L. W. & Sawchenko, P. E. The organization of projections from the central nucleus of the amygdala to brainstem sites involved in central autonomic regulation: a combined retrograde transport-immunohistochemical study. *Brain Res* **303**, 337-357, doi:10.1016/0006-8993(84)91220-4 (1984).

12 Skofitsch, G. & Jacobowitz, D. M. Calcitonin gene-related peptide: detailed immunohistochemical distribution in the central nervous system. *Peptides* **6**, 721-745, doi:10.1016/0196-9781(85)90178-0 (1985).

13 Gustafson, E. L., Card, J. P. & Moore, R. Y. Neuropeptide Y localization in the rat amygdaloid complex. *J Comp Neurol* **251**, 349-362, doi:10.1002/cne.902510306 (1986).

14 McDonald, A. J. Cytoarchitecture of the central amygdaloid nucleus of the rat. *J Comp Neurol* **208**, 401-418, doi:10.1002/cne.902080409 (1982).

15 Gray, T. S., Cassell, M. D. & Kiss, J. Z. Distribution of pro-opiomelanocortin-derived peptides and enkephalins in the rat central nucleus of the amygdala. *Brain Res* **306**, 354-358, doi:10.1016/0006-8993(84)90386-x (1984).

16 Fellmann, D., Bugnon, C. & Gouget, A. Immunocytochemical demonstration of corticoliberin-like immunoreactivity (CLI) in neurones of the rat amygdala central nucleus (ACN). *Neurosci Lett* **34**, 253-258, doi:10.1016/0304-3940(82)90184-7 (1982).
17 Cassell, M. D., Gray, T. S. & Kiss, J. Z. Neuronal architecture in the rat central nucleus of the amygdala: a cytological, hodological, and immunocytochemical study. *J Comp Neurol* **246**, 478-499, doi:10.1002/cne.902460406 (1986).
18 Duarte, C. R., Schütz, B. & Zimmer, A. Incongruent pattern of neurokinin B expression in rat and mouse brains. *Cell Tissue Res* **323**, 43-51, doi:10.1007/s00441-005-0027-x (2006).
19 Yoon, Y. R. & Baik, J. H. Melanocortin 4 Receptor and Dopamine D2 Receptor Expression in Brain Areas Involved in Food Intake. *Endocrinol Metab (Seoul)* **30**, 576-583, doi:10.3803/EnM.2015.30.4.576 (2015).
20 McDonald, A. J. Cortical pathways to the mammalian amygdala. *Prog Neurobiol* **55**, 257-332, doi:10.1016/s0301-0082(98)00003-3 (1998).
21 Amaral, D. G. & Insausti, R. Retrograde transport of D-[3H]-aspartate injected into the monkey amygdaloid complex. *Exp Brain Res* **88**, 375-388, doi:10.1007/bf02259113 (1992).
22 Mascagni, F., McDonald, A. J. & Coleman, J. R. Corticoamygdaloid and corticocortical projections of the rat temporal cortex: a Phaseolus vulgaris leucoagglutinin study. *Neuroscience* **57**, 697-715, doi:10.1016/0306-4522(93)90016-9 (1993).
23 Shi, C. J. & Cassell, M. D. Cortical, thalamic, and amygdaloid connections of the anterior and posterior insular cortices. *J Comp Neurol* **399**, 440-468, doi:10.1002/(sici)1096-9861(19981005)399:4<440::aid-cne2>3.0.co;2-1 (1998).
24 Shi, C. J. & Cassell, M. D. Cascade projections from somatosensory cortex to the rat basolateral amygdala via the parietal insular cortex. *J Comp Neurol* **399**, 469-491, doi:10.1002/(sici)1096-9861(19981005)399:4<469::aid-cne3>3.0.co;2-# (1998).
25 Ledoux, J. E., Ruggiero, D. A., Forest, R., Stornetta, R. & Reis, D. J. Topographic organization of convergent projections to the thalamus from the inferior colliculus and spinal cord in the rat. *J Comp Neurol* **264**, 123-146, doi:10.1002/cne.902640110 (1987).
26 Nakashima, M. *et al.* An anterograde and retrograde tract-tracing study on the projections from the thalamic gustatory area in the rat: distribution of neurons projecting to the insular cortex and amygdaloid complex. *Neurosci Res* **36**, 297-309, doi:10.1016/s0168-0102(99)00129-7 (2000).
27 Turner, B. H. & Herkenham, M. Thalamoamygdaloid projections in the rat: a test of the amygdala's role in sensory processing. *J Comp Neurol* **313**, 295-325, doi:10.1002/cne.903130208 (1991).
28 Bernard, J. F., Alden, M. & Besson, J. M. The organization of the efferent projections from the pontine parabrachial area to the amygdaloid complex: a Phaseolus vulgaris leucoagglutinin (PHA-L) study in the rat. *J Comp Neurol* **329**, 201-229, doi:10.1002/cne.903290205 (1993).
29 LeDoux, J. E., Farb, C. & Ruggiero, D. A. Topographic organization of neurons in the acoustic thalamus that project to the amygdala. *J Neurosci* **10**, 1043-1054, doi:10.1523/jneurosci.10-04-01043.1990 (1990).

30 Shi, C. & Davis, M. Visual pathways involved in fear conditioning measured with fear-potentiated startle: behavioral and anatomic studies. *J Neurosci* **21**, 9844-9855, doi:10.1523/jneurosci.21-24-09844.2001 (2001).
31 McDonald, A. J., Mascagni, F. & Guo, L. Projections of the medial and lateral prefrontal cortices to the amygdala: a Phaseolus vulgaris leucoagglutinin study in the rat. *Neuroscience* **71**, 55-75, doi:10.1016/0306-4522(95)00417-3 (1996).
32 Davis, M. The role of the amygdala in fear and anxiety. *Annu Rev Neurosci* **15**, 353-375, doi:10.1146/annurev.ne.15.030192.002033 (1992).
33 LeDoux, J. E. Emotion: clues from the brain. *Annu Rev Psychol* **46**, 209-235, doi:10.1146/annurev.ps.46.020195.001233 (1995).
34 Maren, S. Building and burying fear memories in the brain. *Neuroscientist* **11**, 89-99, doi:10.1177/1073858404269232 (2005).
35 Rainnie, D. G., Asprodini, E. K. & Shinnick-Gallagher, P. Excitatory transmission in the basolateral amygdala. *J Neurophysiol* **66**, 986-998, doi:10.1152/jn.1991.66.3.986 (1991).
36 Savander, V., Go, C. G., LeDoux, J. E. & Pitkänen, A. Intrinsic connections of the rat amygdaloid complex: projections originating in the basal nucleus. *J Comp Neurol* **361**, 345-368, doi:10.1002/cne.903610211 (1995).
37 Pitkänen, A. *et al.* Intrinsic connections of the rat amygdaloid complex: projections originating in the lateral nucleus. *J Comp Neurol* **356**, 288-310, doi:10.1002/cne.903560211 (1995).
38 *The amygdala: Neurobiological aspects of emotion, memory, and mental dysfunction*. (Wiley-Liss, 1992).
39 Canteras, N. S., Simerly, R. B. & Swanson, L. W. Organization of projections from the medial nucleus of the amygdala: a PHAL study in the rat. *J Comp Neurol* **360**, 213-245, doi:10.1002/cne.903600203 (1995).
40 Jolkkonen, E. & Pitkänen, A. Intrinsic connections of the rat amygdaloid complex: projections originating in the central nucleus. *J Comp Neurol* **395**, 53-72, doi:10.1002/(sici)1096-9861(19980525)395:1<53::aid-cne5>3.0.co;2-g (1998).
41 Petrovich, G. D., Canteras, N. S. & Swanson, L. W. Combinatorial amygdalar inputs to hippocampal domains and hypothalamic behavior systems. *Brain Res Brain Res Rev* **38**, 247-289, doi:10.1016/s0165-0173(01)00080-7 (2001).
42 McDonald, A. J. Topographical organization of amygdaloid projections to the caudatoputamen, nucleus accumbens, and related striatal-like areas of the rat brain. *Neuroscience* **44**, 15-33, doi:10.1016/0306-4522(91)90248-m (1991).
43 LeDoux, J. E., Iwata, J., Cicchetti, P. & Reis, D. J. Different projections of the central amygdaloid nucleus mediate autonomic and behavioral correlates of conditioned fear. *J Neurosci* **8**, 2517-2529, doi:10.1523/jneurosci.08-07-02517.1988 (1988).
44 Behbehani, M. M. Functional characteristics of the midbrain periaqueductal gray. *Prog Neurobiol* **46**, 575-605, doi:10.1016/0301-0082(95)00009-k (1995).
45 Gauriau, C. & Bernard, J. F. Pain pathways and parabrachial circuits in the rat. *Exp Physiol* **87**, 251-258, doi:10.1113/eph8702357 (2002).
46 van der Kooy, D., Koda, L. Y., McGinty, J. F., Gerfen, C. R. & Bloom, F. E. The organization of projections from the cortex, amygdala, and hypothalamus to the nucleus of the solitary tract in rat. *J Comp Neurol* **224**, 1-24, doi:10.1002/cne.902240102 (1984).

47 Swanson, L. W. Cerebral hemisphere regulation of motivated behavior. *Brain Res* **886**, 113-164, doi:10.1016/s0006-8993(00)02905-x (2000).
48 Weiskrantz, L. Behavioral changes associated with ablation of the amygdaloid complex in monkeys. *J Comp Physiol Psychol* **49**, 381-391, doi:10.1037/h0088009 (1956).
49 Fadok, J. P., Markovic, M., Tovote, P. & Lüthi, A. New perspectives on central amygdala function. *Curr Opin Neurobiol* **49**, 141-147, doi:10.1016/j.conb.2018.02.009 (2018).
50 Davis, M. & Whalen, P. J. The amygdala: vigilance and emotion. *Mol Psychiatry* **6**, 13-34, doi:10.1038/sj.mp.4000812 (2001).
51 Everitt, B. J., Cardinal, R. N., Parkinson, J. A. & Robbins, T. W. Appetitive behavior: impact of amygdala-dependent mechanisms of emotional learning. *Ann N Y Acad Sci* **985**, 233-250 (2003).
52 Fadok, J. P. *et al.* A competitive inhibitory circuit for selection of active and passive fear responses. *Nature* **542**, 96-100, doi:10.1038/nature21047 (2017).
53 Yu, K., Garcia da Silva, P., Albeanu, D. F. & Li, B. Central Amygdala Somatostatin Neurons Gate Passive and Active Defensive Behaviors. *J Neurosci* **36**, 6488-6496, doi:10.1523/jneurosci.4419-15.2016 (2016).
54 Cador, M., Robbins, T. W. & Everitt, B. J. Involvement of the amygdala in stimulus-reward associations: interaction with the ventral striatum. *Neuroscience* **30**, 77-86, doi:10.1016/0306-4522(89)90354-0 (1989).
55 Everitt, B. J., Cador, M. & Robbins, T. W. Interactions between the amygdala and ventral striatum in stimulus-reward associations: studies using a second-order schedule of sexual reinforcement. *Neuroscience* **30**, 63-75, doi:10.1016/0306-4522(89)90353-9 (1989).
56 Gallagher, M., Graham, P. W. & Holland, P. C. The amygdala central nucleus and appetitive Pavlovian conditioning: lesions impair one class of conditioned behavior. *J Neurosci* **10**, 1906-1911, doi:10.1523/jneurosci.10-06-01906.1990 (1990).
57 Hatfield, T., Han, J. S., Conley, M., Gallagher, M. & Holland, P. Neurotoxic lesions of basolateral, but not central, amygdala interfere with Pavlovian second-order conditioning and reinforcer devaluation effects. *J Neurosci* **16**, 5256-5265, doi:10.1523/jneurosci.16-16-05256.1996 (1996).
58 Baxter, M. G. & Murray, E. A. The amygdala and reward. *Nat Rev Neurosci* **3**, 563-573, doi:10.1038/nrn875 (2002).
59 Murray, E. & Mishkin, M. Severe tactual as well as visual memory deficits follow combined removal of the amygdala and hippocampus in monkeys. *The Journal of Neuroscience* **4**, 2565-2580, doi:10.1523/jneurosci.04-10-02565.1984 (1984).
60 Murray, E. & Mishkin, M. Amygdalectomy impairs crossmodal association in monkeys. *Science* **228**, 604-606, doi:10.1126/science.3983648 (1985).
61 Gaffan, D. & Harrison, S. Amygdalectomy and disconnection in visual learning for auditory secondary reinforcement by monkeys. *The Journal of Neuroscience* **7**, 2285-2292 (1987).
62 Hiroi, N. & White, N. M. The lateral nucleus of the amygdala mediates expression of the amphetamine-produced conditioned place preference. *J Neurosci* **11**, 2107-2116, doi:10.1523/jneurosci.11-07-02107.1991 (1991).
63 Morrison, S. E. & Salzman, C. D. Re-valuing the amygdala. *Curr Opin Neurobiol* **20**, 221-230, doi:10.1016/j.conb.2010.02.007 (2010).

64 Hatfield, T., Han, J.-S., Conley, M., Gallagher, M. & Holland, P. Neurotoxic Lesions of Basolateral, But Not Central, Amygdala Interfere with Pavlovian Second-Order Conditioning and Reinforcer Devaluation Effects. *The Journal of Neuroscience* **16**, 5256-5265, doi:10.1523/jneurosci.16-16-05256.1996 (1996).
65 Parkinson, J. A., Robbins, T. W. & Everitt, B. J. Dissociable roles of the central and basolateral amygdala in appetitive emotional learning. *Eur J Neurosci* **12**, 405-413, doi:10.1046/j.1460-9568.2000.00960.x (2000).
66 Robinson, M. J., Warlow, S. M. & Berridge, K. C. Optogenetic excitation of central amygdala amplifies and narrows incentive motivation to pursue one reward above another. *J Neurosci* **34**, 16567-16580, doi:10.1523/jneurosci.2013-14.2014 (2014).
67 Carter, M. E., Soden, M. E., Zweifel, L. S. & Palmiter, R. D. Genetic identification of a neural circuit that suppresses appetite. *Nature* **503**, 111-114, doi:10.1038/nature12596 (2013).
68 Kl¸ver, H. & Bucy, P. C. *"Psychic blindness" and other symptoms following bilateral temporal lobectomy in Rhesus monkeys*. ([s.n.], 1937).
69 Sigurdsson, T., Doyère, V., Cain, C. K. & LeDoux, J. E. Long-term potentiation in the amygdala: a cellular mechanism of fear learning and memory. *Neuropharmacology* **52**, 215-227, doi:10.1016/j.neuropharm.2006.06.022 (2007).
70 Balleine, B. W. & Killcross, S. Parallel incentive processing: an integrated view of amygdala function. *Trends Neurosci* **29**, 272-279, doi:10.1016/j.tins.2006.03.002 (2006).
71 LeDoux, J. E. Emotion, memory and the brain. *Sci Am* **270**, 50-57, doi:10.1038/scientificamerican0694-50 (1994).
72 Shi, C. J. & Cassell, M. D. Cortical, thalamic, and amygdaloid projections of rat temporal cortex. *J Comp Neurol* **382**, 153-175 (1997).
73 Royer, S., Martina, M. & Paré, D. An inhibitory interface gates impulse traffic between the input and output stations of the amygdala. *J Neurosci* **19**, 10575-10583, doi:10.1523/jneurosci.19-23-10575.1999 (1999).
74 Pare, D. & Duvarci, S. Amygdala microcircuits mediating fear expression and extinction. *Curr Opin Neurobiol* **22**, 717-723, doi:10.1016/j.conb.2012.02.014 (2012).
75 Blair, H. T., Schafe, G. E., Bauer, E. P., Rodrigues, S. M. & LeDoux, J. E. Synaptic plasticity in the lateral amygdala: a cellular hypothesis of fear conditioning. *Learn Mem* **8**, 229-242, doi:10.1101/lm.30901 (2001).
76 Balleine, B. W. Neural bases of food-seeking: affect, arousal and reward in corticostriatolimbic circuits. *Physiol Behav* **86**, 717-730, doi:10.1016/j.physbeh.2005.08.061 (2005).
77 Bernard, J. F. & Besson, J. M. The spino(trigemino)pontoamygdaloid pathway: electrophysiological evidence for an involvement in pain processes. *J Neurophysiol* **63**, 473-490, doi:10.1152/jn.1990.63.3.473 (1990).
78 Jasmin, L., Burkey, A. R., Card, J. P. & Basbaum, A. I. Transneuronal labeling of a nociceptive pathway, the spino-(trigemino-)parabrachio-amygdaloid, in the rat. *J Neurosci* **17**, 3751-3765, doi:10.1523/jneurosci.17-10-03751.1997 (1997).
79 Samson, R. D. & Paré, D. Activity-dependent synaptic plasticity in the central nucleus of the amygdala. *J Neurosci* **25**, 1847-1855, doi:10.1523/jneurosci.3713-04.2005 (2005).

80 Applegate, C. D., Frysinger, R. C., Kapp, B. S. & Gallagher, M. Multiple unit activity recorded from amygdala central nucleus during Pavlovian heart rate conditioning in rabbit. *Brain Res* **238**, 457-462, doi:10.1016/0006-8993(82)90123-8 (1982).
81 Pascoe, J. P. & Kapp, B. S. Electrophysiological characteristics of amygdaloid central nucleus neurons during Pavlovian fear conditioning in the rabbit. *Behav Brain Res* **16**, 117-133, doi:10.1016/0166-4328(85)90087-7 (1985).
82 Goosens, K. A. & Maren, S. Pretraining NMDA receptor blockade in the basolateral complex, but not the central nucleus, of the amygdala prevents savings of conditional fear. *Behav Neurosci* **117**, 738-750, doi:10.1037/0735-7044.117.4.738 (2003).
83 Wilensky, A. E., Schafe, G. E., Kristensen, M. P. & LeDoux, J. E. Rethinking the fear circuit: the central nucleus of the amygdala is required for the acquisition, consolidation, and expression of Pavlovian fear conditioning. *J Neurosci* **26**, 12387-12396, doi:10.1523/jneurosci.4316-06.2006 (2006).
84 Ehrlich, I. *et al.* Amygdala inhibitory circuits and the control of fear memory. *Neuron* **62**, 757-771, doi:10.1016/j.neuron.2009.05.026 (2009).
85 Smith, Y. & Paré, D. Intra-amygdaloid projections of the lateral nucleus in the cat: PHA-L anterograde labeling combined with postembedding GABA and glutamate immunocytochemistry. *J Comp Neurol* **342**, 232-248, doi:10.1002/cne.903420207 (1994).
86 Tovote, P. *et al.* Midbrain circuits for defensive behaviour. *Nature* **534**, 206-212, doi:10.1038/nature17996 (2016).
87 Viviani, D. *et al.* Oxytocin selectively gates fear responses through distinct outputs from the central amygdala. *Science* **333**, 104-107, doi:10.1126/science.1201043 (2011).
88 Ciocchi, S. *et al.* Encoding of conditioned fear in central amygdala inhibitory circuits. *Nature* **468**, 277-282, doi:10.1038/nature09559 (2010).
89 Delaney, A. J., Crane, J. W. & Sah, P. Noradrenaline modulates transmission at a central synapse by a presynaptic mechanism. *Neuron* **56**, 880-892, doi:10.1016/j.neuron.2007.10.022 (2007).
90 Haubensak, W. *et al.* Genetic dissection of an amygdala microcircuit that gates conditioned fear. *Nature* **468**, 270-276, doi:10.1038/nature09553 (2010).
91 Li, H. *et al.* Experience-dependent modification of a central amygdala fear circuit. *Nat Neurosci* **16**, 332-339, doi:10.1038/nn.3322 (2013).
92 Penzo, M. A., Robert, V. & Li, B. Fear conditioning potentiates synaptic transmission onto long-range projection neurons in the lateral subdivision of central amygdala. *J Neurosci* **34**, 2432-2437, doi:10.1523/jneurosci.4166-13.2014 (2014).
93 Rossi, M. A. & Stuber, G. D. Overlapping Brain Circuits for Homeostatic and Hedonic Feeding. *Cell Metab* **27**, 42-56, doi:10.1016/j.cmet.2017.09.021 (2018).
94 Aponte, Y., Atasoy, D. & Sternson, S. M. AGRP neurons are sufficient to orchestrate feeding behavior rapidly and without training. *Nat Neurosci* **14**, 351-355, doi:10.1038/nn.2739 (2011).
95 Krashes, M. J. *et al.* Rapid, reversible activation of AgRP neurons drives feeding behavior in mice. *J Clin Invest* **121**, 1424-1428, doi:10.1172/jci46229 (2011).
96 Chen, Y., Lin, Y. C., Kuo, T. W. & Knight, Z. A. Sensory detection of food rapidly modulates arcuate feeding circuits. *Cell* **160**, 829-841, doi:10.1016/j.cell.2015.01.033 (2015).

97 Zhan, C. *et al.* Acute and long-term suppression of feeding behavior by POMC neurons in the brainstem and hypothalamus, respectively. *J Neurosci* **33**, 3624-3632, doi:10.1523/jneurosci.2742-12.2013 (2013).
98 Cowley, M. A. *et al.* Leptin activates anorexigenic POMC neurons through a neural network in the arcuate nucleus. *Nature* **411**, 480-484, doi:10.1038/35078085 (2001).
99 Anand, B. K. & Brobeck, J. R. Hypothalamic control of food intake in rats and cats. *Yale J Biol Med* **24**, 123-140 (1951).
100 Hoebel, B. G. & Teitelbaum, P. Hypothalamic control of feeding and self-stimulation. *Science* **135**, 375-377, doi:10.1126/science.135.3501.375 (1962).
101 Jennings, J. H., Rizzi, G., Stamatakis, A. M., Ung, R. L. & Stuber, G. D. The inhibitory circuit architecture of the lateral hypothalamus orchestrates feeding. *Science* **341**, 1517-1521, doi:10.1126/science.1241812 (2013).
102 O'Connor, E. C. *et al.* Accumbal D1R Neurons Projecting to Lateral Hypothalamus Authorize Feeding. *Neuron* **88**, 553-564, doi:10.1016/j.neuron.2015.09.038 (2015).
103 Nieh, E. H. *et al.* Inhibitory Input from the Lateral Hypothalamus to the Ventral Tegmental Area Disinhibits Dopamine Neurons and Promotes Behavioral Activation. *Neuron* **90**, 1286-1298, doi:10.1016/j.neuron.2016.04.035 (2016).
104 Cai, H., Haubensak, W., Anthony, T. E. & Anderson, D. J. Central amygdala PKC-δ(+) neurons mediate the influence of multiple anorexigenic signals. *Nat Neurosci* **17**, 1240-1248, doi:10.1038/nn.3767 (2014).
105 Kishi, T. & Elmquist, J. K. Body weight is regulated by the brain: a link between feeding and emotion. *Mol Psychiatry* **10**, 132-146, doi:10.1038/sj.mp.4001638 (2005).
106 Kask, A. & Schiöth, H. B. Tonic inhibition of food intake during inactive phase is reversed by the injection of the melanocortin receptor antagonist into the paraventricular nucleus of the hypothalamus and central amygdala of the rat. *Brain Res* **887**, 460-464, doi:10.1016/s0006-8993(00)03034-1 (2000).
107 Beckman, T. R., Shi, Q., Levine, A. S. & Billington, C. J. Amygdalar opioids modulate hypothalamic melanocortin-induced anorexia. *Physiol Behav* **96**, 568-573, doi:10.1016/j.physbeh.2008.12.007 (2009).
108 Fekete, E. M., Bagi, E. E., Tóth, K. & Lénárd, L. Neuromedin C microinjected into the amygdala inhibits feeding. *Brain Res Bull* **71**, 386-392, doi:10.1016/j.brainresbull.2006.10.007 (2007).
109 Box, B. M. & Mogenson, G. J. Alterations in ingestive behaviors after bilateral lesions of the amygdala in the rat. *Physiol Behav* **15**, 679-688, doi:10.1016/0031-9384(75)90119-5 (1975).
110 Kemble, E. D., Studelska, D. R. & Schmidt, M. K. Effects of central amygdaloid nucleus lesions on ingestion, taste reactivity, exploration and taste aversion. *Physiol Behav* **22**, 789-793, doi:10.1016/0031-9384(79)90250-6 (1979).
111 Hardaway, J. A. *et al.* Central Amygdala Prepronociceptin-Expressing Neurons Mediate Palatable Food Consumption and Reward. *Neuron* **102**, 1037-1052.e1037, doi:10.1016/j.neuron.2019.03.037 (2019).
112 Comoli, E., Ribeiro-Barbosa, E. R., Negrão, N., Goto, M. & Canteras, N. S. Functional mapping of the prosencephalic systems involved in organizing predatory behavior in rats. *Neuroscience* **130**, 1055-1067, doi:10.1016/j.neuroscience.2004.10.020 (2005).

113 Shammah-Lagnado, S. J., Costa, M. S. & Ricardo, J. A. Afferent connections of the parvocellular reticular formation: a horseradish peroxidase study in the rat. *Neuroscience* **50**, 403-425, doi:10.1016/0306-4522(92)90433-3 (1992).
114 Van Daele, D. J., Fazan, V. P., Agassandian, K. & Cassell, M. D. Amygdala connections with jaw, tongue and laryngo-pharyngeal premotor neurons. *Neuroscience* **177**, 93-113, doi:10.1016/j.neuroscience.2010.12.063 (2011).
115 Han, W. *et al.* Integrated Control of Predatory Hunting by the Central Nucleus of the Amygdala. *Cell* **168**, 311-324.e318, doi:https://doi.org/10.1016/j.cell.2016.12.027 (2017).
116 Gross, C. T. & Canteras, N. S. The many paths to fear. *Nat Rev Neurosci* **13**, 651-658, doi:10.1038/nrn3301 (2012).
117 Isosaka, T. *et al.* Htr2a-Expressing Cells in the Central Amygdala Control the Hierarchy between Innate and Learned Fear. *Cell* **163**, 1153-1164, doi:10.1016/j.cell.2015.10.047 (2015).
118 De Oca, B. M., DeCola, J. P., Maren, S. & Fanselow, M. S. Distinct regions of the periaqueductal gray are involved in the acquisition and expression of defensive responses. *J Neurosci* **18**, 3426-3432, doi:10.1523/jneurosci.18-09-03426.1998 (1998).
119 Vianna, D. M., Graeff, F. G., Landeira-Fernandez, J. & Brandão, M. L. Lesion of the ventral periaqueductal gray reduces conditioned fear but does not change freezing induced by stimulation of the dorsal periaqueductal gray. *Learn Mem* **8**, 164-169, doi:10.1101/lm.36101 (2001).
120 Aguiar, D. C. & Guimarães, F. S. Blockade of NMDA receptors and nitric oxide synthesis in the dorsolateral periaqueductal gray attenuates behavioral and cellular responses of rats exposed to a live predator. *J Neurosci Res* **87**, 2418-2429, doi:10.1002/jnr.22082 (2009).
121 Silva, B. A. *et al.* Independent hypothalamic circuits for social and predator fear. *Nat Neurosci* **16**, 1731-1733, doi:10.1038/nn.3573 (2013).
122 Davis, M., Walker, D. L., Miles, L. & Grillon, C. Phasic vs sustained fear in rats and humans: role of the extended amygdala in fear vs anxiety. *Neuropsychopharmacology* **35**, 105-135, doi:10.1038/npp.2009.109 (2010).
123 Botta, P. *et al.* Regulating anxiety with extrasynaptic inhibition. *Nat Neurosci* **18**, 1493-1500, doi:10.1038/nn.4102 (2015).
124 Tye, K. M. *et al.* Amygdala circuitry mediating reversible and bidirectional control of anxiety. *Nature* **471**, 358-362, doi:10.1038/nature09820 (2011).
125 Bernard, J. F., Peschanski, M. & Besson, J. M. A possible spino (trigemino)-ponto-amygdaloid pathway for pain. *Neurosci Lett* **100**, 83-88, doi:10.1016/0304-3940(89)90664-2 (1989).
126 Han, S., Soleiman, M. T., Soden, M. E., Zweifel, L. S. & Palmiter, R. D. Elucidating an Affective Pain Circuit that Creates a Threat Memory. *Cell* **162**, 363-374, doi:10.1016/j.cell.2015.05.057 (2015).
127 Neugebauer, V. Amygdala pain mechanisms. *Handb Exp Pharmacol* **227**, 261-284, doi:10.1007/978-3-662-46450-2_13 (2015).
128 Neugebauer, V., Li, W., Bird, G. C. & Han, J. S. The amygdala and persistent pain. *Neuroscientist* **10**, 221-234, doi:10.1177/1073858403261077 (2004).

129 Wilson, T. D. *et al.* Dual and Opposing Functions of the Central Amygdala in the Modulation of Pain. *Cell Rep* **29**, 332-346.e335, doi:10.1016/j.celrep.2019.09.011 (2019).
130 Hua, T. *et al.* General anesthetics activate a potent central pain-suppression circuit in the amygdala. *Nat Neurosci* **23**, 854-868, doi:10.1038/s41593-020-0632-8 (2020).
131 Leib, D. E., Zimmerman, C. A. & Knight, Z. A. Thirst. *Curr Biol* **26**, R1260-r1265, doi:10.1016/j.cub.2016.11.019 (2016).
132 Hull, C. L. *Principles of behavior : an introduction to behavior theory*. (D. Appleton-Century Company, Incorporated, 1943).
133 Miller, N. E. Experiments on motivation. Studies combining psychological, physiological, and pharmacological techniques. *Science* **126**, 1271-1278, doi:10.1126/science.126.3286.1271 (1957).
134 Oatley, K. Brain mechanisms and motivation. *Nature* **225**, 797-801, doi:10.1038/225797a0 (1970).
135 Berridge, K. C. Motivation concepts in behavioral neuroscience. *Physiol Behav* **81**, 179-209, doi:10.1016/j.physbeh.2004.02.004 (2004).
136 Anderson, D. J. Circuit modules linking internal states and social behaviour in flies and mice. *Nat Rev Neurosci* **17**, 692-704, doi:10.1038/nrn.2016.125 (2016).
137 *Learning, motivation, and cognition: The functional behaviorism of Robert C. Bolles*. (American Psychological Association, 1997).
138 Allen, W. E. *et al.* Thirst-associated preoptic neurons encode an aversive motivational drive. *Science* **357**, 1149-1155, doi:10.1126/science.aan6747 (2017).
139 Saker, P. *et al.* Regional brain responses associated with drinking water during thirst and after its satiation. *Proc Natl Acad Sci U S A* **111**, 5379-5384, doi:10.1073/pnas.1403382111 (2014).
140 Johnson, A. K. & Thunhorst, R. L. The neuroendocrinology of thirst and salt appetite: visceral sensory signals and mechanisms of central integration. *Front Neuroendocrinol* **18**, 292-353, doi:10.1006/frne.1997.0153 (1997).
141 McKinley, M. J. & Johnson, A. K. The physiological regulation of thirst and fluid intake. *News Physiol Sci* **19**, 1-6, doi:10.1152/nips.01470.2003 (2004).
142 Mandelblat-Cerf, Y. *et al.* Bidirectional Anticipation of Future Osmotic Challenges by Vasopressin Neurons. *Neuron* **93**, 57-65, doi:10.1016/j.neuron.2016.11.021 (2017).
143 Curtis, K. S. & Stricker, E. M. Enhanced fluid intake by rats after capsaicin treatment. *Am J Physiol* **272**, R704-709, doi:10.1152/ajpregu.1997.272.2.R704 (1997).
144 Wood, R. J., Maddison, S., Rolls, E. T., Rolls, B. J. & Gibbs, J. Drinking in rhesus monkeys: role of presystemic and systemic factors in control of drinking. *J Comp Physiol Psychol* **94**, 1135-1148, doi:10.1037/h0077745 (1980).
145 Gibbs, J., Rolls, B. J. & Rolls, E. T. in *The Physiology of Thirst and Sodium Appetite* (eds G. de Caro, A. N. Epstein, & M. Massi) 287-294 (Springer US, 1986).
146 Hyde, T. M. & Miselis, R. R. Area postrema and adjacent nucleus of the solitary tract in water and sodium balance. *Am J Physiol* **247**, R173-182, doi:10.1152/ajpregu.1984.247.1.R173 (1984).
147 Edwards, G. L. & Ritter, R. C. Area postrema lesions increase drinking to angiotensin and extracellular dehydration. *Physiol Behav* **29**, 943-947, doi:10.1016/0031-9384(82)90348-1 (1982).

148 Ryan, P. J., Ross, S. I., Campos, C. A., Derkach, V. A. & Palmiter, R. D. Oxytocin-receptor-expressing neurons in the parabrachial nucleus regulate fluid intake. *Nat Neurosci* **20**, 1722-1733, doi:10.1038/s41593-017-0014-z (2017).
149 Menani, J. V., De Luca, L. A., Jr. & Johnson, A. K. Role of the lateral parabrachial nucleus in the control of sodium appetite. *Am J Physiol Regul Integr Comp Physiol* **306**, R201-210, doi:10.1152/ajpregu.00251.2012 (2014).
150 Sawchenko, P. E. Central connections of the sensory and motor nuclei of the vagus nerve. *J Auton Nerv Syst* **9**, 13-26, doi:10.1016/0165-1838(83)90129-7 (1983).
151 Dong, H. W., Petrovich, G. D. & Swanson, L. W. Topography of projections from amygdala to bed nuclei of the stria terminalis. *Brain Res Brain Res Rev* **38**, 192-246, doi:10.1016/s0165-0173(01)00079-0 (2001).
152 Galaverna, O., De Luca, L. A., Jr., Schulkin, J., Yao, S. Z. & Epstein, A. N. Deficits in NaCl ingestion after damage to the central nucleus of the amygdala in the rat. *Brain Res Bull* **28**, 89-98, doi:10.1016/0361-9230(92)90234-o (1992).
153 Zardetto-Smith, A. M., Beltz, T. G. & Johnson, A. K. Role of the central nucleus of the amygdala and bed nucleus of the stria terminalis in experimentally-induced salt appetite. *Brain Res* **645**, 123-134, doi:10.1016/0006-8993(94)91645-4 (1994).
154 Johnson, A. K., de Olmos, J., Pastuskovas, C. V., Zardetto-Smith, A. M. & Vivas, L. The extended amygdala and salt appetite. *Ann N Y Acad Sci* **877**, 258-280, doi:10.1111/j.1749-6632.1999.tb09272.x (1999).
155 Smith, G. P. & Jerome, C. Effects of total and selective abdominal vagotomies on water intake in rats. *J Auton Nerv Syst* **9**, 259-271, doi:10.1016/0165-1838(83)90146-7 (1983).
156 Andrade-Franzé, G. M. F. *et al.* Lateral parabrachial nucleus and opioid mechanisms of the central nucleus of the amygdala in the control of sodium intake. *Behavioural Brain Research* **316**, 11-17, doi:https://doi.org/10.1016/j.bbr.2016.08.035 (2017).
157 Swanson, L. W. & Kuypers, H. G. The paraventricular nucleus of the hypothalamus: cytoarchitectonic subdivisions and organization of projections to the pituitary, dorsal vagal complex, and spinal cord as demonstrated by retrograde fluorescence double-labeling methods. *J Comp Neurol* **194**, 555-570, doi:10.1002/cne.901940306 (1980).
158 Zimmerman, C. A., Leib, D. E. & Knight, Z. A. Neural circuits underlying thirst and fluid homeostasis. *Nat Rev Neurosci* **18**, 459-469, doi:10.1038/nrn.2017.71 (2017).
159 Bourque, C. W. Central mechanisms of osmosensation and systemic osmoregulation. *Nat Rev Neurosci* **9**, 519-531, doi:10.1038/nrn2400 (2008).
160 Farrell, M. J. *et al.* Cortical activation and lamina terminalis functional connectivity during thirst and drinking in humans. *Am J Physiol Regul Integr Comp Physiol* **301**, R623-631, doi:10.1152/ajpregu.00817.2010 (2011).
161 Gizowski, C. & Bourque, C. W. The neural basis of homeostatic and anticipatory thirst. *Nat Rev Nephrol* **14**, 11-25, doi:10.1038/nrneph.2017.149 (2018).
162 Denton, D. A., McKinley, M. J. & Weisinger, R. S. Hypothalamic integration of body fluid regulation. *Proc Natl Acad Sci U S A* **93**, 7397-7404, doi:10.1073/pnas.93.14.7397 (1996).
163 Oka, Y., Ye, M. & Zuker, C. S. Thirst driving and suppressing signals encoded by distinct neural populations in the brain. *Nature* **520**, 349-352, doi:10.1038/nature14108 (2015).

164 Abbott, S. B., Machado, N. L., Geerling, J. C. & Saper, C. B. Reciprocal Control of Drinking Behavior by Median Preoptic Neurons in Mice. *J Neurosci* **36**, 8228-8237, doi:10.1523/jneurosci.1244-16.2016 (2016).
165 Chow, B. Y. *et al.* High-performance genetically targetable optical neural silencing by light-driven proton pumps. *Nature* **463**, 98-102, doi:10.1038/nature08652 (2010).
166 Otchy, T. M. *et al.* Acute off-target effects of neural circuit manipulations. *Nature* **528**, 358-363, doi:10.1038/nature16442 (2015).
167 Zhang, F., Aravanis, A. M., Adamantidis, A., de Lecea, L. & Deisseroth, K. Circuit-breakers: optical technologies for probing neural signals and systems. *Nat Rev Neurosci* **8**, 577-581, doi:10.1038/nrn2192 (2007).
168 Mattis, J. *et al.* Principles for applying optogenetic tools derived from direct comparative analysis of microbial opsins. *Nat Methods* **9**, 159-172, doi:10.1038/nmeth.1808 (2011).
169 Allen, B. D., Singer, A. C. & Boyden, E. S. Principles of designing interpretable optogenetic behavior experiments. *Learn Mem* **22**, 232-238, doi:10.1101/lm.038026.114 (2015).
170 Chuong, A. S. *et al.* Noninvasive optical inhibition with a red-shifted microbial rhodopsin. *Nat Neurosci* **17**, 1123-1129, doi:10.1038/nn.3752 (2014).
171 Boyden, E. S., Zhang, F., Bamberg, E., Nagel, G. & Deisseroth, K. Millisecond-timescale, genetically targeted optical control of neural activity. *Nat Neurosci* **8**, 1263-1268, doi:10.1038/nn1525 (2005).
172 Nagel, G. *et al.* Channelrhodopsin-2, a directly light-gated cation-selective membrane channel. *Proc Natl Acad Sci U S A* **100**, 13940-13945, doi:10.1073/pnas.1936192100 (2003).
173 Zhang, F. *et al.* Multimodal fast optical interrogation of neural circuitry. *Nature* **446**, 633-639, doi:10.1038/nature05744 (2007).
174 Ihara, K. *et al.* Evolution of the archaeal rhodopsins: evolution rate changes by gene duplication and functional differentiation. *J Mol Biol* **285**, 163-174, doi:10.1006/jmbi.1998.2286 (1999).
175 Yizhar, O., Fenno, Lief E., Davidson, Thomas J., Mogri, M. & Deisseroth, K. Optogenetics in Neural Systems. *Neuron* **71**, 9-34, doi:https://doi.org/10.1016/j.neuron.2011.06.004 (2011).
176 Wiegert, J. S., Mahn, M., Prigge, M., Printz, Y. & Yizhar, O. Silencing Neurons: Tools, Applications, and Experimental Constraints. *Neuron* **95**, 504-529, doi:10.1016/j.neuron.2017.06.050 (2017).
177 Mahn, M. *et al.* Optogenetic silencing of neurotransmitter release with a naturally occurring invertebrate rhodopsin. *bioRxiv*, 2021.2002.2018.431673, doi:10.1101/2021.02.18.431673 (2021).
178 Atasoy, D., Aponte, Y., Su, H. H. & Sternson, S. M. A FLEX switch targets Channelrhodopsin-2 to multiple cell types for imaging and long-range circuit mapping. *J Neurosci* **28**, 7025-7030, doi:10.1523/jneurosci.1954-08.2008 (2008).
179 Kügler, S., Lingor, P., Schöll, U., Zolotukhin, S. & Bähr, M. Differential transgene expression in brain cells in vivo and in vitro from AAV-2 vectors with small transcriptional control units. *Virology* **311**, 89-95, doi:10.1016/s0042-6822(03)00162-4 (2003).
180 Chen, T. W. *et al.* Ultrasensitive fluorescent proteins for imaging neuronal activity. *Nature* **499**, 295-300, doi:10.1038/nature12354 (2013).

181 Resendez, S. L. & Stuber, G. D. In vivo calcium imaging to illuminate neurocircuit activity dynamics underlying naturalistic behavior. *Neuropsychopharmacology* **40**, 238-239, doi:10.1038/npp.2014.206 (2015).
182 Svoboda, K. & Yasuda, R. Principles of two-photon excitation microscopy and its applications to neuroscience. *Neuron* **50**, 823-839, doi:10.1016/j.neuron.2006.05.019 (2006).
183 Ziv, Y. *et al.* Long-term dynamics of CA1 hippocampal place codes. *Nat Neurosci* **16**, 264-266, doi:10.1038/nn.3329 (2013).
184 Cui, G. *et al.* Deep brain optical measurements of cell type-specific neural activity in behaving mice. *Nat Protoc* **9**, 1213-1228, doi:10.1038/nprot.2014.080 (2014).
185 Gunaydin, L. A. *et al.* Natural neural projection dynamics underlying social behavior. *Cell* **157**, 1535-1551, doi:10.1016/j.cell.2014.05.017 (2014).
186 Fenno, L. E. *et al.* Comprehensive Dual- and Triple-Feature Intersectional Single-Vector Delivery of Diverse Functional Payloads to Cells of Behaving Mammals. *Neuron* **107**, 836-853.e811, doi:https://doi.org/10.1016/j.neuron.2020.06.003 (2020).
187 Madisen, L. *et al.* A robust and high-throughput Cre reporting and characterization system for the whole mouse brain. *Nat Neurosci* **13**, 133-140, doi:10.1038/nn.2467 (2010).
188 Ray, R. S. *et al.* Impaired respiratory and body temperature control upon acute serotonergic neuron inhibition. *Science* **333**, 637-642, doi:10.1126/science.1205295 (2011).
189 Sciolino, N. R. *et al.* Recombinase-Dependent Mouse Lines for Chemogenetic Activation of Genetically Defined Cell Types. *Cell Rep* **15**, 2563-2573, doi:10.1016/j.celrep.2016.05.034 (2016).
190 Lu, J. *et al.* MIN1PIPE: A Miniscope 1-Photon-Based Calcium Imaging Signal Extraction Pipeline. *Cell Rep* **23**, 3673-3684, doi:10.1016/j.celrep.2018.05.062 (2018).
191 Sheintuch, L. *et al.* Tracking the Same Neurons across Multiple Days in Ca(2+) Imaging Data. *Cell Rep* **21**, 1102-1115, doi:10.1016/j.celrep.2017.10.013 (2017).
192 Miri, A., Daie, K., Burdine, R. D., Aksay, E. & Tank, D. W. Regression-based identification of behavior-encoding neurons during large-scale optical imaging of neural activity at cellular resolution. *J Neurophysiol* **105**, 964-980, doi:10.1152/jn.00702.2010 (2011).
193 Luuk, H. *et al.* Distribution of Wfs1 protein in the central nervous system of the mouse and its relation to clinical symptoms of the Wolfram syndrome. *J Comp Neurol* **509**, 642-660, doi:10.1002/cne.21777 (2008).
194 Madisen, L. *et al.* A toolbox of Cre-dependent optogenetic transgenic mice for light-induced activation and silencing. *Nat Neurosci* **15**, 793-802, doi:10.1038/nn.3078 (2012).
195 Carleton, A., Accolla, R. & Simon, S. A. Coding in the mammalian gustatory system. *Trends Neurosci* **33**, 326-334, doi:10.1016/j.tins.2010.04.002 (2010).
196 Yamamoto, T. & Ueji, K. Brain mechanisms of flavor learning. *Front Syst Neurosci* **5**, 76, doi:10.3389/fnsys.2011.00076 (2011).
197 Chamberlin, N. L. & Saper, C. B. Topographic organization of cardiovascular responses to electrical and glutamate microstimulation of the parabrachial nucleus in the rat. *J Comp Neurol* **326**, 245-262, doi:10.1002/cne.903260207 (1992).

198 Yamaguchi, M. Functional Sub-Circuits of the Olfactory System Viewed from the Olfactory Bulb and the Olfactory Tubercle. *Front Neuroanat* **11**, 33, doi:10.3389/fnana.2017.00033 (2017).
199 McDonald, A. J., Shammah-Lagnado, S. J., Shi, C. & Davis, M. Cortical afferents to the extended amygdala. *Ann N Y Acad Sci* **877**, 309-338, doi:10.1111/j.1749-6632.1999.tb09275.x (1999).
200 Schiff, H. C. *et al.* An Insula–Central Amygdala Circuit for Guiding Tastant-Reinforced Choice Behavior. *The Journal of Neuroscience* **38**, 1418-1429, doi:10.1523/jneurosci.1773-17.2017 (2018).
201 Knapska, E. *et al.* Differential involvement of the central amygdala in appetitive versus aversive learning. *Learn Mem* **13**, 192-200, doi:10.1101/lm.54706 (2006).
202 Schultz, W. Updating dopamine reward signals. *Curr Opin Neurobiol* **23**, 229-238, doi:10.1016/j.conb.2012.11.012 (2013).
203 Swanson, L. W. Anatomy of the soul as reflected in the cerebral hemispheres: neural circuits underlying voluntary control of basic motivated behaviors. *J Comp Neurol* **493**, 122-131, doi:10.1002/cne.20733 (2005).
204 Baldo, B. A. & Kelley, A. E. Discrete neurochemical coding of distinguishable motivational processes: insights from nucleus accumbens control of feeding. *Psychopharmacology (Berl)* **191**, 439-459, doi:10.1007/s00213-007-0741-z (2007).
205 Everitt, B. J. *et al.* Review. Neural mechanisms underlying the vulnerability to develop compulsive drug-seeking habits and addiction. *Philos Trans R Soc Lond B Biol Sci* **363**, 3125-3135, doi:10.1098/rstb.2008.0089 (2008).
206 DiFeliceantonio, A. G. & Berridge, K. C. Which cue to 'want'? Opioid stimulation of central amygdala makes goal-trackers show stronger goal-tracking, just as sign-trackers show stronger sign-tracking. *Behav Brain Res* **230**, 399-408, doi:10.1016/j.bbr.2012.02.032 (2012).
207 Mahler, S. V. & Berridge, K. C. Which cue to "want?" Central amygdala opioid activation enhances and focuses incentive salience on a prepotent reward cue. *J Neurosci* **29**, 6500-6513, doi:10.1523/jneurosci.3875-08.2009 (2009).
208 Yu, K. *et al.* The central amygdala controls learning in the lateral amygdala. *Nat Neurosci* **20**, 1680-1685, doi:10.1038/s41593-017-0009-9 (2017).
209 Cornea-Hébert, V., Riad, M., Wu, C., Singh, S. K. & Descarries, L. Cellular and subcellular distribution of the serotonin 5-HT2A receptor in the central nervous system of adult rat. *J Comp Neurol* **409**, 187-209, doi:10.1002/(sici)1096-9861(19990628)409:2<187::aid-cne2>3.0.co;2-p (1999).
210 Moga, M. M. & Gray, T. S. Evidence for corticotropin-releasing factor, neurotensin, and somatostatin in the neural pathway from the central nucleus of the amygdala to the parabrachial nucleus. *J Comp Neurol* **241**, 275-284, doi:10.1002/cne.902410304 (1985).
211 Warden, M. K. & Young, W. S., 3rd. Distribution of cells containing mRNAs encoding substance P and neurokinin B in the rat central nervous system. *J Comp Neurol* **272**, 90-113, doi:10.1002/cne.902720107 (1988).
212 Zirlinger, M., Kreiman, G. & Anderson, D. J. Amygdala-enriched genes identified by microarray technology are restricted to specific amygdaloid subnuclei. *Proceedings of the National Academy of Sciences* **98**, 5270-5275, doi:10.1073/pnas.091094698 (2001).

6. Appendix

6.1 Abbreviations

AAA Anterior Amygdala Area

AAV Adeno-associated Virus

AgRP Agouti-related peptide

AP Area postrema

Arch Archaerhodopsin

BA Basal Amygdala

BM Basomedial Amygdala

BLA Basolateral Amygdala

BNST Bed Nucleus of the Stria Terminalis

Calcr1 Calcitonin receptor 1

CaM Calmodulin

CCK Cholecystokinin

CeA Central Amygdala

CeC Capsular part of the Central Amygdala

CeI Intermediate subdivision of the Central Amygdala

CeL Lateral subdivision of the Central Amygdala

CeM Medial subdivision of the Central Amygdala

CGRP Calcitonin gene-related peptide

ChR Channelrhodopsin

COA Cortical nucleus of Amygdala

cpGFP Circularly permuted green fluorescent protein

CRH Corticotropin-Releasing-Hormone

CS Conditioned Stimulus

Ctx Cortex

D2R Dopamine D2 receptor

dPAG Dorsal periaqueductal gray

DREADD Designer receptors exclusively activated by designer drugs

DVC Dorsal vagal complex

ECF Extracellular fluid

ENK Enkephalin

EPM Elevated plus maze

EYFP Enhanced Yellow Fluorescent protein

GLP1R Glucagon-like peptide 1 receptor

GRIN Gradient index

HYP Hypothalamus

HPC Hippocampus

Htr2a 5-Hydroxytryptamine receptor 2A

IC Insular Cortex

iC ++ Selective chloride-conducting-channelrodopsin

LA Lateral Amygdala

LH Lateral hypothalamus

LiCl Lithium chloride

LPB Lateral parabrachial nucleus

LPS Lipopolysaccharide

LTP Long term potentiation

MeA Medial Amygdala

MB Midbrain

MC4R Melanocortin 4 receptor

MGM Medial portion of the Medial Geniculate

MnPO Median preoptic nucleus

NAc Nucleus accumbens

NaCl Sodium Chloride

NLOT Nucleus of the Lateral Olfactory Tract

NMDA N-methyl-D-aspartate-receptor

nNOS Nitric oxide synthase neurons

NpHR Halorhodopsin from *Natronomonas*

NPY Neuropeptide Y

Nts Neurotensin

NTS Nucleus of the solitary tract

Ob Olfactory bulbs

ORF Open Reading Frame

OVLT Organum vascolosum of the lamina terminalis

Ox-A Orexin-A

Ox-B Orexin-B

Oxtr Oxytocin-receptor

PAA Piriform Amygdalar Area

PAG Periaqueductal grey

PBN Parabrachial Nucleus

Penk1 Proenkaphalin1

PFC Prefrontal cortex

PKCδ Protein kinase C δ

Pnoc Prepronociceptive-expressing cells

POMC Pro-opiomelanocortin

PVH Paraventricular hypothalamic nucleus

PVT Paraventricular nucleus of the thalamus

RTPP Real time place preference

S Stimulus

SFO Subfornical organ

SI Substantia Innominata

SON Supraoptic nucleus

Sst Somatostastin

Tac2 Tachykinin 2

TH Thalamus

US Unconditioned Stimulus

VIP Vasoactive Intestinal Peptide

vPAG Ventral periaqueductal gray

vlPAG Ventrolateral periaqueductal grey

VP_{PP} Vasopressin neurons projecting to the posterior pituitary

VTA Ventral Tegmental Area

Wfs1 Wolframin1

6.2 Acknowledgments

First, I would like to thank my supervisor Prof. Dr. Rüdiger Klein for his supervision and for providing me with guidance and counsel during my PhD. I am very grateful for the opportunity to work in very stimulating environment!

Thanks to Dr. Jan Deussing and Dr. Nadine Gogolla, members of my TAC, for supporting and encouraging me during these years and for providing scientific feedbacks.
Thanks to all the Klein-lab for the years we spent together! In particular I would like to thank Marion for sharing with me a scientific project and going through all the ups and downs. I enjoyed a lot collaborating with you! Thanks to Louise for helping me with lots of histology, never complaining about the high amount of work. Thanks to Pilar who has engineered essential transgenic mouse lines. Thanks to Christian, Hansol, Seung-Hee, Ylenia, Sonia, Rubia, Tobias and Dani for all the scientific discussions and funny moments we shared together.

My deepest thank to my dad, thanks for standing by me for all your life and loving me so much. I can still remember how my Bachelor and Master thesis defenses made you cry. I know that even if not physically here you will be close to me also this time. I hope to continue make you proud of me!

My warmest thank to my mum, the pillar of my life! Thanks for your infinite love!

Last, but not least, thanks to Simon. Apart from all the scientific suggestions and your help in solving many of my work-related problems, thanks for holding my hand and sharing your life with me. Thank you for being you, because you make my life complete!